TECHNICAL REPORT STANDARD PAGE

1. Report No. FHWA/LA-92/254	2. Government Accession No.	3. Recipient's Catalog No.
4. Title and Subtitle ENGINEERING PROPERTIES OF BRITTLE REPAIR MATERIALS	5. Report Date SEPTEMBER 1992	
	6. Performing Organization Code	
7. Author(s) G. Z. VOYIADJIS, C. CHANNAKESHAVA, T.M. ABU-LEBDEH, F. BARZEGAR	8. Performing Organization Report No. 254	
9. Performing Organization Name and Address Department of Civil Engineering Louisiana State University Baton Rouge, LA 70803	10. Work Unit No.	
	11. Contract or Grant No. 89-2C	
12. Sponsoring Agency Name and Address Louisiana Transportation Research Center P.O. Box 94245, Capitol Station Baton Rouge, LA 70804-9245	13. Type of Report and Period Covered Final Report - Volume I & Volume II July 1989 - June 1992	
	14. Sponsoring Agency Code	

15. Supplementary Notes
Conducted in cooperation with the U.S. Department of Transportation, Federal Highway Administration.

16. Abstract

Most codes of practice prescribe procedures for selecting patch configuration and materials based on test devised for evaluating new pavement materials. This study is aimed at examining the special consideration to be given to such evaluation procedures and to suggest improved procedures for brittle repair materials, based on additional tests and computer analysis.

The first part of the present investigation covers the experimental study, in which three different repair materials, namely plain concrete, steel fiber concrete, and rapid patch material (Duracel cement) are investigated. Tests are conducted on two different patch configurations (transition and rectangular) and three different patch depths (2, 4 and 6 inches). The experimental procedure to evaluate a brittle repair material consider four tests, namely, uniaxial strength test, biaxial strength test, bond strength tests, and shear test of a repaired pavement joint. As a result of the experimental study, it is concluded that the proposed biaxial testing set-up has been shown to provide a better understanding by which the strength and behavior of brittle repair materials can be fully investigated. It is observed that the strength of the repair material under combined tension and compression is lower than under uniaxial compression, and the strength decreases as the applied tensile stress in increased.

In the second part of this study, a mechanistic patched pavement analysis program is developed to assist in the evaluation of patching procedures and materials. Such a program can be used to develop curves which aid in the selection process. It can also be used for a case by case analysis for specific problems. This program can analyze both intact and patched concrete pavements considering different loading and support conditions, material properties, patch configurations, and depths. In this study, for the first time a complete distress simulation capability has been built into a three dimensional analysis program and it is expected that analysis using this program would enable better understanding of pavement behavior, which can lead to proper guidelines for evaluation of different materials and repair procedures in rehabilitating rigid-jointed pavements.

This report is presented in two volumes. Volume II contains the Appendices. A separate Summary Report is issued as report number FHWA/LA-92/253.

17. Key Words concrete, bi-axial testing, concrete pavement modeling, concrete engineering properties testing	18. Distribution Statement Unrestricted. This document is available to the public through the National Technical Information Service, Springfield, VA 22161.

ENGINEERING PROPERTIES OF BRITTLE REPAIR MATERIALS

FINAL REPORT

Volume I

by

G. Z. VOYIADJIS
PROFESSOR OF CIVIL ENGINEERING
C. CHANNAKESHAVA
RESEARCH ASSOCIATE
T. M. ABU-LEBDEH
DOCTORAL CANDIDATE
F. BARZEGAR
ASSISTANT PROFESSOR OF CIVIL ENGINEERING
DEPARTMENT OF CIVIL ENGINEERING
LOUISIANA STATE UNIVERSITY
BATON ROUGE, LA 70803

CONDUCTED FOR

LOUISIANA DEPARTMENT OF TRANSPORTATION AND DEVELOPMENT
LOUISIANA TRANSPORTATION RESEARCH CENTER
in Cooperation with
U.S. Department of Transportation
FEDERAL HIGHWAY ADMINISTRATION

FEBRUARY 1992

ABSTRACT

Most codes of practice prescribe procedures for selecting patch configuration and materials based on tests devised for evaluating new pavement materials. This study is aimed at examining the special considerations to be given to such evaluation procedures and to suggest improved procedures for brittle repair materials, based on additional tests and computer analysis.

The first part of the present investigation covers the experimental study, in which three different repair materials, namely, plain concrete, steel fiber concrete, and rapid patch material (Duracal cement) are investigated. Tests are conducted on two different patch configurations (transition and rectangular) and three different patch depths (2, 4 and 6 inches). The experimental procedure to evaluate a brittle repair material consider four tests, namely, uniaxial strength test, biaxial strength test, bond strength tests, and shear test of a repaired pavement joint. As a result of the experimental study, it is concluded that the proposed biaxial testing set-up has been shown to provide a better understanding by which the strength and behavior of brittle repair materials can be fully investigated. It is observed that the strength of the repair material under combined tension and compression is lower than under uniaxial compression, and the strength decreases as the applied tensile stress is increased.

In the second part of this study, a mechanistic patched pavement analysis program is developed to assist in the evaluation of patching procedures and materials. Such program can be used to develop curves which aid in the selection process. It can also be used for a case by case analysis for specific problems. This program can analyze both intact and patched concrete pavements considering different loading and support conditions, material properties, patch configurations, and depths. In this study, for the first time a complete distress simulation capability has been built into a three-dimensional analysis program and it is expected hat analysis using this program would enable better understanding of pavement behavior, which can lead to proper guidelines for evaluation of different materials and repair procedures in rehabilitating rigid-jointed pavements.

This report is presented in two volumes. Volume II contains the Appendices. A separate Summary Report is issued as report number FHWA/LA-92/253.

ACKNOWLEDGMENTS

This work was carried out under contract to the Louisiana Transportation Research Center sponsored by the Federal Highway Administration and the Louisiana Department of Transportation and Development. The authors gratefully acknowledge this support and the encouragement of Harold Paul and William Temple.

We would also like to express our appreciation for the help provided by the laboratory technicians of LTRC, Richard P. Desselles, Randy C. Young, and Matt A. Tircuit, and the LTRC concrete research engineer, Nick Rabalais.

PROGRAM IMPLEMENTATION

A mechanistic patched pavement analysis program has been developed to assist in the evaluation of patching procedures and materials. The program could be used to develop curves which aid in the selection process. It could also be used for a case by case analysis for specific problems. Further, detailed information of stresses in pavement sections can be obtained from the program. The applications of the program can be enhanced by minor modifications. Only the development of the curves necessary for evaluating the patch repair materials and configurations need some special knowledge which can be obtained through special training. Not much training or effort is necessary to use these curves. If guidelines for basic inputs and range of variation are supplied the authors assure assistance in developing these curves, or in training the personnel of the user departments in the use of the program.

TABLE OF CONTENTS

Volume I

Volume II

LIST OF TABLES

LIST OF FIGURES

Chapter 1

INTRODUCTION

Jointed concrete pavements constitute substantial mileage of the U.S. road network. The state of Louisiana has most of its interstate roads made of this type of pavement. They are durable, have a longer life than flexible pavements, and can be placed over relatively poor subgrade. However, several problems are encountered in the design, construction, and maintenance of jointed concrete pavements. Structural and serviceability failure of pavements are encountered due to improper design, construction, maintenance, and use. Structural failures of rigid pavements can occur either at the slab center or near the joints. Center-slab failures are mostly due to the loss of support because curling of pavements lead to cracking during the passage of heavy wheel loads. In Louisiana, the center-slab failures are due to: (1) shrinkage on 58 ft slabs, and (2) loss of subgrade support due to drainage problems and pumping. However, more common failures occur at joints. Such failures could be due to the loss of support, restraint at joints, and impact action of heavy axle loads. The cause of most of these failures is not fully understood. It may be impossible to avoid failure of rigid concrete pavements. Hence, repair procedures have been developed to rehabilitate failed concrete pavements. The repair procedures are based on limited test results and empirical guidelines. However, increase in axle loads, speed of vehicles, and also the cost of rehabilitation works have forced engineers to look at the rehabilitation procedures critically. There is a need for assessing and evaluating the cause of pavement failure and for selecting the most appropriate rehabilitation procedure. For this purpose, pavement failure should be clearly understood. The cost of materials and experimental investigations has made full scale testing of pavements a difficult proposition. The objective of this study is to devise evaluation methods for the repair materials employed for rehabilitation of damaged pavements based on simple experimental procedures and a computer based analytical procedure. For this purpose, special testing procedures are developed to obtain data for use in the analytical study. The causes for pavement failure are then examined through a specially-developed computer program. Finally, the experimental data is employed in studying the effect of pavement repair procedures and materials by using the computer program. The method of evaluating the suitability of the selected material is proposed.

Most standard tests for determining the quality and suitability of the materials for pavement rehabilitations are based on simple one-dimensional load applications, such as the standard cylinder test for compression and the splitting or tensile tests for tension. However, the field stress conditions are quite different from these test conditions. In general, the state of stress is three-dimensional. For pavements, the

most important property is the flexural or tensile strength of the material. It is well known that the tensile strength of concrete and most other similar materials depends upon the lateral compressive stresses. Under high lateral compression, the tensile strength may drop to about 50 percent of its original value. In spite of this knowledge, all design procedures still employ only the standard tensile strength, disregarding the actual stress conditions in the field. Although the permitted tensile stresses are only a fraction of the tensile strength and are not exceeded even if the decrease in strength under lateral compression is considered, under repeated applications of load, it is possible that fatigue effects reduce the actual tensile strength to a much smaller value. This effect depends upon the ratio of maximum tensile stress to the tensile strength at that stress state (biaxial or triaxial), and hence, under biaxial compression-tension stress fields, the fatigue life of pavements may be reduced drastically. Hitherto, no test procedure has been developed to determine the strength of the pavement materials under biaxial stress states. The present study attempts to do this using testing equipment normally available in any materials testing laboratory. The parameters obtained from such testing will be compared and validated with respect to more sophisticated test results available in literature.

The next phase of the experimental work involves determining the effect of repair procedures on the strength of rehabilitated pavement specimens. In particular, the study concentrates on whether or not the bond between the old and new materials is sufficient. Further testing is also done to obtain the properties of two different repair materials with respect to the strengths and initial elastic moduli for use in the computer-based analytical model.

The analytical part of the study involves the development of a reasonably sophisticated model to analyze pavements considering the various nonlinear effects involved, such as loss of support, loss of dowel force transfer stiffness due to local yielding and cracking, cracking of pavement slabs, and also the effects of temperature, self weight, and initial strains such as shrinkage strains. To achieve this objective, a special purpose finite element program is developed for three-dimensional nonlinear analysis of jointed concrete pavements. This program is employed to evaluate the causes of failure of pavements under condition of wheel loads, temperature effects, and effects of loss of support. Finally, the computer program is employed to study the effect of shrinkage of various repair materials employed in rehabilitations of damaged pavements on the operational life of pavements.

The main objectives of this study are as follows:

(1) Devising simple test procedures using commonly available testing equipment to test pavement concrete under general biaxial loads.

(2) Developing test methods for studying the interaction between repair materials and existing materials.

(3) Studying the effect of different materials on the effectiveness of patching procedures.

(4) Development of a computer-based analytical model to simulate and study the response of jointed concrete pavements.

(5) Studying the effect of axle and temperature loads on the static response of concrete pavements under different conditions of dowel-support and subgrade support.

(6) Studying the effect of patch materials and patching procedures through numerical simulation on the stresses in concrete pavements.

(7) Development of additional testing and analysis procedures to evaluate and select repair materials for rehabilitation of damaged rigid pavements.

Chapter 2

EXPERIMENTAL INVESTIGATIONS

2.1 INTRODUCTION

Recent research related to brittle repair material indicates that repairing existing highways and bridges will reduce expenses, effort, and time needed for new construction. Recent developments in patching materials technology have shown no considerable improvements in patching operations and their testing procedures. Substantial information exists on mild temperature patching procedures *[1], [2]* and a large number of materials were tested for strength development at temperatures of 15 to 20°F (-9 to -7°C), but very little data exists on material performance at subfreezing temperatures *[3]*.

An evaluation of the general state-of-the-practice in testing and formulating the response of brittle materials indicates that it has lagged state of the art considerably. The ASTM and AASHTO *[4]* specifications for concrete used in new construction has not undergone a major change since the 1960's. There are no specifications for evaluating repair materials and investigating their performance within damaged concrete. Such specifications are needed to provide the basis for selecting proper repair materials for use in different maintenance and rehabilitation projects. Therefore, new test techniques and response formulations for brittle repair materials have become an urgent need. This study will attempt to provide a better understanding of material behavior such as concrete as it responds in the field and particularly in repaired regions of rigid pavements. Such an extended understanding can help to conduct more realistic testing of existing and new brittle materials.

Generally, in selecting the proper repair material for a project, the following properties should be considered: (1) ability to stop the deterioration of the structure, particularly by preventing further cracks; (2) strength and stiffness properties of the patch repair material should be similar to those of the parent material; and (3) the material should provide acceptable workability and easy finish of the surfaces. Based on these requirements, concrete will be used as patching repair material.

At the present stage of evolution of computers, finite element method, and associated numerical techniques, important advances have been made in the procedures for obtaining numerical solutions to structural engineering problems and model simulation of nonlinear structural behavior. Unfortunately, our capability for numerical prediction of the behavior of such structures is frequently limited by the inadequacy of the material model for concrete.

In spite of the theoretical and experimental advances pertaining to the study of concrete behavior, it has not been possible to understand and formulate all the

important features of material response which would make it possible to predict element or structural response. Therefore, it is necessary to develop sophisticated analysis capabilities for accurate predictions of the response of such structures. Theoretically, one may use a mode involving a large number of state variables and parameters in order to accurately predict the responses of the material. However, consideration of the statistical scatter of the concrete properties, combined with the desire for computational feasibility, calls for the development of a mathematically simple model.

Before starting the scope of this investigation, it is necessary to review the main aspects of concrete behavior which will lead to a better understanding of the previous studies and the appropriate choices in the theoretical formulation of concrete.

Concrete is considered an aggregate-matrix composite material consisting of three components: the cement matrix, the aggregate, and the interface between the matrix and aggregate. The last component is the most porous part of this composite material and therefore, its weakest zone. The failure behavior of concrete is governed by complex degradation processes within the aggregate-matrix interface. An important feature of the aggregate-matrix interface is that it contains very fine cracks (microcracks) even before any load has been applied to the concrete shown in Figure 2.1a. The formation of such cracks is due primarily to the strain and stress concentrations resulting from the incompatibility of the elastic moduli of the aggregate and paste components. Volume changes in concrete due to shrinkage or thermal effects can cause strain constrations at aggregate-paste interface. These microcracks (bond cracks) spread causing major cracks at failure.

Many investigations *[5], [6], [7]* have shown that fracture characteristics and behavior of concrete subjected to uniaxial compression may be explained by the creation and propagation of microcracks within the concrete. Under applied loading, four stages of behavior can be distinguished in the stress-strain response. Consider, as an example, the stress-strain curve under uniaxial compression, shown in Figure 2.2.

As a first stage, consider the region up to 30-60 percent of the ultimate strength (shown as 45 percent in Figure 2.2). In this initial stage, microcracks in addition to those pre-existing in the material are initiated at isolated points where the tensile strain concentration is the highest shown in Figure 2.1b. At this load stage, localized cracks are initiated, but they do not propagate. Stresses up to 70-90 percent of the ultimate strength (shown as 85 percent in Figure 2.2) characterize the second stage (stage II in Figure 2.2). In this stage, as the applied load is increased, the crack system multiplies and propagates (Figure 2.1c), although in a slow, stable manner. If loading is stopped and the stress level is maintained at a certain value, crack propagation ceases. The increasing internal damage, revealed by deviation of the linear elastic behavior, causes irrecoverable deformation upon unloading. Although the relief of strain concentration

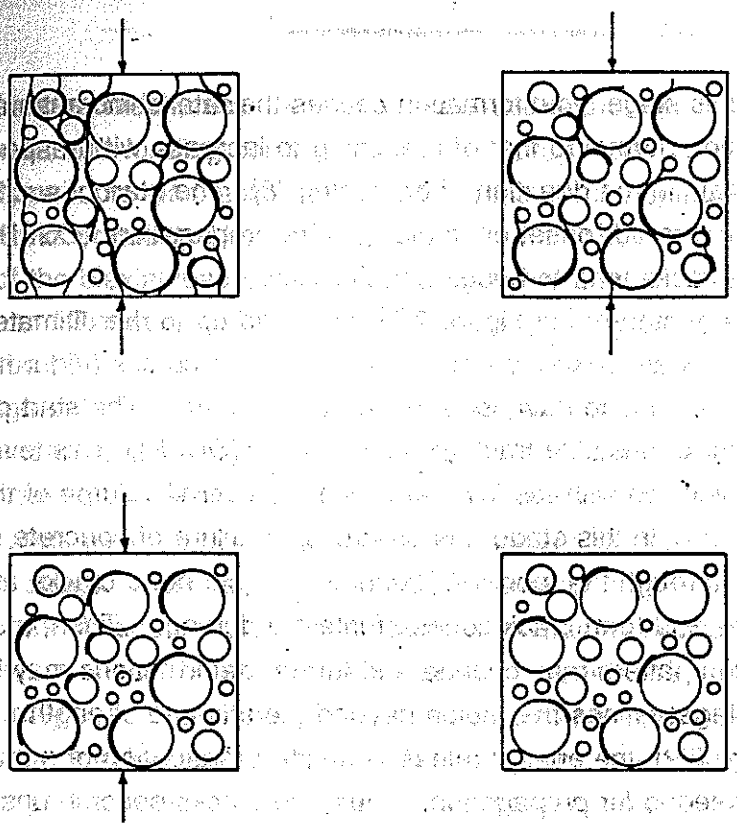

Figure 2.1
Crack patterns obtained from x-ray examination

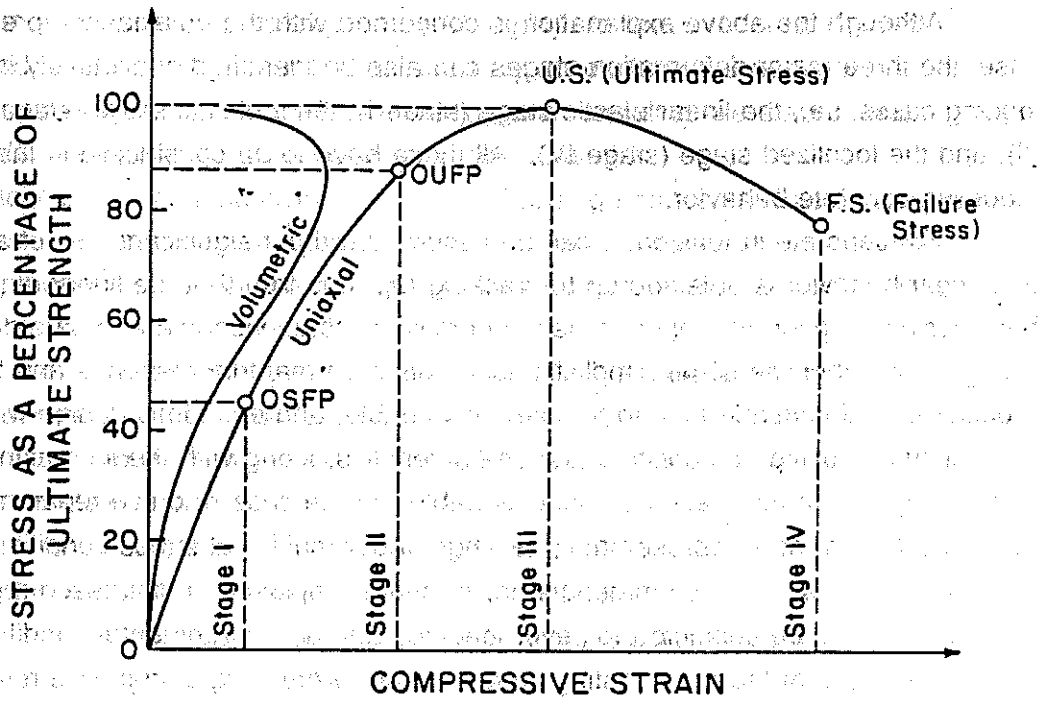

Figure 2.2
Uniaxial stress-strain curve for concrete

continues during this stage, void formation causes the rate of increase at the tensile strain in the direction normal to that of branching to increase with respect to the rate of increase of the strain in the direction of branching *[8]*. The start of such deformation behavior has been termed "onset of stable fracture propagation" (OSFP). In this load stage, the mortar cracks tend to bridge bond cracks.

A third stage (stage III in Figure 2.2) is applied up to the ultimate strength. Interface microcracks are linked to each other by mortar cracks (Figure 2.1c), and void formation (dilation) begins to have its effect on deformation. The start of this stage has been termed "onset of unstable fracture propagation" (OUFP). This level is easily defined since it coincides with the level at which the overall volume of the material becomes a minimum. In this stage, the progressive failure of concrete is primarily caused by cracks through the mortar. These cracks join bond cracks at the surface of nearby aggregates and form crack zones of internal damage. Then, a smoothly varying deformation pattern may change and further deformations may be localized.

A fourth stage defines the region beyond the ultimate strength. In this region (stage IV in Figure 2.2), the energy released by the propagation of a crack is greater than the energy needed for propagation. Thus, the cracks become unstable and self propagating until complete disruption and failure occurs. In this stage, the major cracks form parallel to the direction of applied load, causing failure of the concrete. The volume of voids increases dramatically, causing a rapid dilation of the overall volume of concrete (Figure 2.1d).

Although the above explanation is concerned with the uniaxial compression case, the three major deformation stages can also be identified qualitatively in other loading cases, i.e., the linear elastic stage (stage I), the inelastic stage (stage II and III), and the localized stage (stage IV). All these have to be considered in the modeling concrete behavior.

For concrete in tension, it can be assumed without significant loss of accuracy that linear behavior is obtained up to cracking *[9]*. It is true that the linear elastic-brittle behavior assumption for concrete has generally led to serviceable and safe design. However, whether the same simplistic assumption on material response and test procedures will continue to lead to safe, serviceable, and economic design with the constantly improving composition and characteristics, along with the increasingly challenging use of the material, is questionable. In the case of brittle repair materials, the demands on more representative testings under multiaxial stress conditions are even higher, because these materials are normally employed in distressed regions of structures which are subjected to sever loadings and/or environmental conditions.

The state-of-the-art in testing concrete and formulating constitutive relations and failure theories for this material has advanced significantly. The advances in the analytical and computational aspects of brittle material have led to a wide range of constitutive laws and failure relations, some of which are based on esoteric theories of

plasticity and fracture mechanics. A variety of equations that describe the behavior of concrete under various loading conditions has been proposed. In most of these models, the microscopic mechanism of concrete behavior is neglected. The experimental works conducted by Kupfer et al. *[10]* and Tasuji et al. *[11]* nearly cover the full range of the biaxial load cases. The triaxial stress states were covered by the results of Mills and Zimmerman *[12]*, Launay and Gachon *[13]*, and Gerstle et al. *[14]*.

Within the framework of continuum mechanics, there are several models for the short-term, range independent stress-strain behavior of concrete. These include nonlinear incrementally orthotropic, nonlinear-elastic isotropic models, hypoelastic model, models based on plasticity theory, and endochronic nonlinear elastic model *[9]*, *[15]*. These models have demonstrated their applicability for only limited combinations of biaxial stress states. More recently, the model developed by Romstad, Taylor and Herrmann *[16]* has obtained a good match with the overall monotonic biaxial behavior of plain concrete. It should be noted that these three models are suitable for use in finite element analysis. These have generally been incorporated with "tension cut-off" assumption. Coon and Evans *[17]* developed a model for multiaxial loading of plain concrete and can be applied to nonmonotonic and nonproportional loading.

Based on a hypoelastic orthotropic approach, Elwi and Murray *[18]* developed a nonlinear three-dimensional stress-strain relationship for concrete, which incorporates the equivalent uniaxial strain concepts of Darwin and Pecknold *[19]*.

Some of the earliest nonlinear concrete models have been obtained by direct application of associated plasticity theory *[20]*, *[21]*. In these models, concrete is considered as elastic-strain hardening, and they account for the dependence of deformations of the stress path, but unloading and reloading are elastic, and a reasonable description of cyclic behavior is not obtained.

Models involving plasticity theories and damage concepts (fracturing model) have been developed. These include the endochronic model *[22]*, *[23]*, plastic-fracturing model *[24]*, elastic progressive fracturing model *[25]*, *[26]*, *[27]*, *[28]*, and bounding surface model *[29]*, *[30]*.

In the second part of the experimental study, it will be attempted to provide a better understanding of the behavior of other repair material such as steel fibrous concrete and rapid patch material, particularly when subjected to biaxial tension-compression state of stress.

Before starting the scope of this investigation, it is necessary to review the main aspect of the behavior of steel fibrous concrete and the rapid patch material, which will guide one to the better understanding of the previous studies and the appropriate choices in the theoretical formulation of concrete.

Concrete is considered an aggregate-matrix composite material consisting of three components: the cement matrix, the aggregate, and the interface between the matrix and aggregate. The last component is the most porous part of this composite

material and therefore, its weakest zone. It contains microcracks even before a load has been applied to the concrete. The formation of such cracks is due primarily to the strain and stress concentrations resulting from the incompatibility of the elastic moduli of the aggregate and paste components. Introducing steel fiber to the concrete will make up the weakness in resisting tensile stresses. Indeed, the rapid propagation of the microcracks under applied stress is considered responsible for the weakness of concrete in tensile strength *[31]*. It seems reasonable to assume that tensile properties of concrete can be increased by adding the steel fiber. These fibers would arrest the microcracks' propagation, and hence delay the onset of tensile cracks and increase the tensile strength of the concrete.

Since Romualdi and Batson first introduced the idea of steel fibrous concrete in the early 1960's, research was undertaken to explore the usefulness of steel fibers as reinforcement of concrete. Since then, laboratory results and field experience have shown that steel fibers do indeed provide significant improvement in many of the engineering properties of concrete. The most dramatic improvements are seen in the uniaxial tensile or flexural behavior. Few studies have been made on the behavior of steel fibrous concrete subjected to compression loading. The reason might be that experimental studies *[32]*, *[33]*, *[34]* have shown that introducing fibers to the concrete has very little effect on its uniaxial compressive strength. However, the experimental studies *[10]*, *[35]*, *[36]* have demonstrated that plain concrete fails by tensile splitting under both uniaxial and biaxial compression loading. Hence, it seems reasonable to assume that the failure of concrete under compressive loading is governed by the tensile property,and the compressive strength of concrete should be increased substantially by the addition of the steel fibers. The test results of Yin et al. *[31]* have shown that the biaxial compressive strength of concrete is increased significantly by the addition of fibers. In the present study, it will be attempted to investigate the behavior of two repair materials, namely, steel fibrous concrete and rapid patch material subjected to biaxial tension-compression state of stress. The influence of adding steel fiber to the concrete on the ultimate strength and on the deformational characteristics will be studied herein.

Although fibers of various characteristics are produced from steel, plastic, glass, and natural material, steel fiber is the most commonly used in structures. In the present work, the Ribtec's XOREX steel fiber will be used as reinforcement for the concrete. To get the higher level of property improvements gained from the selected steel fiber, the following factors will be considered:

1. concrete mix design
2. concrete age
3. steel fiber content
4. steel fiber aspects ratio (length/diameter)
5. fiber/matrix bond

The last two factors are the most important factors, since the efficiency of the steel fibers in the concrete strongly depends on them. It should be noted that the corrugated shape of XOREX steel fibers (used in the present work) enhanced the bonding of the steel fiber to the concrete matrix.

2.2 GENERAL OBJECTIVE

As mentioned before, the behavior of ordinary concrete has been studied to some extent. Nevertheless, most of the experimental investigations on the concrete behavior have employed rather sophisticated costly testing apparatus and data acquisition systems which are not normally available in testing laboratories. On the other hand, with the introduction of the new and expensive brittle repair materials which are used in retrofit and/or rehabilitation tasks, evaluating their improved stiffness and strength characteristics under different stress conditions is becoming vital.

The main objective of this investigation is to study the behavior of materials such as concrete, steel fibrous concrete, and rapid patch material as they respond in the field and particularly in repaired regions of rigid pavements. The following factors, which are of practical interest, are studied:

1. Improving the standard ASTM procedures currently used in testing brittle repair materials by subjecting the material to a biaxial state of stress
2. Devising a simple testing method to study the interaction between repair materials and ordinary concrete
3. Testing repaired doweled joints in rigid pavements up to failure to investigate the performance of the repair material in the field and to assess the effectiveness of the joint rehabilitation measures
4. Analyzing the test specimens to verify the analytical methods and numerical procedures to diagnose the causes of failure, and to identify the parameters affecting the test specimen responses
5. The influence of adding steel fibers to the normal concrete, particularly on the ultimate strength and the deformational characteristics of steel fibrous concrete
6. The behavior of rapid patch material subjected to a biaxial tension-compression state of stress
7. Biaxial stress-strain relationship for both steel fibrous concrete and rapid patch material
8. Making recommendations regarding the use of repair materials in rigid pavements rehabilitation projects

2.3 SCOPE OF WORK

Most of the materials laboratories in research centers have not adopted the recent advances in laboratory test techniques. The experimental capability available in

an advanced material test laboratory would be capable of subjecting a sample of material to a general multiaxial state of stress. Significant analytical and computational capabilities are required to complete the experimental activities in such a laboratory.

Most of the research related to steel fiber concrete has investigated the effect of adding steel fiber on the uniaxial tensile or flexural behavior. Few studies have been made on the deformational and microcracking behavior of steel fiber concrete subjected to the biaxial tension-compression state of stress.

The overall approach of this study is to investigate the properties of brittle repair materials, particularly plain concrete, fiber concrete, and rapid patch material. It will attempt to propose an adequate performance criteria of patching materials. The general approach includes:

1. Devising more realistic sampling and testing procedures for brittle repair materials and their bonding behavior with the surrounding regular concrete.
2. Modifying the parameters obtained from the newly devised as well as existing standard material test.
3. Investigating the behavior of repair materials under service conditions by testing a number of repaired rigid pavement joints with different patching configuration and depths.

To reach the first objective, repair material test samples will be designed, cast, cured, and tested to explore practical but realistic manners of improving the existing standard sampling and testing procedures. In addition, samples of composite repair material-concrete will be tested to assess the bond characteristics between regular concrete and patching material used in pavement.

To reach the second objective, a simple stress-strain model under biaxial state of stress will be formulated. In calibrating this model, the experimental results will be utilized. Also, based on the bond test results, appropriate criteria to establish unbonding between regular concrete used in roadway construction and brittle repair material will be employed.

To reach the third objective, specimens of repaired rigid pavement joints will be prepared and tested under transverse loads applied at the joints. Different patching sizes and depths will be included to identify the patching procedure.

2.4 EXPERIMENTAL DESIGN AND PROCEDURE

Strength properties are not the only criteria in the performance of patching material. Durability is also considered. Each of these general categories, however, involves several parameters. Bond strength and the strength of the repair material itself fall under the strength category. Freeze-thaw durability, shrinkage, and thermal movement fall under the durability category.

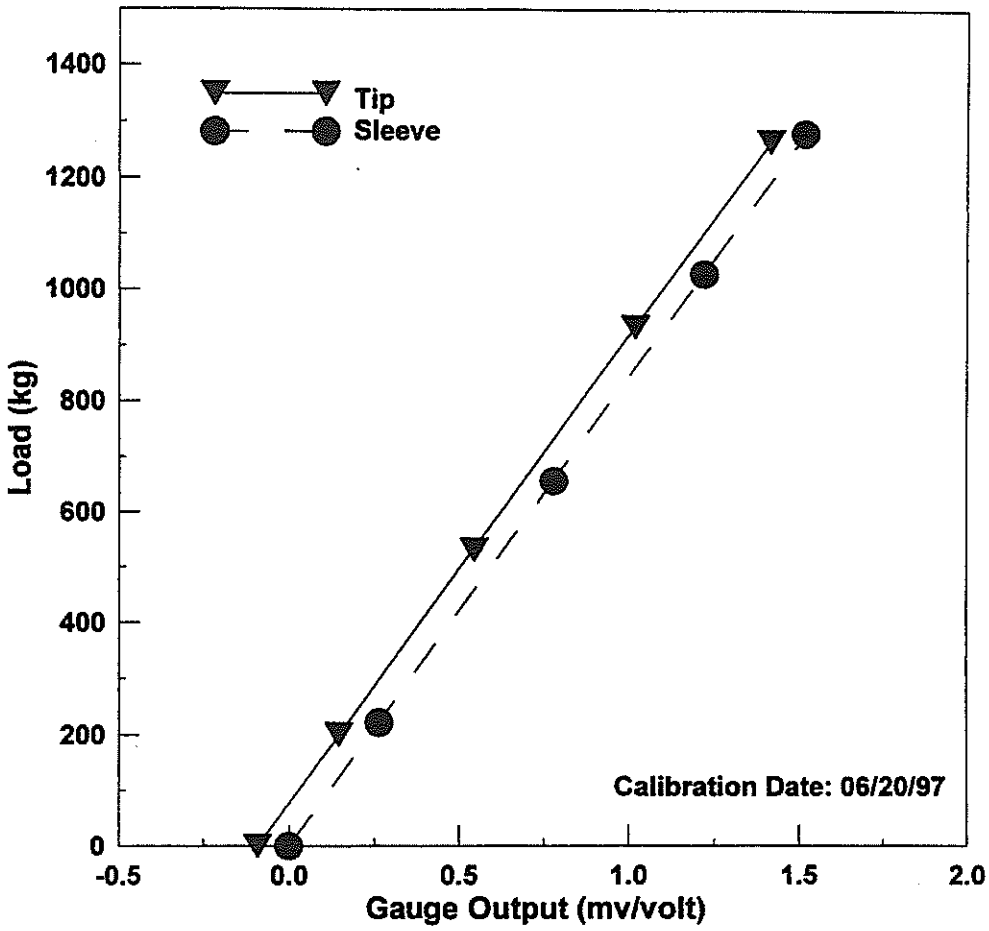

Figure 6
Load calibration of the miniature cone penetrometer

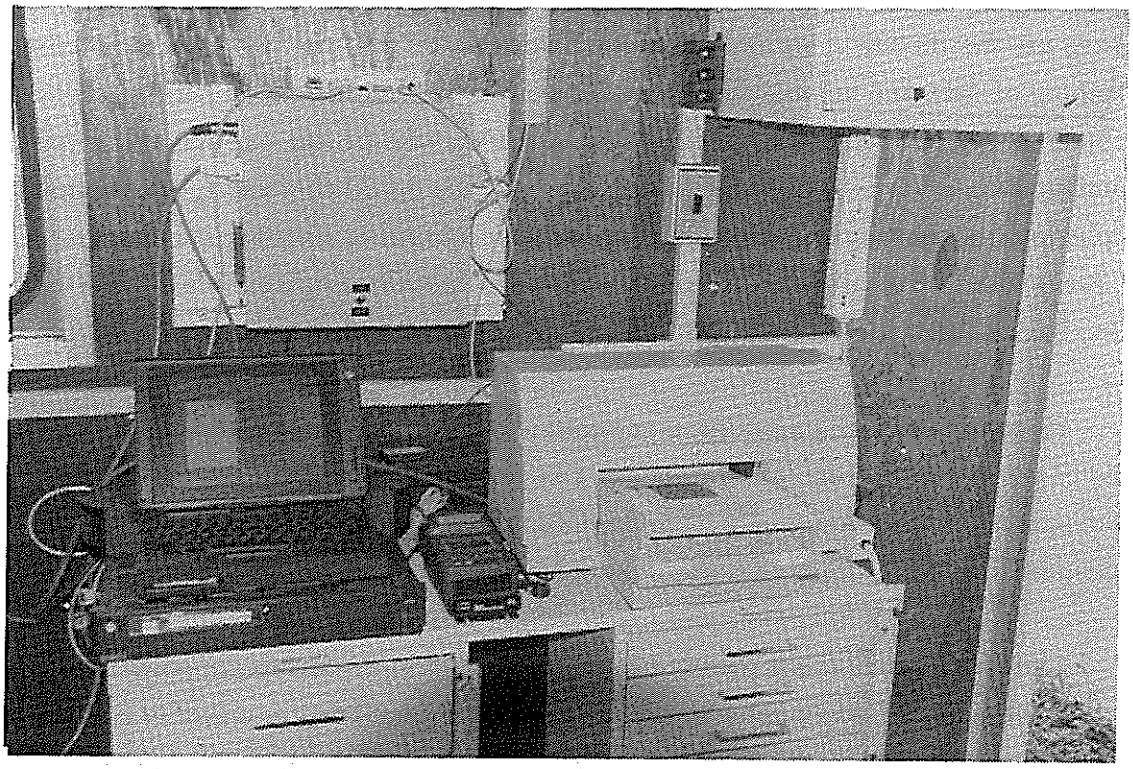

Figure 7
The complete data acquisition system

sleeve friction. For the data collection of five measurements (penetration depth, tip resistance, sleeve friction, pore pressure, and inclination), a system of dedicated smart-digital-sensors modules are used to collect, hold, and communicate to a personal computer the measured data from each sensor. The schematics of the DGH modules are given in figure 8. These modules along with a power supply housed in a metal box comprise the data acquisition hardware (figure 9).

The dedicated smart-digital-sensors modules, manufactured by DGH corporation, are sensor to computer interfaces, designed primarily for data acquisition based on personal computers with standard serial I/O ports. These modules collect analog or digital output signals from sensors, within and/or out of the cone, convert them into digital signals, and send them to a computer's standard RS-485 or RS-232C serial port. The computer itself can be used to communicate to the DGH module to program the module's various data conditioning features, such as scaling of data output, smoothing of data, and noise filtration. Also, interfacing communication parameters between the computer and module, such as baud rates and parity, can be set through the serial port. All communications to and from the modules are in printable ASCII characters, which allows for easy deciphering of output signals. This means a high level computer language such as BASIC, Pascal, or C can be used for programing a data acquisition system by issuing a simple ASCII command and getting back a result in an ASCII string.

Physically, each DGH module is enclosed in a plastic case measuring 7.7 x 3.6 x 1.1 cm, with a labeled screw terminal on one of its edges. DGH modules are selected by model number for the type of sensor to be monitored. A total of five DGH modules are used for a miniature piezocone data acquisition system, one for each sensor. The following is a list of the different DGH modules used.

- One DGH D1622 event counter module is used as a pulse counter for counting digital pulses from a optical incremental encoder. The encoder is axially mounted to a wheel, which is located within the cone pushing device, that rotates as the cone rod is unwound and pushed into the soil.
- Two DGH D1102 voltage modules are used to capture millivolt readings from the tip and sleeve strain gauges.
- One DGH D1512 bridge input module is connected to an Entran miniature accelerometer, located within the cone, to measure the inclination during intrusion.
- One DGH D1532 bridge input is use to measure the millivolt readings from the an Entran miniature pressure transducer.

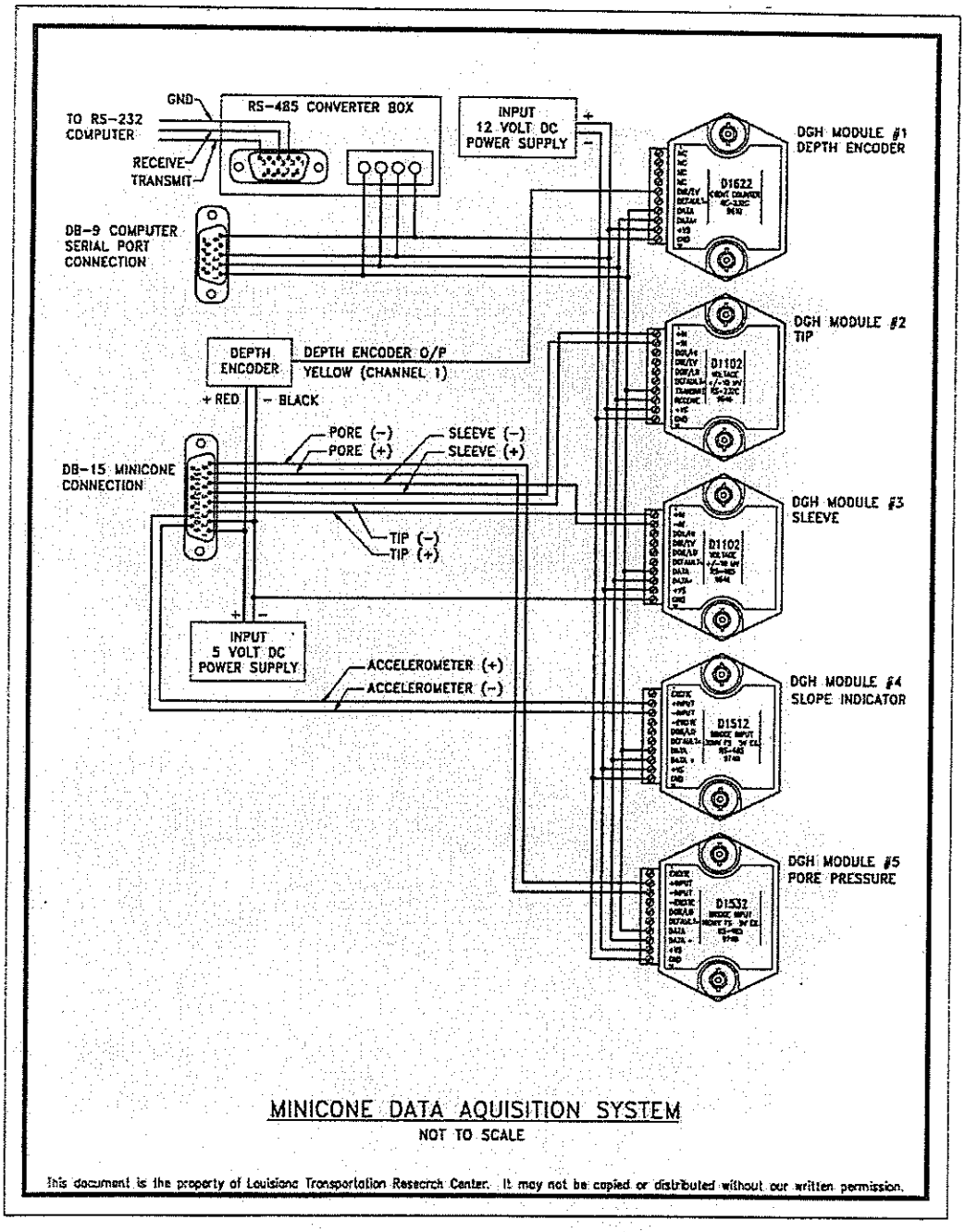

Figure 8
The DGH data acquisition modules (wiring diagram)

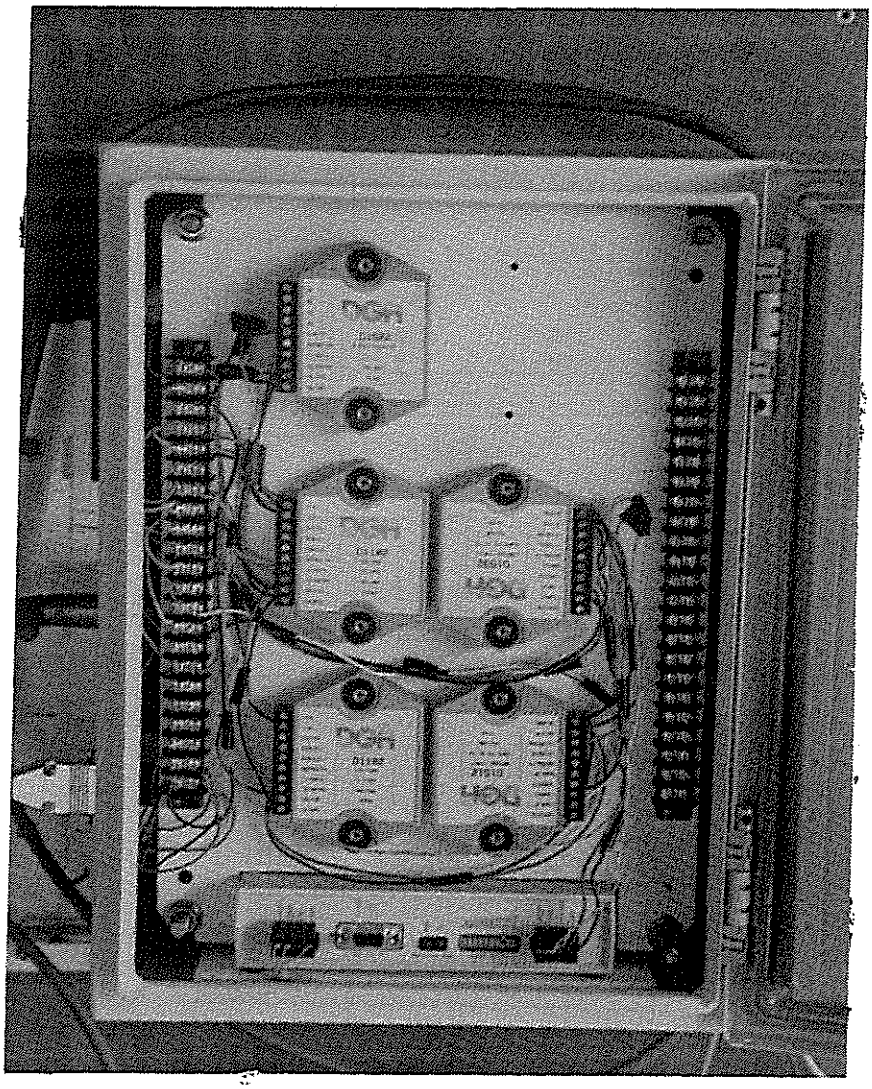

Figure 9
General view of housing for the DGH data acquisition modules

All modules are mounted on a panel within a weather-resistant 30 x 43 x 18 cm metal box. The metal box also houses a 5 and 12 volt power supply to supply power to the DGH modules and excitation voltage to the cone's sensors. To exhaust the heat generated by the modules and the power supply, an electric fan, rated at 32 CFM, is used to vent air though two 3-inch diameter holes fitted with air filters and finger guards. Also housed within the box is a serial signal converter for converting RS485 to RS232C, which is compatible to the standard serial ports of almost any personal computer. Converting the serial signal before it comes out of the box allows for any personal computer to be hooked up to the minicone data acquisition system without the need to install special equipment in the computer itself.

A data acquisition, processing, and display software has been developed in Turbo C ++ to acquire and display data on screen in real time. The software part of the data acquisition system consists of two main parts; the communications part and the graphic part. The communications part consists of the software interacting with hardware to get data. Once the data from the modules are acquired, the software converts the data into engineering units and plots them onto a computer screen in a graphic form in real time. Simultaneously, the data is written to a data file. The graphical user interface is designed to be user-friendly. A pentium notebook computer running at 100 MHz with 16 MB RAM and 810 MB hard drive capacity is used for data acquisition, processing, and analysis. A printer is also available to obtain hard copy output and plots of the cone penetration profiles.

Global Positioning System (GPS)

A Global Positioning System (GPS) installed in the vehicle outputs test locations directly to the computer via an RS-232 port. This is accomplished by a MARCH I unit, an all purpose Global Positioning System (GPS) Data Recorder and navigator, developed by Corvallis Microtechnology, Inc. (figure 10). The unit is practically a handheld computer. It uses a ten MHz CMOS 80c88 CPU with one megabyte internal RAM disk as its main operating platform to run an eight channel Motorola GPS module. Its physical dimensions are 7.9 x 4.9 x 3.0 and weighs 33 ounces. For corrections a Leica differential receiver, tuned to marine Coast Guard frequency is used. With Coast Guard RTCM corrections and a dilution of precision (DOP) less than four (DOP < 4) it has an accuracy of 2 meters under CEP (50 percent), 2.5 meters under RMS (63 percent), and 5 meters under 2DRMS (95 percent). Without any corrections the unit on its own has an accuracy anywhere from 40 to 100 meters. The MARCH GPS unit essentially consists of a MARCH Field Data Recorder, a built-in GPS antenna, and a GPS receiver for satellite signals. The unit is used to collect accurate position data. When the GPS unit is turned on, the tracking status indicator on the screen indicates the quality of the constellation of satellites being tracked by the unit.

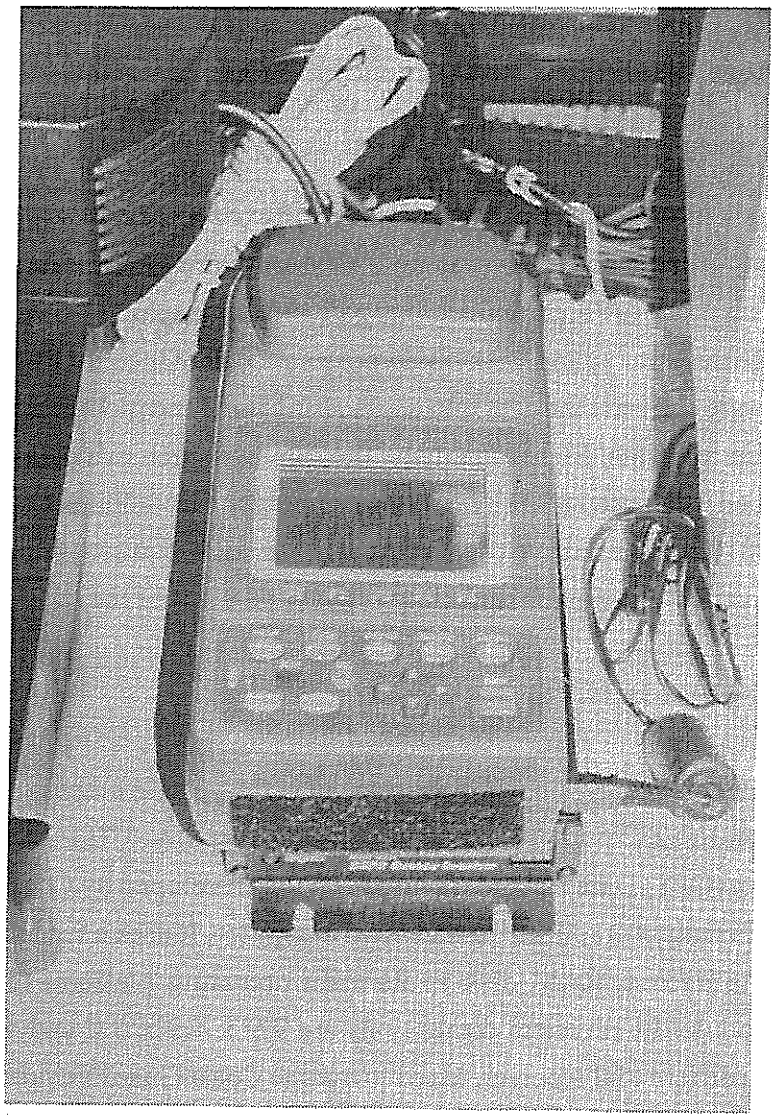

Figure 10
MARCH I - Global Positioning System (GPS)

The appropriate status is "N3D4" which means MARCH GPS is navigating in 3-D and tracking four or more satellites. If differential correction is being used with the RTCM_104 function, the "D" in the indicator will become a "C" indicating correction. The differential correction is received from the Coast Guard radio beacon receiver.

A program module written in Turbo C receives data from the COM port and extracts the latitude and longitude from the reading. The program receives ten corrected readings and computes the average of the latitude and longitude. A listing of the program code is given in appendix 1a. The MARCH GPS unit is provided with two RS-232 interface ports (COM ports) for communication with the external PC. The NMEA function enables the MARCH GPS to output its current calculated coordinates through a COM port for use by the external device. The RTCM_104 function is used to apply the differential correction to the data collected by the GPS unit. These two functions are used in conjunction with each other to produce corrected data and output it to the computer port. The RTCM_104 message is received on COM1, and the NMEA message with the corrected GPS position is sent from COM2 to the PC. It is essential to maintain the same baud rate and other communication parameters between the device providing the correction (LEICA beacon receiver) and the GPS for the RTCM_104 function. Similarly the same parameters are set between the NMEA function and the PC. In this project, the following communication parameters have been set:

Baud Rate	9600
Data bits	8
Parity	None
Stop Bit	1
RTCM_104	Auto (This indicates that the March GPS will use the RTCM_104 message whenever it is received.)
Output Frequency	3 (This indicates how often the NMEA messages will be outputted in this case it is 3 seconds)

A typical output from the GPS is shown in appendix 1b.

DISCUSSION OF RESULTS

Field testing and calibration of the CIMCPT system

The implementation of the miniature cone penetrometer was tested and verified by comparing the penetration profiles with those obtained using a standard 10 cm^2 cross-sectional area reference cone penetrometer developed by Fugro. The 10 cm^2 electronic cone penetrometer has a friction sleeve area of 150 cm^2 and a 60^0 cone apex angle. For field calibration, it is essential to conduct tests at well-documented sites with homogeneous soil deposits to minimize the effect of soil variability on the measured data. The miniature cone is capable of detecting thin layers compared to the large size cones and this feature must be taken into account while interpreting MCPT data. Penetrations by the 10 cm^2 reference cone penetrometer and the 15 cm^2 cone penetrometer have greater radial influence, than the MCPT's. Hence the MCPT's were conducted first before conducting the reference CPT's to minimize interaction and influence of soil disturbance on the tests results. In situ calibration of the CIMCPT system was conducted at a highway embankment site in Baton Rouge, Louisiana; and also at two of the National Geotechnical Experimentation Sites (NGES): University of Houston, and the Texas A & M University. A description of the soil properties at the sites followed by the in situ test results are given below.

Site description and results of in situ tests

Highland Road Site in Baton Rouge, Louisiana. The CIMCPT was field tested and calibrated near the intersection of Highland Road and Interstate 10 (LA SR-42) in Baton Rouge, Louisiana *[6], [7]*. The soil at the test site was overconsolidated, desiccated silty clay/clayey silt formed during the Pleistocene period and deposited in a deltaic environment. The soil is of stiff consistency, low moisture content, and fissured with slickensides and occasional sand pockets *[8]*. The ground water table was located at a depth of 4.5 m. Detailed piezocone penetration tests, soil sampling, and laboratory tests have been performed by Chen and Mayne *[9]* to a depth of 34 meters. Since the CIMCPT system was used to test only the top eight meters, the description of soil properties were limited up to this depth. The liquid limit ranges from 52 to 76 percent with an average of 64 $\pm$ 12 percent. The plasticity index ranges from 26 to 40 percent with an average of 33 $\pm$ 7 percent. The soil is classified as CH material in the Unified Soil Classification System (USCS). The natural water content varies from 30 to 42 percent (36 $\pm$ 6 percent) and is very close to the plastic limit, indicating a stiff deposit. The liquidity index ranges from 0.142 to 0.154. Consolidation test results indicated an overconsolidated deposit with OCR decreasing from 15.6 at a depth of 5.5 meters to an OCR of 11.9 at a depth of 7.9 meters. The compression index (C_c) varies from 0.47 to

0.62, and the swelling index (C_s) ranges from 0.14 to 0.22 ($C_s = 0.18 \pm 0.04$). Isotropically consolidated undrained triaxial compression tests (CIUC) show that the undrained shear strengths range from 60 kN/m^2 to 120 kN/m^2 [*9*].

Figure 11 shows the location and test plan at the calibration site. Five MCPT's (MCPT1, MCPT2, MCPT3, MCPT4, and MCPT5) were performed at the corners of two equilateral (2.22 m each side) triangular grids. Two 10 cm^2 reference cone penetration tests (CPT1 and CPT2) were conducted at the centroid of each triangles. The distance between two adjacent MCPT's was 2.22 m, and that between the two reference CPT's was 2.56 m (144 times the radius of the reference cone). Hence the influence of soil disturbance and effects of consolidation (due to the proximity of tests) on the data was minimal. At this site it was possible to conduct MCPT's to maximum depths ranging from 7.75 m to 8.75 m. Beyond this depth the total resistance due to friction and tip load exceeded the thrust capacity of the continuous push device. The homogeneity at this site can be easily seen in figure 12 that compares the CPT1 and CPT2 profiles. Figure 13 shows CPT1 profiles compared with those of MCPT1, MCPT2, and MCPT3. Figure 14 shows CPT2 profiles compared with those of MCPT3, MCPT4, and MCPT5. Very good comparison is seen between the 2 cm^2 MCPT profiles and the standard 10 cm^2 CPT profiles. Soil classification by the computerized probabilistic method by Zhang and Tumay, 1999 *[10]* using the mean CPT profiles and the mean MCPT profile are shown in figures 15 and 16.

National Geotechnical Experimentation Sites. A system of test sites is now available in the United States through the National Geotechnical Experimentation Sites (NGES) program funded by the National Science Foundation (NSF) and the Federal Highway Administration (FHWA)[*11*],[*12*]. The NGES system of multiple user test sites provides easy access to well-documented field sites, allowing geotechnical researchers to select the most appropriate site for their needs on the basis of soil type, site location, and available geotechnical data. These well-documented field, well-referenced test sites greatly facilitate the development and validation of new techniques for soil characterization. Associated with the NGES program is a central data repository which provides a database designed to promote exchange of information, resulting in a more cost effective use of available research funds.

Five of the forty-two sites have been selected at an NSF/FHWA workshop and classified as level I or level II sites. The remaining sites are classified as level III. level I sites are those sites which most closely fit the combined criteria of research areas identified through several workshops as being of significant national importance and possessing favorable site characteristics. Theme research areas are geotechnical earthquake engineering (liquefaction, site amplification,

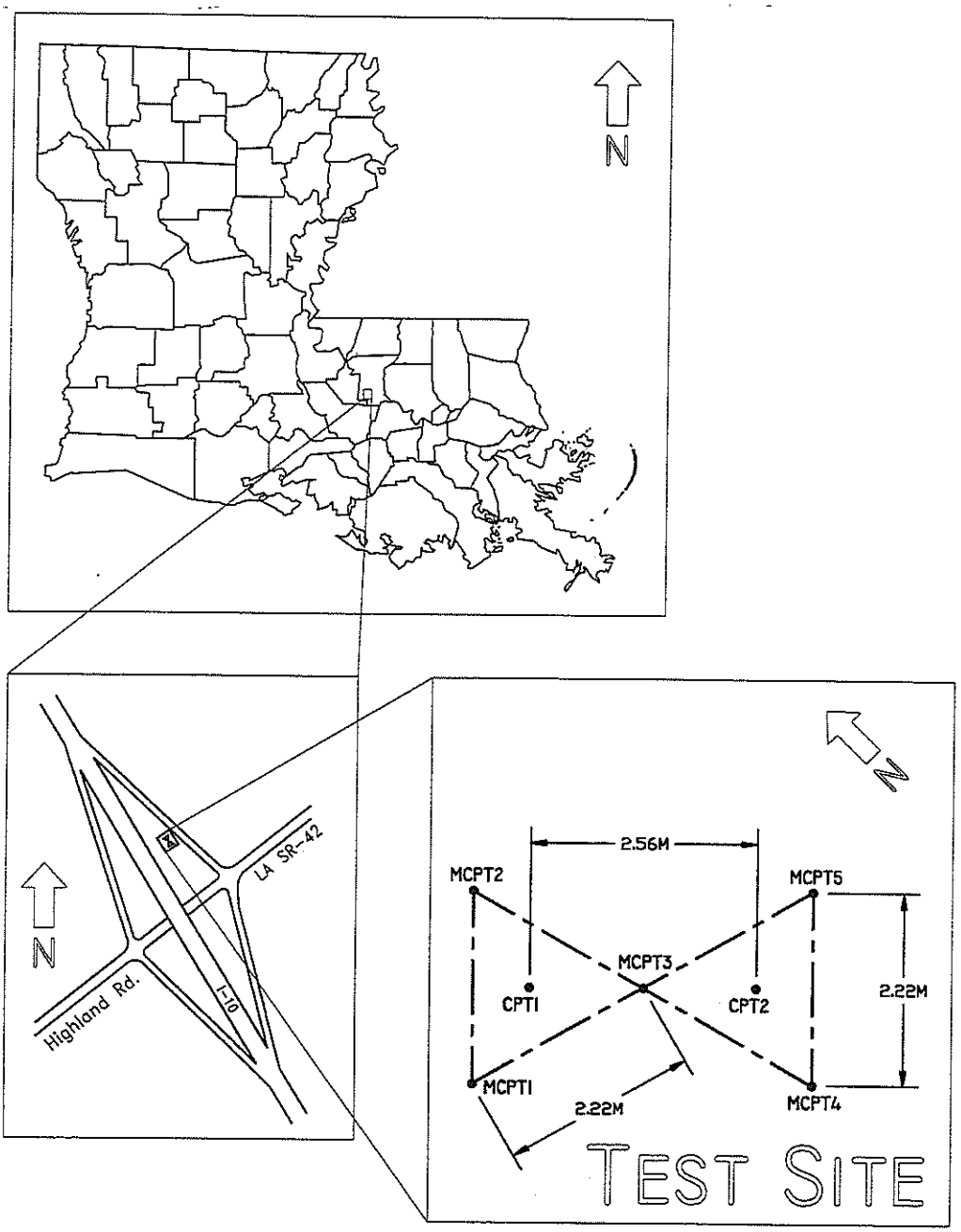

Figure 11
Location and test plan at the Highland Road site in Louisiana

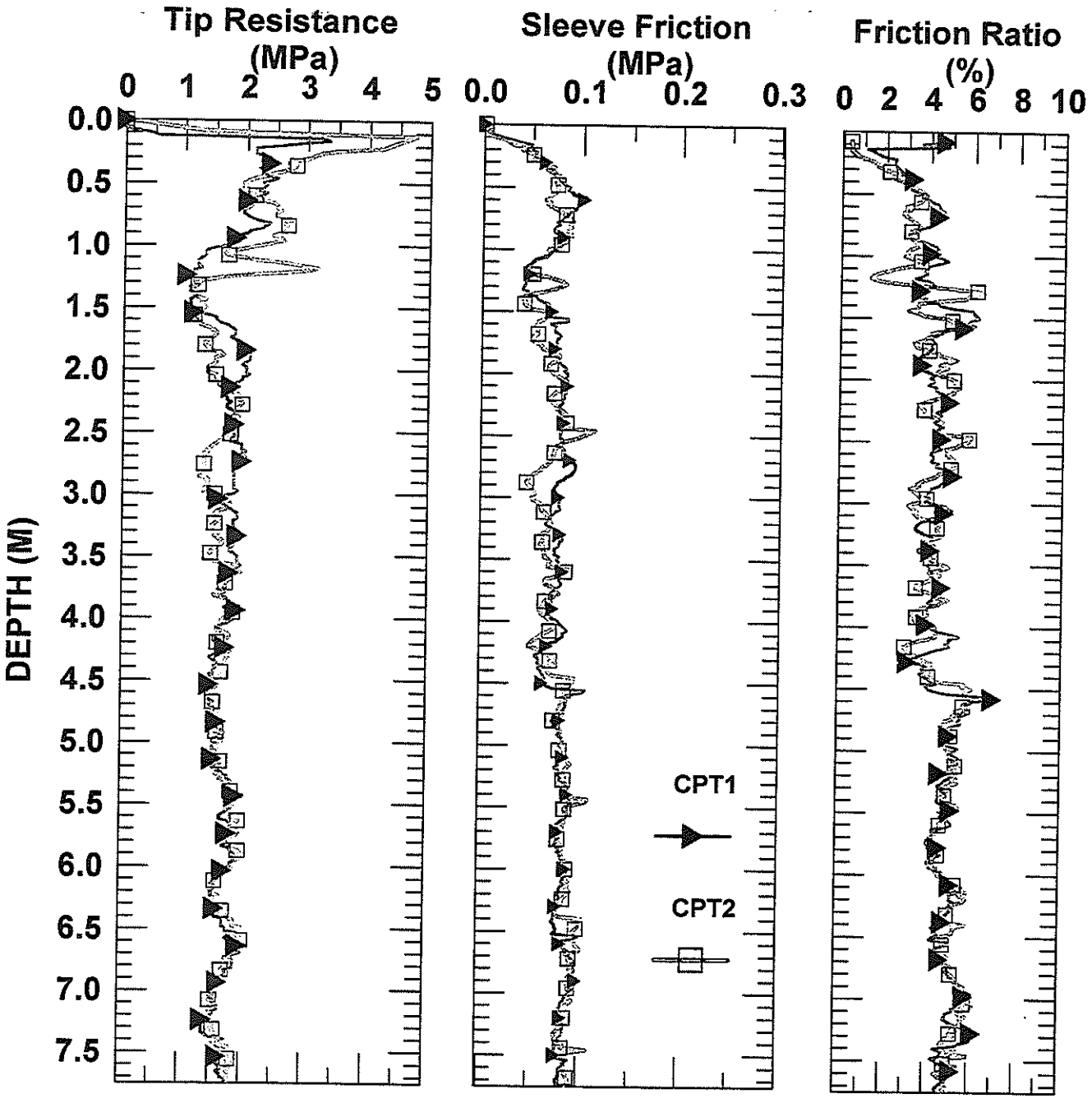

Figure 12
Comparison of penetration profiles of CPT1 and CPT2 at the Highland Road site in Louisiana

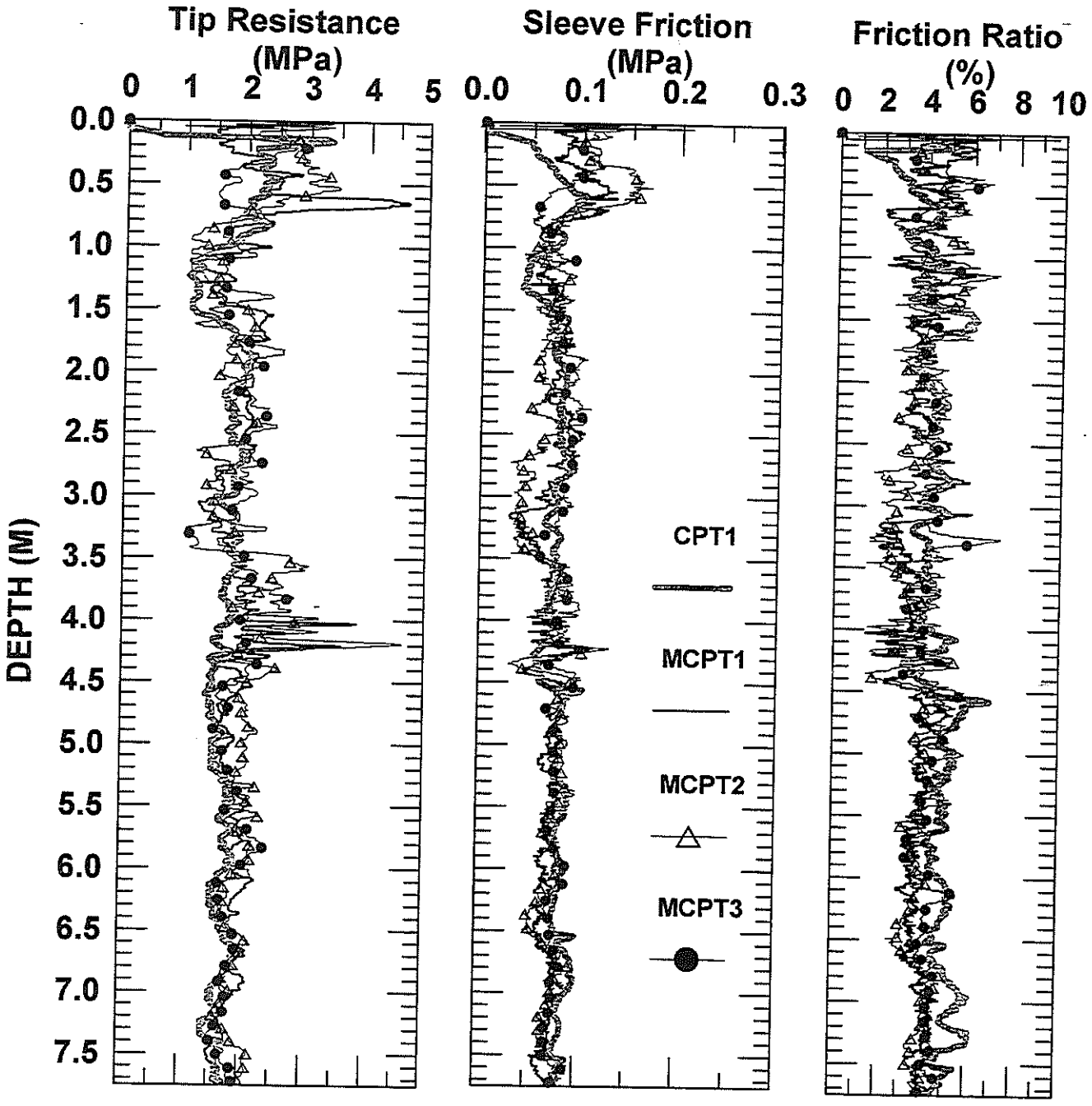

Figure 13
Comparison of penetration profiles of MCPT1, MCPT2 MCPT3 and CPT1 at the Highland Road site in Louisiana

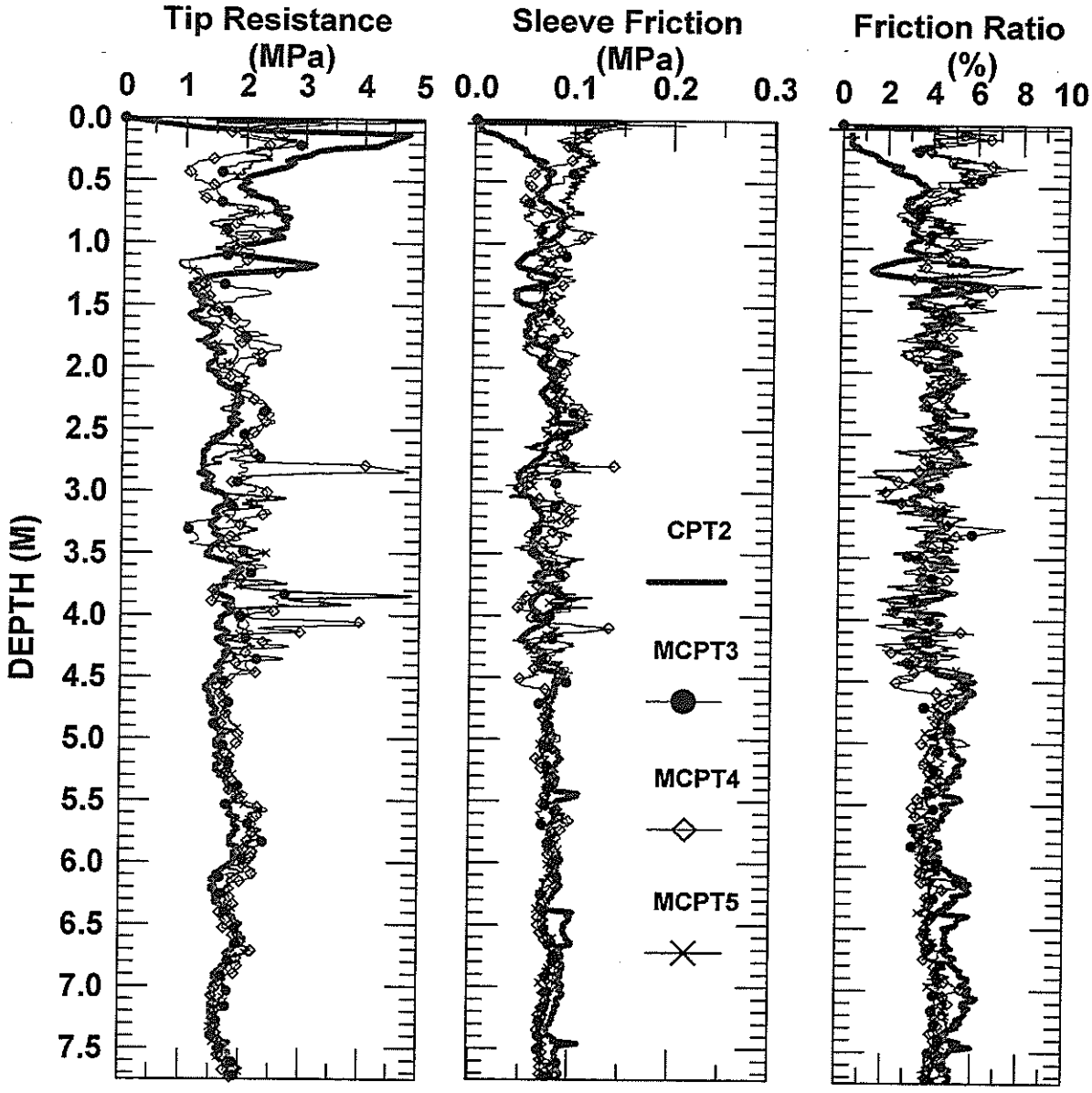

Figure 14
Comparison of penetration profiles of MCPT3, MCPT4, MCPT5 and CPT2 at the Highland Road site in Louisiana.

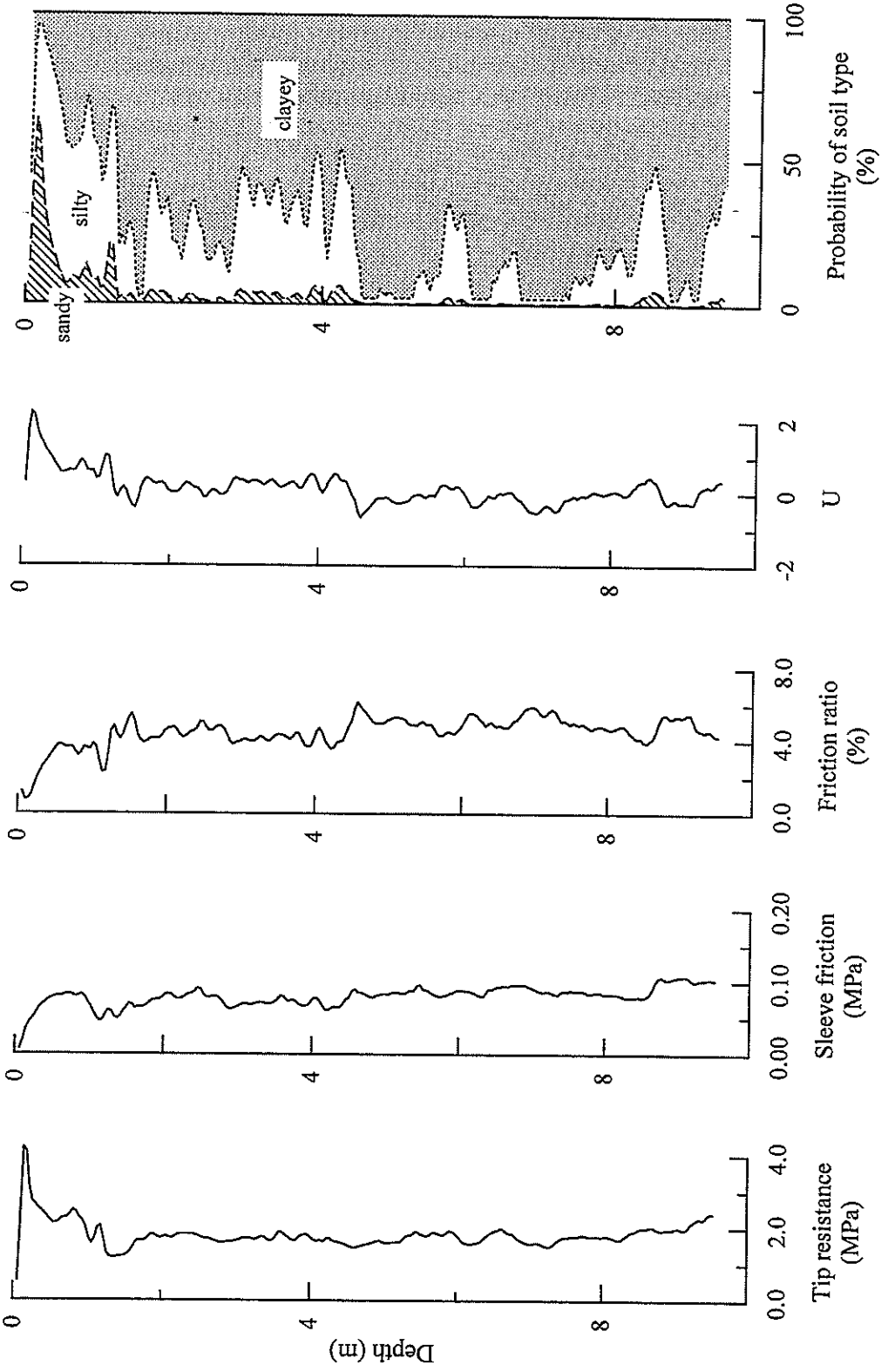

Figure 15
CPT soil classification at the Highland Road site

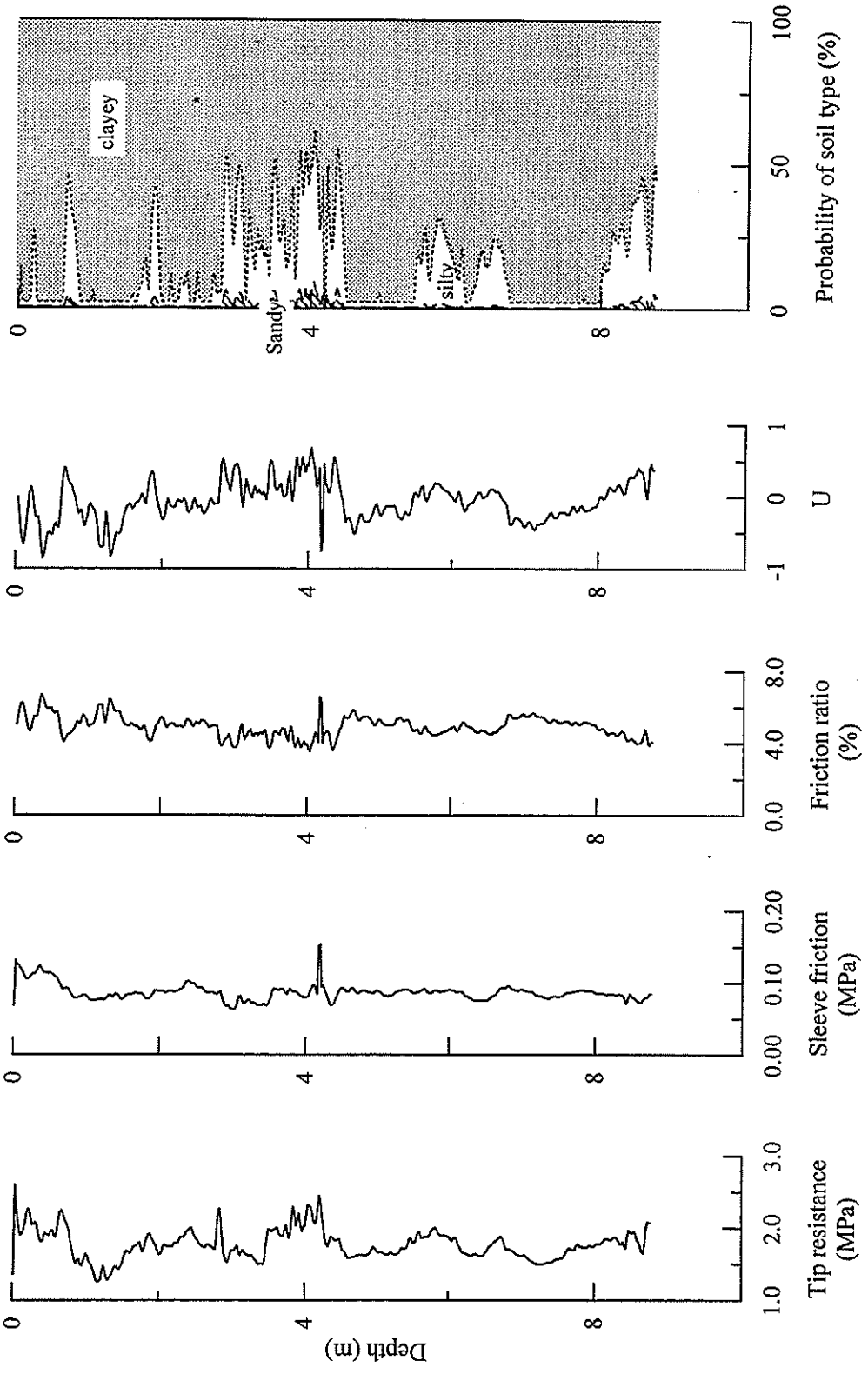

Figure 16
MCPT soil classification at the Highland Road site

and permanent deformations), calibration of new equipment, proof-testing site improvement techniques, geo-environmental problems, expansive clay problems, and foundation prototype testing. Sites qualifying in the theme areas were also screened based on a short list of site characteristics consisting of soil types, stratification, site size, interest and energy of site proponents, security, and long-term accessibility. For level I and II sites, detailed individual field and laboratory test results are accessible on the Internet to potential users and researchers, allowing them to review the quality and numerical details of the results.

The CIMCPT testing at the National Geotechnical Experimentation sites was conducted using the newly developed MPCPT. The MPCPT has the same frame size and geometric configuration of the MCPT, however, in order to accommodate the pressure transducer for pore pressure measurment, a circular cavity in the load cell component of the probe had to be created. CIMCPT results have indicated that this configuration tends to increase the moment sensitivity of the probe which leads to lower friction sleeve readings when tip resistance is higher than two MPa, especially in sandy soils. The sleeve resistance correction due to moment sensitivity was investigated by subjecting the minicone to a simple four-point bending test in the laboratory which resulted in the following empirical relationship based on statistical analysis:

$$f_s \text{ (corrected, MPa)} = f_s \text{ (measured, MPa)} + 0.015*[q_c \text{ (measured, MPa)}]^{1/2}$$

This correction is reflected in the MPCPT data presented for CIMCPT investigations performed at the National Geotechnical Experimentation Sites of Texas A&M University and University of Houston, Texas.

National Geotechnical Experimentation Site at Texas A&M University. The CIMCPT system was tested in the clay site, at Texas A&M University, Riverside Campus, College Station, Texas*[12], [13]*. This Level I site (with Site I.D.: TXAMCLAY) essentially consists of highly plastic, stiff clay (CH) up to a depth of 6.5 meters. Below this is a hard clay deposit 5.7 m thick, with high shrink-swell potential, over hard clay/clay shale 23 m thick. The ground water table is normally located between 7 and 7.3 m. The site has been used in the past by various investigators for a variety of tests on full-scale deep and shallow foundations, as well as for extensive in situ testing.

Figure 17 shows the test plan layout for the in situ tests performed at this site. In figure 17 the test numbers with prefix MPCPT are the miniature piezocone penetration tests, those beginning with letters CPT are the 10 cm^2 standard friction cone penetration tests. MPCPT profiles MPCPT-TXAM1, MPCPT-TXAM3 and MPCPT-TXAM4 are compared with the mean of CPT18 and CPT22

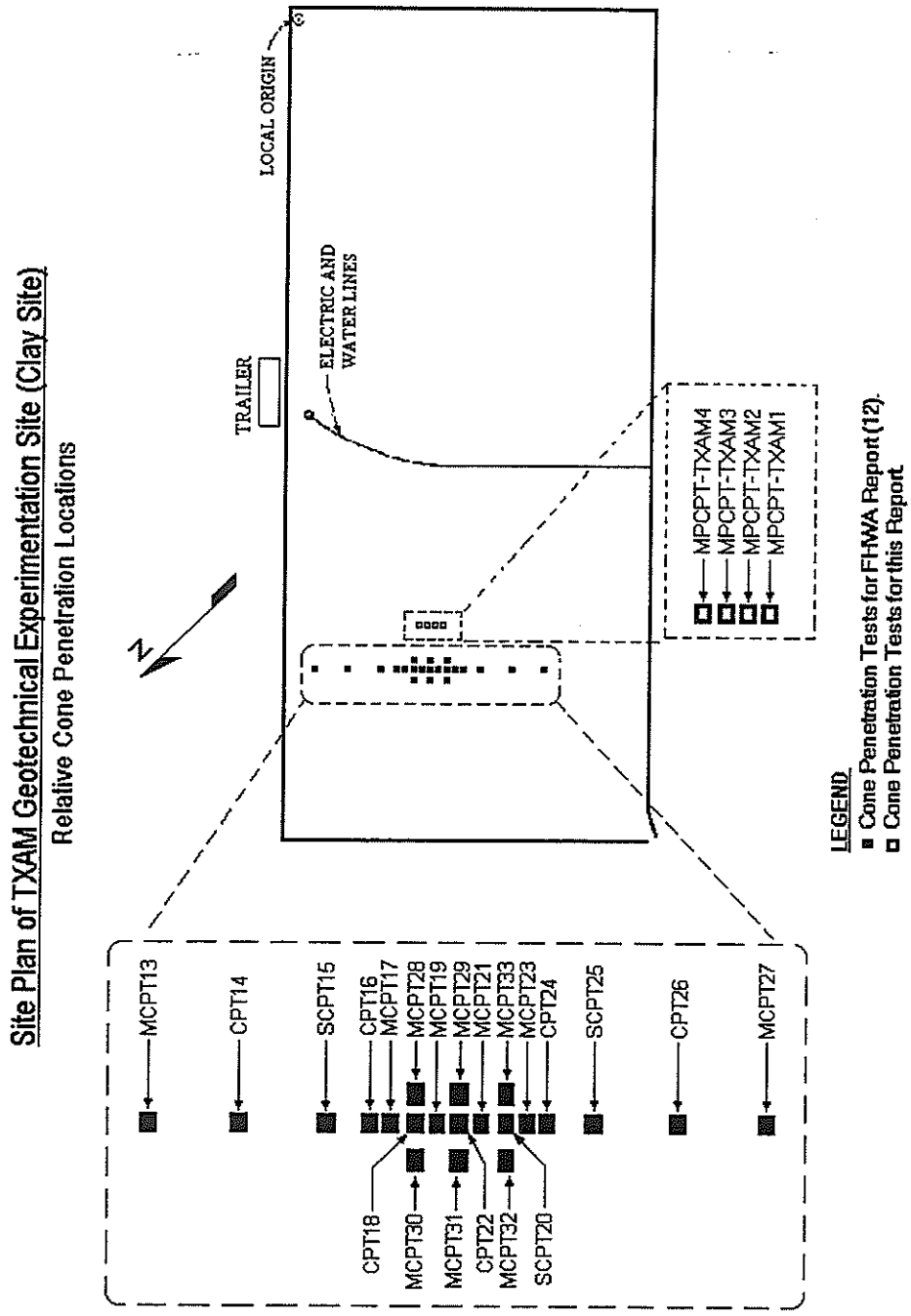

Figure 17
Location and test plan at the NGES in Texas A&M University

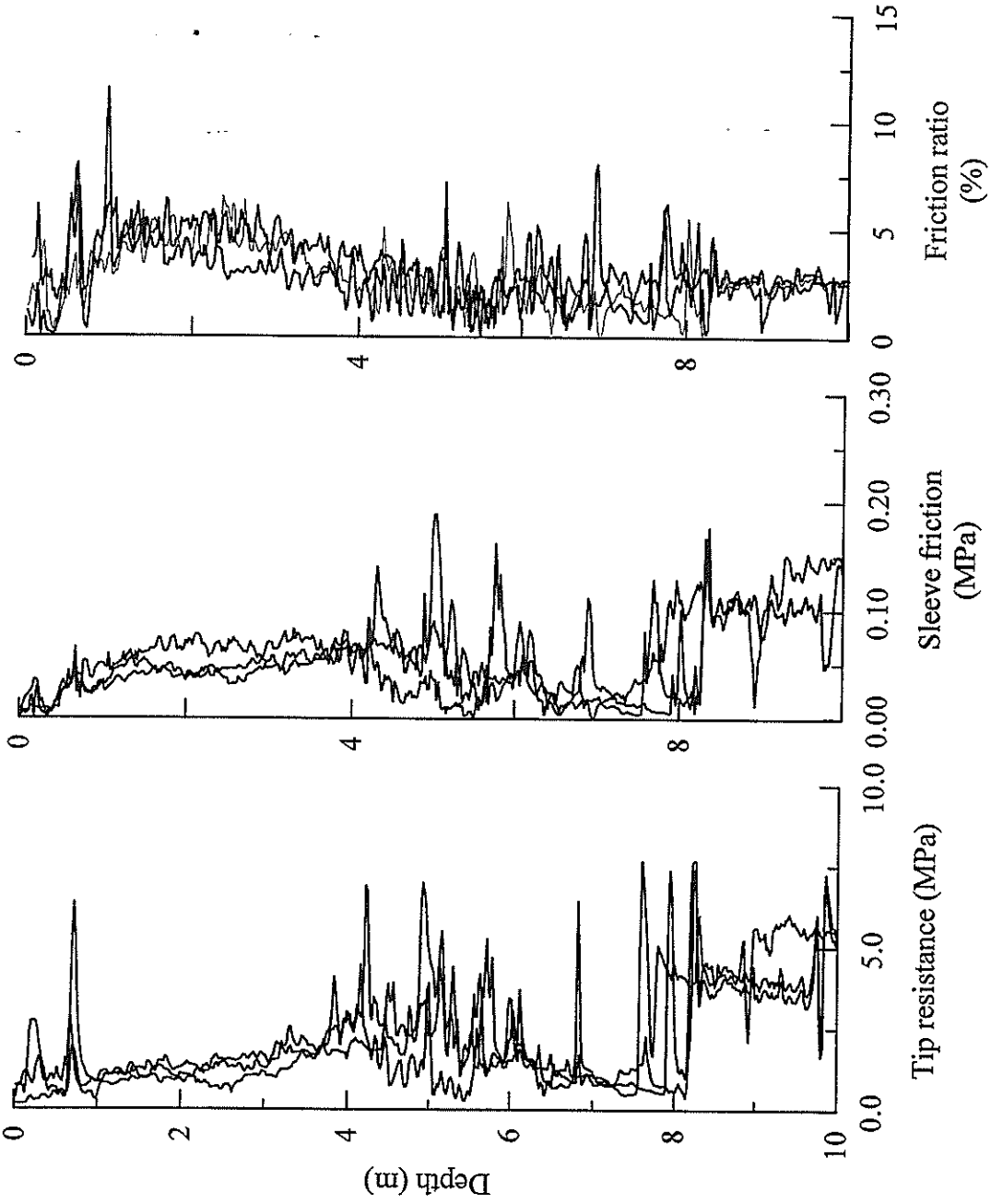

Figure 18
Comparison of penetration profiles of MPCPT-TXAM1, MPCPT-TXAM3, MPCPT-TXAM4 with the means of CPT18 and CPT22 at the NGES in Texas A&M University

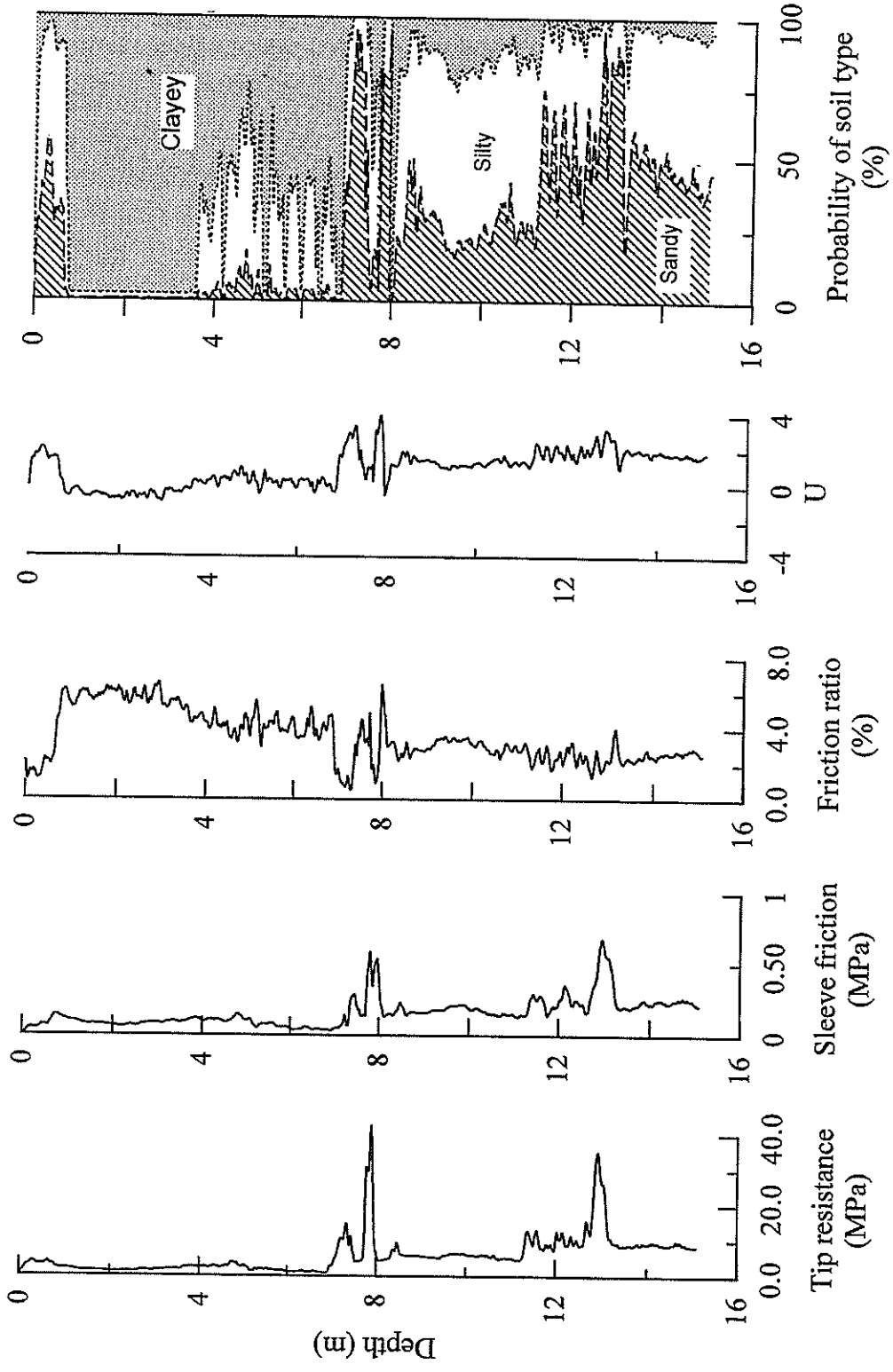

Figure 19
CPT Soil classification at the NGES at Texas A&M University

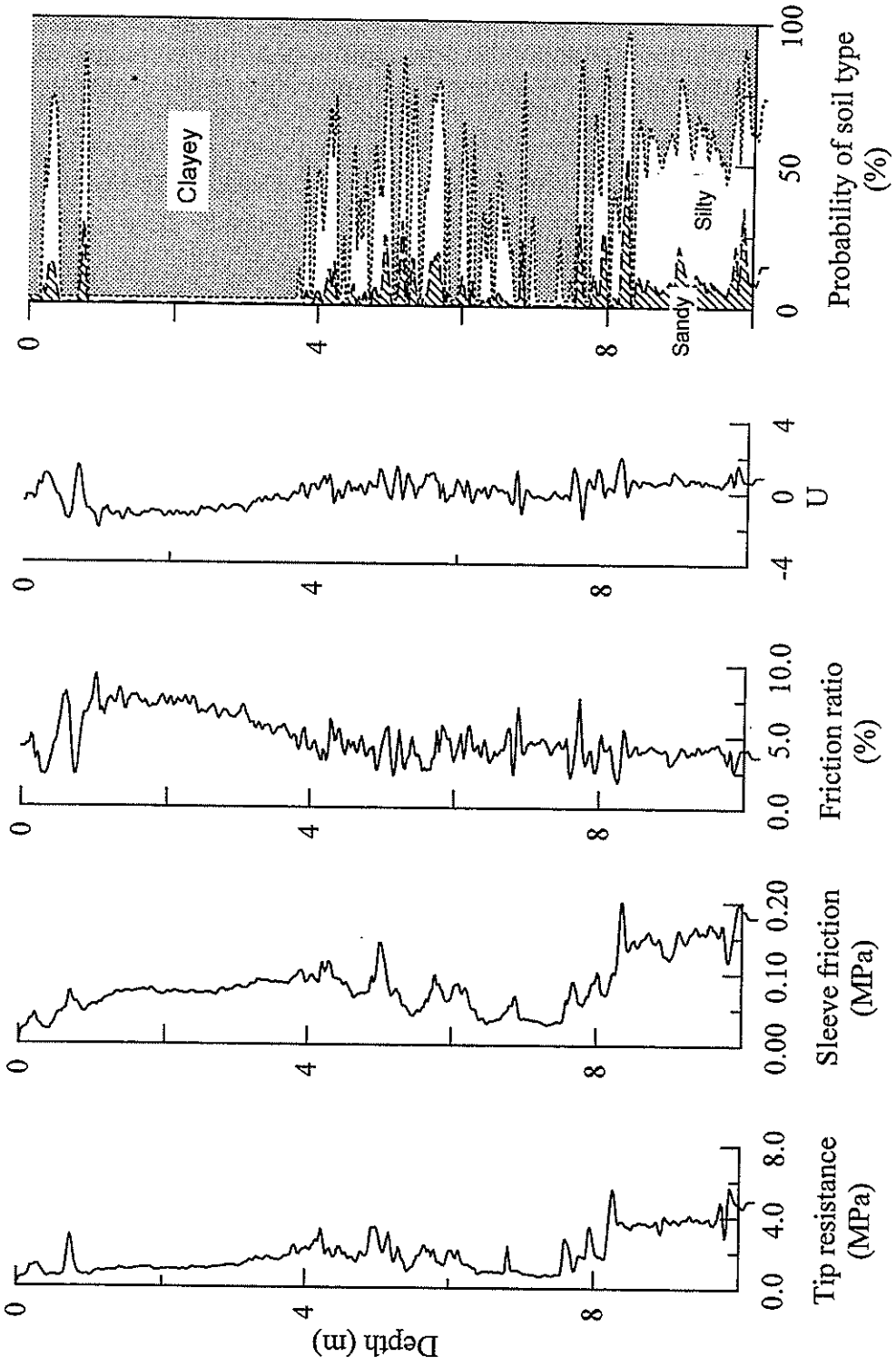

Figure 20
MCPT classification at the NGES in Texas A&M University

profiles in figure 18. Soil classification by the computerized probabilistic method [*10*] using the mean CPT profile and the mean MPCPT profile are shown in figures 19 and 20.

National Geotechnical Experimentation Site at University of Houston, Texas. The CIMCPT system was tested in the level II site at the University of Houston (figure 21). This site (with Site I.D.: TXHOUSTO) essentially consists of overconsolidated stiff to hard clay (CH to CL) up to a depth of 30 meters [*12*], [*14*]. The ground water table is located at 2.1 m. The site has been used in the past by various investigators for individual and group behavior of deep foundations. Extensive in situ and laboratory testing data are available.

Figure 22 shows the test plan layout for the in situ tests performed at this site. MPCPT profiles MPCPT-UH1, MPCPT-UH2, MPCPT-UH3 and MCPT-UH4 are compared with the mean CPT profile in figure 23. The mean CPT profile is the mean of C3, C4, C4A, and C5 (figure 22). Soil classification by the computerized probabilistic method *[10]* using the mean CPT profile and the mean MPCPT profile are shown in figures 24 and 25.

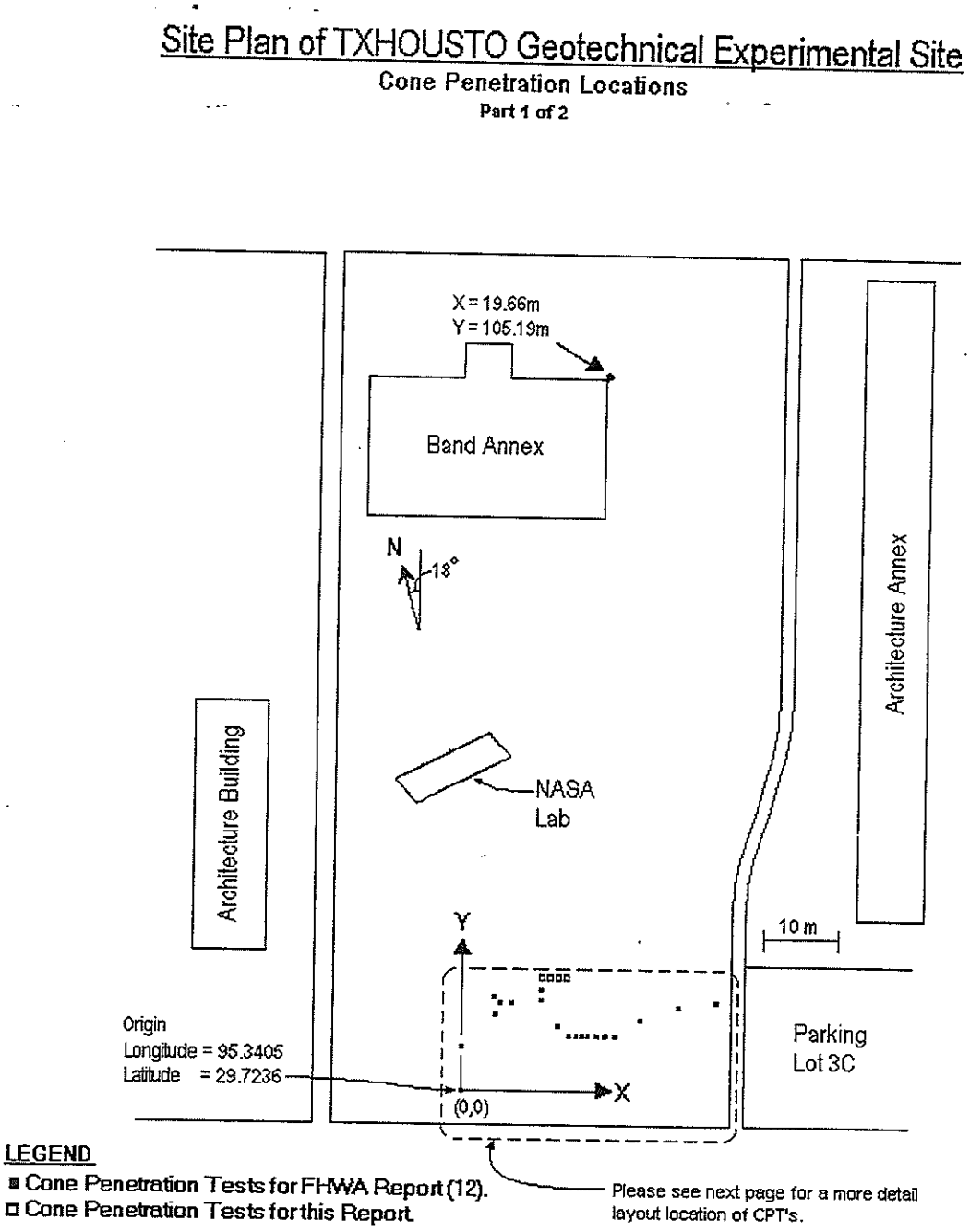

Figure 21
Location of the NGES in the University of Houston

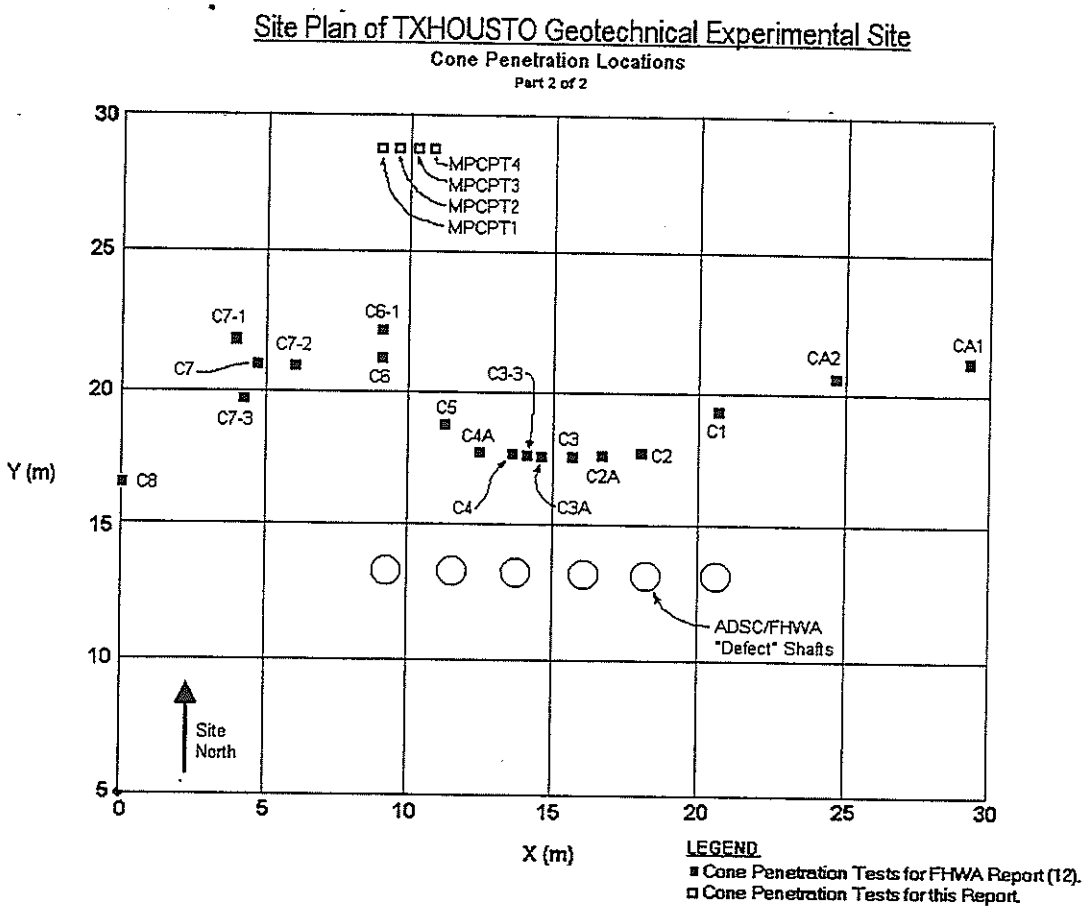

Figure 22
Test plan at the NGES in the University of Houston

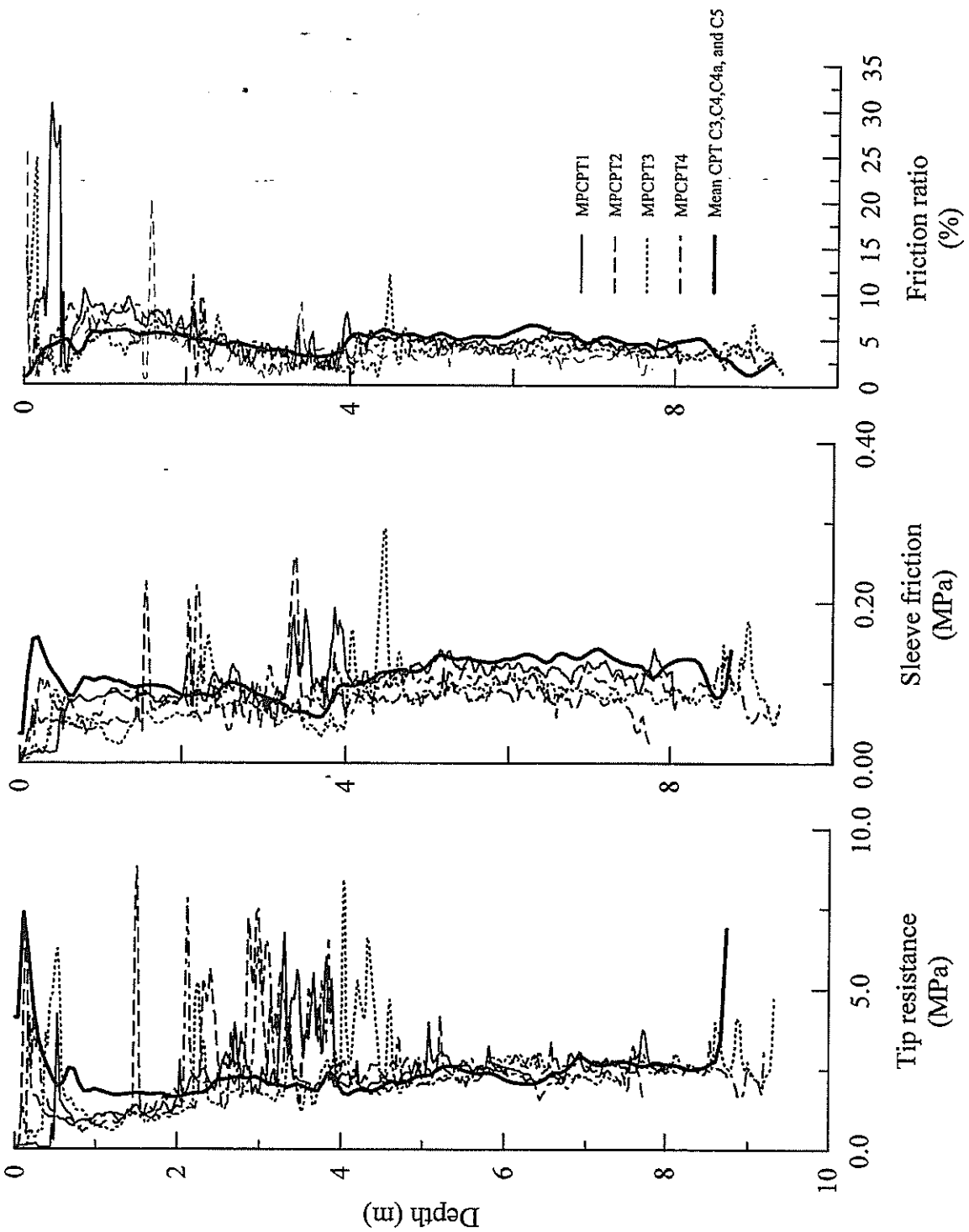

Figure 23
Comparison of the penetration profiles MPCPT-UH1, MPCPT-UH2, MPCPT-UH3 and MPCPT-UH4 with the mean of CPT profiles C3, C4, C4a, and C5 at the NGES in the University of Houston

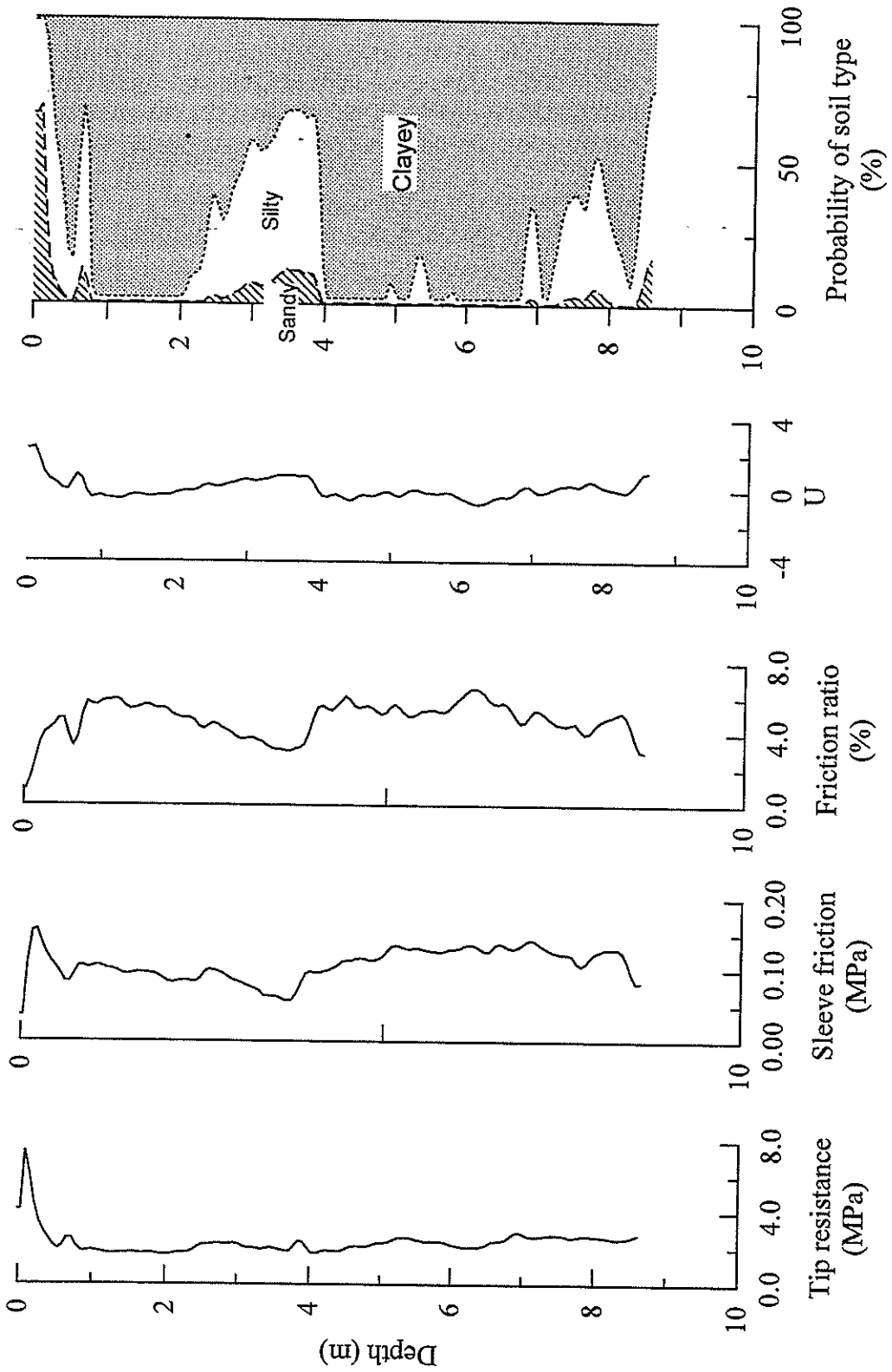

Figure 24
CPT soil classification at the NGES in the University of Houston

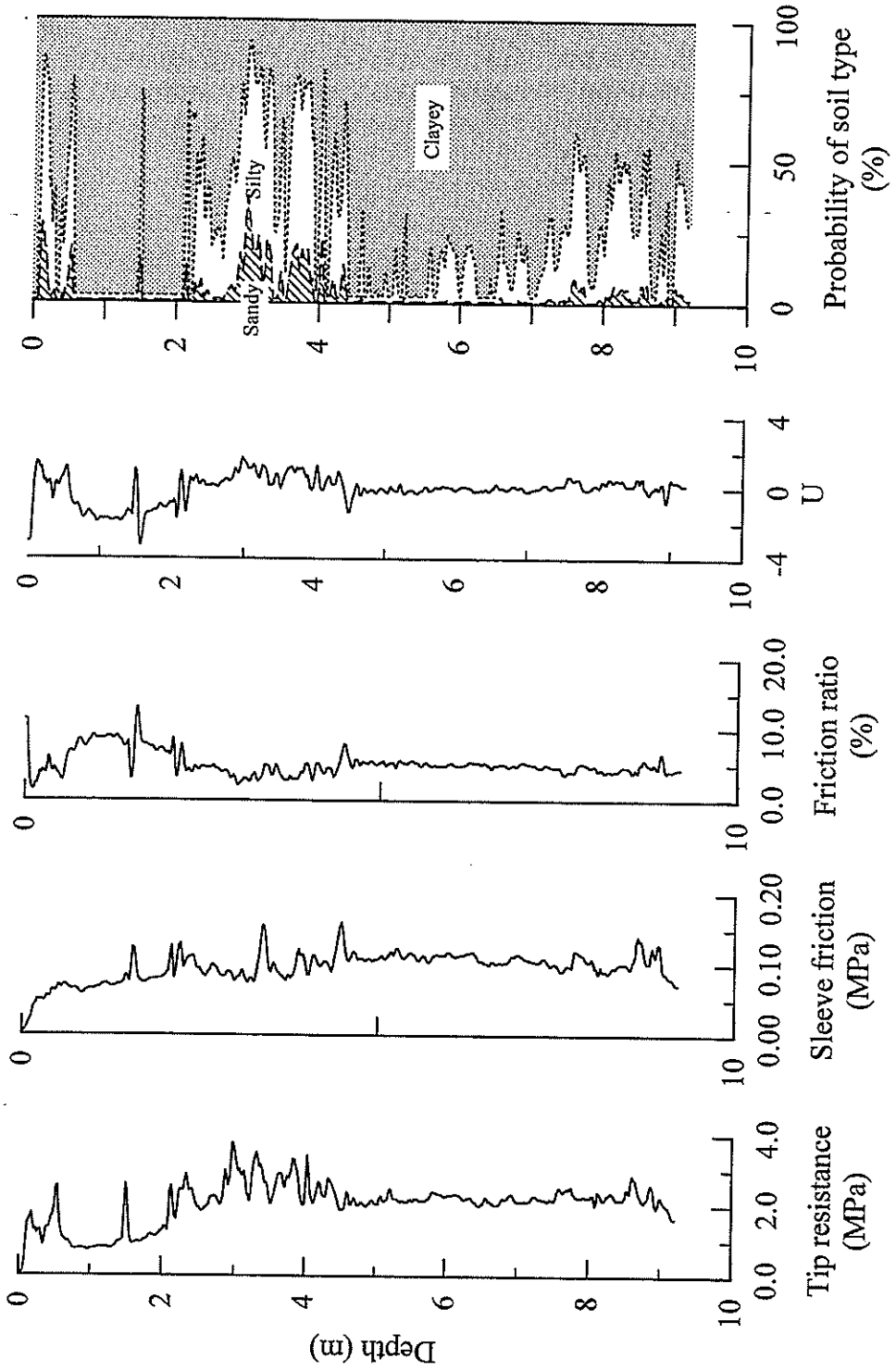

Figure 25
MPCPT soil classification at the NGES in the University of Houston

CONCLUSIONS

The validity of the CIMCPT system is readily verified by comparing the 2 cm^2 MCPT and MPCPT profiles with the 10 cm^2 CPT profiles performed at the Highland Road site in Baton Rouge, Louisiana, and at the National Geotechnical Experimentation Sites at Texas A&M University and the University of Houston (figures 13, 14, 18 and 23).

At each of these sites, comparison between the MCPT, MPCPT and CPT test profiles indicate "scale" (size and rate) effects. Table 1. summarizes the scale effects at the three test sites.

TABLE 1
Scale effects at the test sites

TEST SITE (Minicone Type)	Depths	$q_{c(2\ cm2)}/q_{c(10\ cm2)}$	$f_{s(2\ cm2)}/f_{s(10\ cm2)}$
Highland Road(1) Baton Rouge, LA	4.5 m - 7.5 m	1.10	0.89
NGES (2) Texas A&M Univ.	1.5 m - 7.0 m	1.13	0.91
NGES (2) Univ. of Houston	1.0 m - 8.5 m	1.11	0.87

(1) MCPT

(2) MPCPT (Sleeve resistance corrected for moment sensitivity)

The CIMCPT was field-tested at sites where the tip resistance of the sediments were less than eight MPa. The range of depths chosen for analyses at these sites are such that the probability of clay is about 75 percent, using the computerized probabilistic method for soil classification *[10]*. The scale effects are valid provided the probability of sand is less than ten percent.

A continuous intrusion miniature cone penetration test system (CIMCPT) was developed for transportation applications. CIMCPT was validated by testing at a Highland Road test site in Baton Rouge, Louisiana and also at two well documented, well referenced, National Geotechnical Experimentation Sites (University of Houston, and at the clay site, at Texas A&M University). Penetration profiles obtained using the 2 cm^2 cross-sectional area miniature cone penetrometers showed the existence of "scale effects" when compared to penetration profiles obtained using a 10

cm^2 cross-sectional area reference cone penetrometer. The average CIMCPT (MCPT and MPCPT) tip resistance was found to be 11 percent higher than that of the reference CPT. The average CIMCPT (MCPT and MPCPT) sleeve friction was found to be 11 percent lower than the reference CPT sleeve friction. These correction factors can be easily implemented into the computer programs for calculation of the tip resistance q_c and sleeve resistance, f_s. These trends in the results compare very well with previous research.

Penetration records of CIMCPT generally render much more detailed soil identification/classification profiles than penetration records obtained by CPT.

RECOMMENDATIONS

The CIMCPT system may be used for shallow and semi-deep subsurface investigations for highway subgrade characterization, embankment construction control, and for the assessment of ground improvement effectiveness for transportation applications.

The following recommendations are proposed for future enhancement of the equipment and for field testing:

1. The 2 cm^2 miniature cone penetrometer that has been implemented and tested in this project is a basic friction cone penetrometer, MCPT, which gives cone resistance and sleeve friction profiles with depth. With the inclusion of a pressure transducer and an inclinometer, the capabilities of MCPT were modified to measure pore pressures generated during cone penetration and the inclination during intrusion. It is recommended that the 2 cm^2 miniature "piezocone" penetrometer test (MPCPT) capability of the CIMCPT system be further developed for locating the depth of the ground water table, detailed profiling of soil stratigraphy, and for estimating flow and consolidation characteristics of fine grained soils from the dissipation of excess pore pressure data.

2. The inclusion of the pore pressure transducer and the inclinometer in the limited space of the MPCPT probe requires a hole in the load cell configuration thus increasing the moment sensitivity. This sensitivity tends to decrease friction sleeve readings in stiffer layers where tip resistance in excess of 2 MPa are encountered (i.e. sandy soils). It is recommended to modify the sleeve friction load cell design to strengthen the structural integrity of the probe to remedy this hardware problem.

3. More in situ calibration tests in well-characterized and well-documented sites should be conducted to further refine and correlate MCPT and MPCPT data with engineering soil properties (such as resilient modulus, shear strength, deformation, consolidation, and flow characteristics) needed for highway design and construction control.

REFERENCES

1. Tumay, M.T., *Implementation of Louisiana Electronic Cone Penetrometer System (LECOPS) for Design of Transportation Facilities*, Executive Summary, FHWA/LA Report No. LA - 94/280 A&B, 1994, p.118.

2. Tumay, M. T., and Kurup, P. U., *Calibration and Implementation of Miniature Electronic Cone Penetrometers for Road and Highway Design and Construction Control*, LTRC State Project No. 736-13-0036,1997, p.71.

3. de Lima, D. C., *Development, Fabrication and Verification of the LSU In Situ Testing Calibration Chamber*. Ph.D. Dissertation, Louisiana State University, Baton Rouge, LA, 1990.

4. de Lima, D. C., and Tumay, M. T., "Scale Effects in Cone Penetration Tests." *Proc., Geotechnical Engineering Congress*, GT Div/ASCE, Special Publication No. 27, Boulder, CO, 1991, pp. 38-51.

5. Tumay, M. T., and de Lima, D. C., *Calibration and Implementation of Miniature Electronic Cone Penetrometer and Development, Fabrication and Verification of the LSU In-situ Testing Calibration Chamber (LSU/CALCHAS)*, LTRC/FHWA Report No. GE-92/08, 1992, 240 p.

6. Kurup, P.U., and Tumay, M.T., "Calibration of a Miniature Cone Penetrometer for Highway Applications" Transportation Research Record No. 1614: In Situ Testing Devices and Strain Measurements, 1998, pp. 8-14.

7. Tumay, M.T., Kurup, P.U. and Boggess, R.L., "A Continuous Feed Electronic Miniature Cone Penetrometer System for Site Characterization," Geotechnical Site Characterization, (eds. Robertson, P.K. and Mayne, P.W.), A.A. Balkema, Rotterdam, Proceedings of the First International Conference on Site Characterization (ISC'98), Atlanta, April 19-22, 1998, Vol. 2, pp. 1183-1188.

8. Arman, A., and McManis, K. L., "The Effect of Conventional Soil Sampling Methods on the Engineering Properties of Cohesive Soils in Louisiana." *Engineering Research Bulletin No. 117*, Louisiana State University, Baton Rouge, Louisiana, 1977, 294 p.

9. Chen, B. S., and Mayne, P. W., *Profiling the Overconsolidation Ratio of Clays by Piezocone Tests*. Report No. GIT-CEEGEO-94-1, Georgia Tech Research Corporation, Georgia Institute of Technology, Atlanta, Georgia, 1994, p. 279.

10. Zhang, Z., and Tumay, M. T., "Statistical to Fuzzy Approach Toward CPT Soil Classification," *Journal of Geotechnical & Geoenvironmental Engineering*, ASCE, Vol. 125, No. 3, 1999, pp. 179-186.

11. DiMillio, A.F., and Prince, G., "National Geotechnical Experimentation Sites," *Public Roads*, FHWA, U.S. DOT, Vol. 57, No. 2, pp 17-22.

12. Tumay, M. T., "In Situ Testing at National Geotechnical Experimentation Sites - Phase 2," Contract DTFH61-97-P-00161, Final Report, U.S. Department of Transportation, Federal Highway Administration, February 1998, 154 pp + CD-ROM.

13. Simon, P.A., and Briaud, J-L., " The National Geotechnical Experimentation Sites at the Texas A & M University: Clay and Sand," NGES-TA&M-006, December 1996, Texas A & M University, College Station, Texas.

14. O'Neill, M.W., Professor of Civil Engineering, University of Houston, Personal Communication, 1998.

APPENDIX 1

1a. Listing of the GPS program code

1b. Typical output from the Global Positioning System

1a. Listing of the GPS program code:

```
/* GPS MODULE ************************************************************/
/*                                                                       */
/* by Ramya Sarma                                                        */
/*                                                                       */
/* This module uses Borland C++ function bioscom to initialize com       */
/* port and collect data from GPS on COM 2.  Ten latitude and             */
/* longitude values are collected and averaged.  GPS correction           */
/* reception is verified.  If corrections are not present, the            */
/* module notifies operator and asks if another collection should         */
/* occur.                                                                */
/*************************************************************************/

/* The following variables and functions are responsible for receiving
   GPS data and convert them into suitable form to be displayed in
   th computer screen */
#define COM2 1
#define COM1 0
#define DATA_READY 0x100
#define TRUE 1
#define FALSE 0
#define SETTINGS (0xE0|0x00|0x00|0x03)
struct gpsreading {
        char reading[100];
        char slatitude[30];
        char slongitude[30];
        float flatitude;
        float flongitude;
        char fix;
        } gpsdata[10];
char latitudedirection,longitudedirection;
int gpsnumber=0;
int uncorrected=FALSE;
void gps(void)
{
        int count = 0;
        char ch;
        /*Declare variables*/
        int in, out, status, DONE=FALSE;
        int gpscount=0;
        char format[7];
        char c;
        /*set the communications parameters*/
        bioscom(0,SETTINGS,COM2);
        gpsnumber=0;
        printf("\n\n");
        printf("                                GPS Readings");
        printf("\n");
        while(!DONE) {
                status=bioscom(3,0,COM2);
                if ((status & DATA_READY))
                {
                        if(((out=bioscom(2, 0, COM2) & 0x7F) != 0) && (out!='\n') ){
```

```
                        gpsdata[gpscount].reading[count]=out;
                        count++;
                        if (count==71) {
                                if ((strncmp("$GPGGA",gpsdata[gpscount].reading,6)==0)) {
                                        gpsdata[gpscount].reading[count]='\0';
                                        gpsnumber++;
                                        printf("\n#%d:
%s",gpsnumber,gpsdata[gpscount].reading);
                                        count=0;
                                        gpscount=gpsnumber;
                                        delay(2000);
                                        DONE=FALSE;
                                        if (gpsnumber==10) {
                                                DONE=TRUE;
                                                getlatlong();
                                                getaverage();
                                                return(1);
                                        }
                                }
                        }
                }
        }
}
/* Subroutine to display latitude and longitude*/
getlatlong()
{
 int i=0;
 char *promptstring;
 char degrees[3],minutes[7];
 int count=0;
 int gpscount=0;
        for (gpscount=0; gpscount<=gpsnumber-1; gpscount++) {
                count=0;
                /*get the latitude reading*/
                for (i=14;i<=21;i++) {
                        gpsdata[gpscount].slatitude[count]=gpsdata[gpscount].reading[i];
                        count++;
                }
                latitudedirection=gpsdata[gpscount].reading[23];
                /*make it a string*/
                gpsdata[gpscount].slatitude[count]='\0';
                /*convert slatitude into a float and fill the array element*/
                gpsdata[gpscount].flatitude=atof(gpsdata[gpscount].slatitude);
                /*reinitialize count to get the longitude reading*/
                count=0;
                /*get the longitude string*/
                for (i=26;i<=33;i++) {
                        gpsdata[gpscount].slongitude[count]=gpsdata[gpscount].reading[i];
                        count++;                }
                longitudedirection=gpsdata[gpscount].reading[35];
                /*make it a string*/
                gpsdata[gpscount].slongitude[count]='\0';
                /*convert slongitude into a float and fill the array element*/
```

```
                gpsdata[gpscount].flongitude=atof(gpsdata[gpscount].slongitude);
                /*store the fix*/
                gpsdata[gpscount].fix=gpsdata[gpscount].reading[39];
                /*check for corrected fix*/
                if (gpsdata[gpscount].reading[37] != '2')
                        uncorrected=TRUE;
                else uncorrected=FALSE;
        }
        /* get the latitude and lonitude direction*/
        return;
}

getaverage()
{
float avglatitude=0.0, avglongitude=0.0;
char *stemplatitude, *stemplongitude;
int ilatdigits=7;
int ilongdigits=8;
int idec,isign;
int count=0;
int gpscount=0;
char c;
        /*get the average of the ten latitude readings obtained in flatitude*/
        for (gpscount=0;gpscount<=gpsnumber-1;gpscount++) {
                avglatitude=avglatitude+gpsdata[gpscount].flatitude;
        }
        avglatitude=avglatitude/gpscount;
        /*convert the latitude into a string*/
        stemplatitude= fcvt(avglatitude, ilatdigits, &idec, &isign);
        /*get the degree component - the first two characters*/
        count=idec-2;
        strncpy(sfinallatitude,stemplatitude,count);
        sfinallatitude[count]='\0';
        /*attach "deg" string to it*/
        strcat(sfinallatitude," deg ");
        count=strlen(sfinallatitude);
        /* get the minute component*/
        sfinallatitude[count]= stemplatitude[2];
        count++;
        sfinallatitude[count]=stemplatitude[3];
        count++;
        sfinallatitude[count]='.';
        count++;
        sfinallatitude[count]= stemplatitude[4];
        count++;
        sfinallatitude[count]=stemplatitude[5];
        count++;
        sfinallatitude[count]= stemplatitude[6];
        count++;
        sfinallatitude[count]='\'';
        count++;
        /*get the direction*/
        sfinallatitude[count]=latitudedirection;
        count++;
```

```
        sfinallatitude[count]='\0';
        /*get the average of the ten longitude readings obtained in flongitude*/
        for (gpscount=0;gpscount<=gpsnumber-1;gpscount++) {
                avglongitude=avglongitude+gpsdata[gpscount].flongitude;
        }
        avglongitude=avglongitude/gpscount;
        /*convert the longitude into a string*/
        stemplongitude= fcvt(avglongitude, ilongdigits, &idec, &isign);
        /*get the degree component - the first two characters*/
        count=idec-2;
        strncpy(sfinallongitude,stemplongitude,count);
        sfinallongitude[count]='\0';
        /*attach "deg" string to it*/
        strcat(sfinallongitude," deg ");
        count=strlen(sfinallongitude);
        /* get the minute component*/
        sfinallongitude[count]= stemplongitude[2];
        count++;
        sfinallongitude[count]=stemplongitude[3];
        count++;
        sfinallongitude[count]='.';
        count++;
        sfinallongitude[count]= stemplongitude[4];
        count++;
        sfinallongitude[count]=stemplongitude[5];
        count++;
        sfinallongitude[count]= stemplongitude[6];
        count++;
        sfinallongitude[count]='\'';
        count++;
        /*get the direction*/
        sfinallongitude[count]=longitudedirection;
        count++;
        sfinallongitude[count]='\0';
        /*print the average latitude and longitude*/
        printf("\n\n");
        printf("\n\n            Average Latitude:       %s",sfinallatitude);
        printf("\n             Average Longitude:      %s",sfinallongitude);

       printf("\n\n\n\n");
       gotoxy(1,24);
       if (uncorrected==FALSE || uncorrected==TRUE)
       {
               if (uncorrected==TRUE)
               {
                       puts("The gps data contains uncorrected values. Proceed to redetermine
the location?");
                       do
                       {
                       gotoxy(80,24);
                       c=getch();
                       if (toupper(c)=='Y') gpsmain();
                       else return;
                       } while(toupper(c)!='Y' || toupper(c)!='N');
```

```
                }
                else
                {
                        puts("The gps data contains corrected values. Proceed to redetermine the
location?");
                        do
                        {
                        gotoxy(78,24);
                        c=getch();
                        if (toupper(c)=='Y') gpsmain();
                        else return;
                        } while(toupper(c)!='Y' || toupper(c)!='N');
                }
        }


 }

/*subroutine to create the output window*/
makewindow(left,top,right,bottom,text,back)
int left,top,right,bottom,text,back;
{
        window(left,top,right,bottom);
        textcolor(text);
        textbackground(back);
        return;
}


gpsmain()
{
int c;
int text=15;
int back=4;

        clrscr();

        /*make a window*/
        makewindow(1,1,80,25,text,back);
        clrscr();

        /*prompt the user to get the gps reading*/
        /*gotoxy(5,12);
        puts("Press G to get the GPS reading or Esc to quit.");

        do
        {
                gotoxy(60,12);*/
                /*get a keystroke from the keyboard*/
                /*c=(getch());
                gotoxy(60,12);
                putch(c);
                delay(500);
                if (toascii(c)!=27 || toascii(c)!=71)
```

```
        {
                gotoxy(60,12);
                cputs(" ");
        } */
        /*if Esc is pressed*/
        /*if (toascii(c)==27) {*/
                /*quit the program*/
                /*return;
        }*/
        /*if G or g is pressed*/
        /*if(toascii(toupper(c))==71) { */
                text=15;
                back=1;
                makewindow(1,1,80,15,text,back);
                clrscr();
                /*run the gps module*/
                gps();
/*      }

}while (c!='g' || c!='G' || toascii(c)!=27);*/}
```

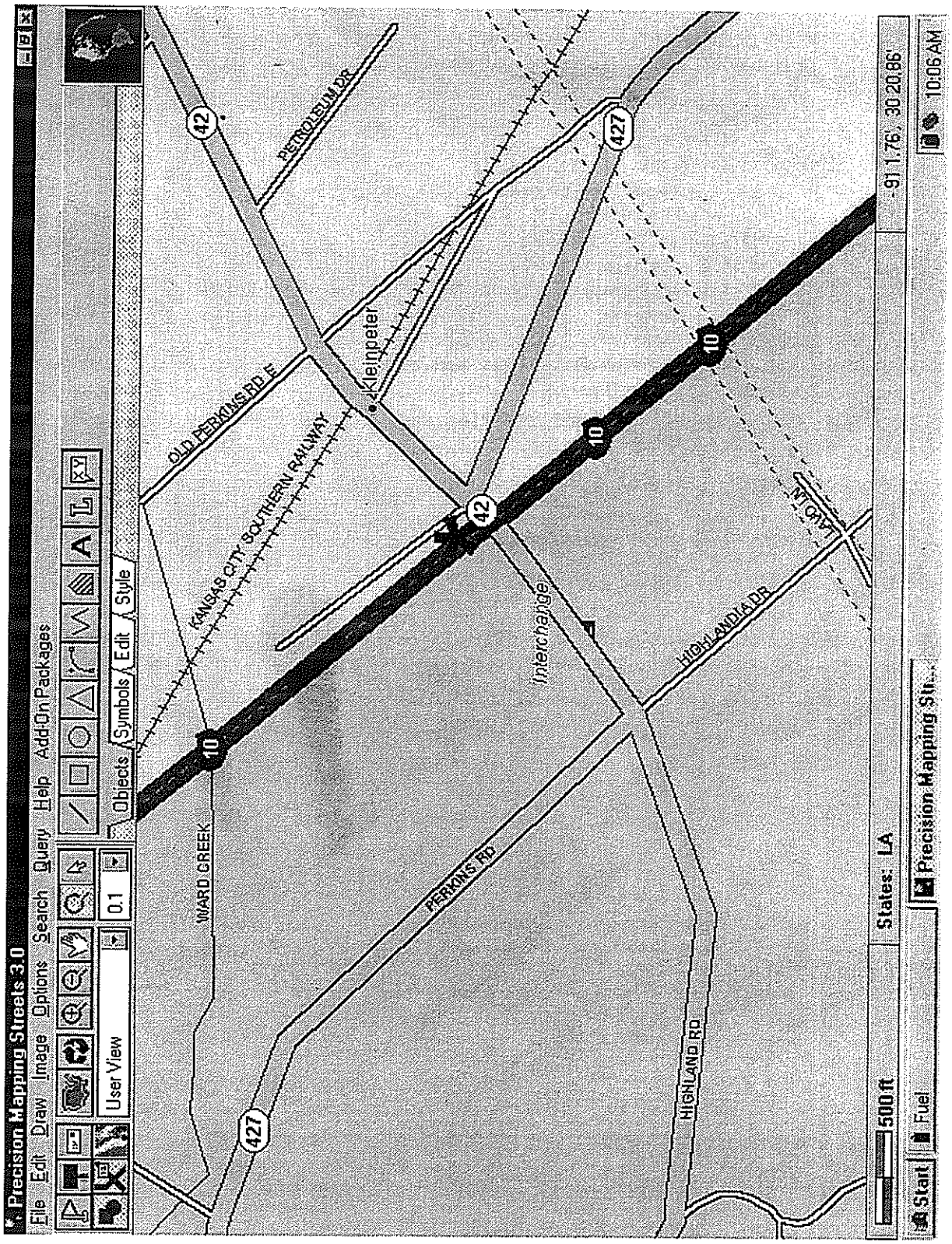

1b. Typical output from the Global Positioning System

APPENDIX 2 CD-ROM (1)

(a) Continuous Intrusion Miniature Cone Penetration Test (CIMCPT) 9:00 min.
(b) Research Vehicle for Geotechnical In Situ Testing & Support (REVEGITS) 4:30 min.

This public document is published at a total cost of $1741.18. Four hundred copies of this public document were published in this first printing at a cost of $1191.18. The total cost of all printings of this document including reprints is $1741.18. This document was published by Louisiana State University, Graphic Services, 3555 River Road, Baton Rouge, Louisiana 70802, to report and publish research findings of the Louisiana Transportation Research Center as required by R.S.48:105. This material was printed in accordance with standards for printing by state agencies established pursuant to R.S.43:31. Printing of this material was purchased in accordance with the provisions of Title 43 of the Louisiana Revised Statutes.

The investigation uses three different materials: ordinary concrete, steel fibrous concrete, and rapid patch material. To study as many performance parameters as possible, the following experiments are conducted:

1. Uniaxial strength of patching material
2. Strength of patching material under biaxial state of stress
3. Bond strength of patched cylinder specimens
4. Shear test of a repaired pavement joint

The design and experimental procedure adopted for these experiments are discussed in detail in the following sections. With these tests and by appropriate interpretation of the test data, a more rigorous evaluation of the material and hence, a more confident assessment of its performance in a specific repair task can be made.

As mentioned before, most materials laboratories in research centers have not adopted the recent advances in laboratory test techniques. It would be easy to recommend sophisticated multiaxial computer-servocontrolled electro-hydraulic test equipment. A meaningful utilization of such equipment, however, would be possible in only a handful of research institutions. But to be successful, modernization in testing and formulating material response for design should be carried out so that the existing standard universal testing machines may be employed with only minor changes. The specimens should be more informative than the currently recommended cylinder and beam tests. This task requires perhaps greater ingenuity and effort than conducting advanced research on materials science with the new sophisticated test and computational equipment.

In the present study, the experimental work is carried out using the "LTRC" concrete test facilities. The existing 400-kip universal testing machine in this laboratory is used as the main test equipment.

An interesting feature of the experimental program will be its overall planning and design. It will be conducted based on accompanying analytical verification. The specimens were designed, fabricated, and cured based on prior analytical studies so that the specimens and their testing will simulate conditions existing within the repaired rigid pavement sections as closely as possible, and certainly closer than the standard cylinder test. On the other hand, the instrumentation and loading were designed to provide response information which will be compatible with the anticipated response of material within a pavement. Studying the material response recovered through this a concept as opposed to the standard ASTM test will lead to useful information regarding ways to improve material testing to answer the needs for special applications, instead of conducting a standard material test for all types of structures and material.

After testing repair material, its stress-strain relation will be expressed using a simple constitutive model. In the analytical part of the study, an attempt will be made to select appropriate models from the available constitutive models for regular concrete and modifying them to reflect the response of tested material.

applied tensile stress to the actual biaxial cracking strength of concrete in such regions, the expected equivalent wheel load factor (EWLF) to cause failure of the repaired slab will be greatly decreased. Such examples are clear indications that for realistic assessment of properties of brittle repair materials, such stress conditions should be given particular attention during testing. Considering the effect of other stress inducing factors, such as dowel bars at the repaired joints, it becomes clear that the evaluation of performance of repair materials based on the parameters obtained from uniaxial standard tests can lead to serviceability problems at certain critical locations within rigid pavements. Recurrence of cracking and spalling of concrete in the repaired regions of rigid pavements may be avoided by a better understanding of the behavior of the repair material under the complex stress states which occur at those regions, and by improving the material application procedures accordingly.

In order to simulate such effects, a simplified biaxial testing method for brittle repaired materials such as plain concrete, fiber concrete, and rapid patch material, was introduced and devised with the following objectives:

(a) To carry out the test method such that the influence of tension-compression state of stress can be studied

(b) To design specimens and testing procedure to yield the most reliable information with the simplest, most practical testing which may be routinely carried out in a concrete material test laboratory equipped to conduct standard ASTM tests

(c) To design the testing set-up such that different specimens of brittle repair material can be tested under various ratios of tension-compression stresses and the results can be compared with those of previous studies to verify the validity of the proposed simplified testing procedures

(d) To instrument specimens to make it possible to develop stress-strain curves and biaxial failure envelopes

In order to simplify procedures to produce a tension-compression state of stress, it may be possible to use the existing standard universal testing machine with some modification in order to apply tension to the specimen.

Unfortunately, most of the experimental investigations on the concrete behavior have employed rather sophisticated and costly testing apparatus and data acquisition system which are not normally available in testing laboratories of the state highway department. In this study, a simplified biaxial testing method for brittle repair materials was introduced. The proposed simplified testing procedure was carried out such that the existing standard universal testing machines could be employed along with hydraulic jacks in the orthogonal direction. Details of the biaxial testing set-up are shown in Figure 2.3.

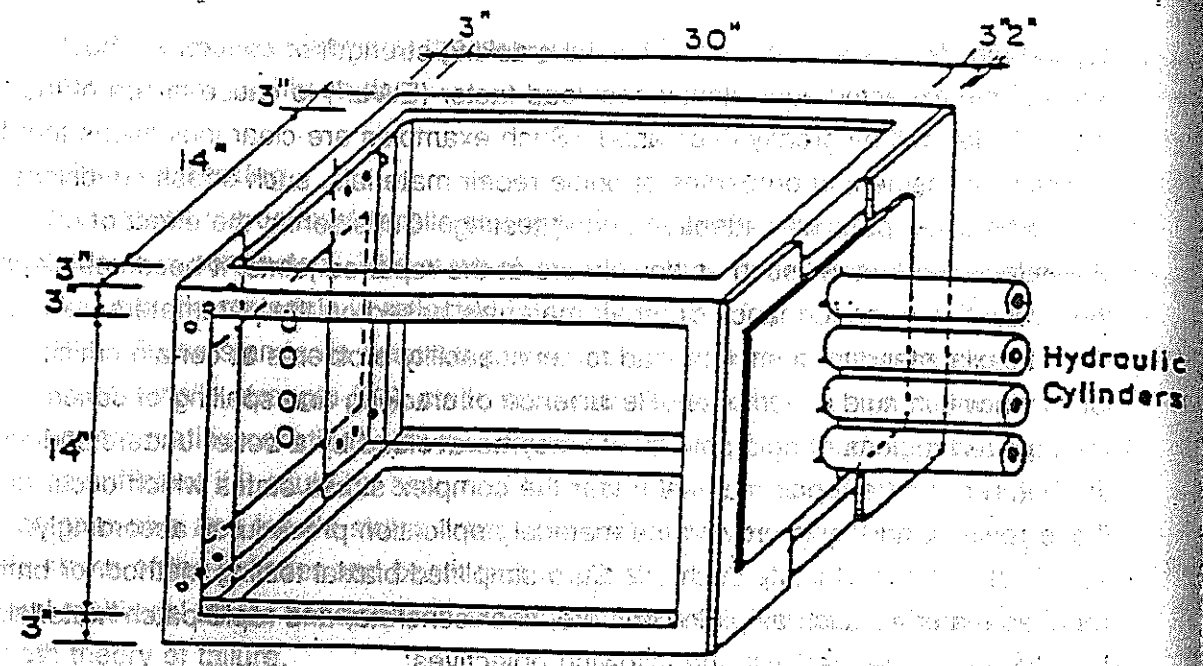

(a) Details of the biaxial test set-up

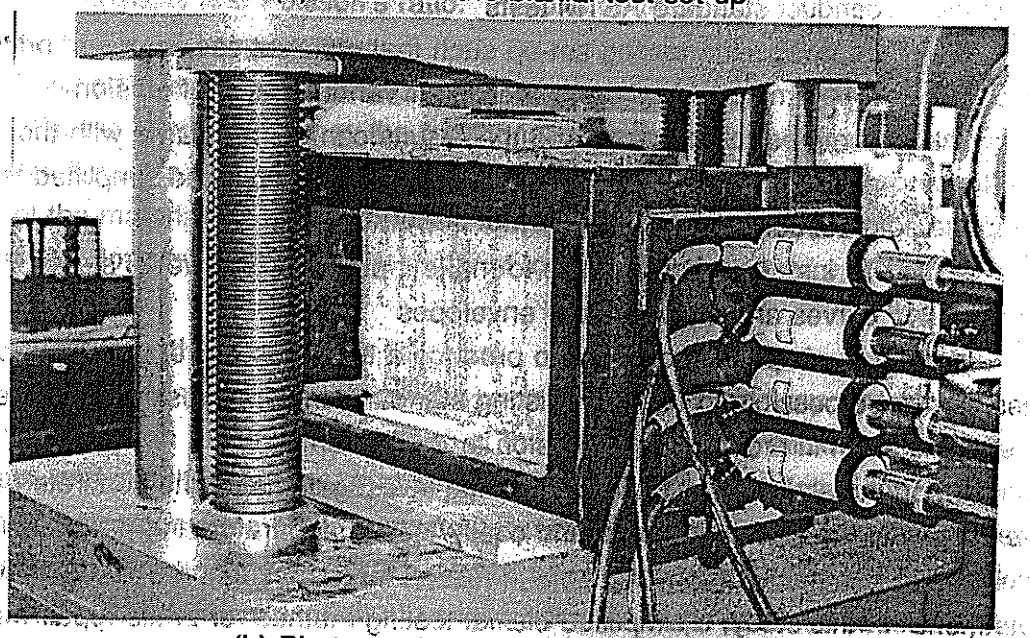

(b) Photograph of the biaxial test set-up

Figure 2.3
Set-up for biaxial test

In order to prevent a brittle failure upon cracking, the specimen is slightly reinforced. This will permit the load to be increased after cracking and hence strain measurements up to failure may be possible to record. The test specimen shown in Figure 2.4 includes wire mesh to ensure transfer of tension to the specimen in the event cracking occurs outside the gaged region. The vertical bars were introduced to facilitate placement of the horizontal bars during casting.

Alignment of the testing frame and the specimen is very important, otherwise unstable conditions will arise. Therefore, the following factors were considered:

1. The strands in the specimen in Figure 2.4 were kept horizontal during casting, curing, and testing.
2. The opposite side of the hydraulic jacks in the testing machine in Figure 2.3 was made movable so that alignment can be adjusted easily.

To ensure transfer of uniform compression load to the specimen, three plates (1" thick each) were used as loading plates. Moreover, one plate of teflon was placed on the top and one on the bottom of the specimen to eliminate friction between specimen surface and loading plate.

In order to apply a biaxial state of stress to normal concrete material, experimental specimens similar to the one shown in Figure 2.4 were cast, cured, and tested. Seventy-four specimens were used to assess the employed materials' biaxial properties. Half of them were cured under controlled conditions in the laboratory and tested after 28 days. The other half were cured under normal temperature and moisture conditions for 3 months. In addition, twelve standard ASTM beams, twelve cylinders for compressive strength and six cylinders for splitting tensile tests were used to determine the uniaxial properties at the time of biaxial testing.

Additional biaxial tests were conducted on specimens of regular concrete patched with different shapes and depths of a repair material, shown in Figure 2.5. The patched specimens were cured under different conditions and for varying periods of time. Different ratios of biaxial stress and predominantly tension-compression stresses were applied to the patched regions to investigate the performance of the repair materials within rigid pavement slab subjected to surface loading conditions. The patching depths were also varied to better represent the actual field conditions for the repaired pavements. Fifty specimens, similar to the one shown in Figure 2.4 with patching material, were tested in this phase of the study.

2.4.3 Bond Strength

Concrete repairing operations commonly include removing damaged concrete and replacing it with patches and overlay materials. In repair and rehabilitation of existing rigid pavements, compatibility and bonding characteristics of the repair material with the parent are significant factors that should be considered in selecting the repair material.

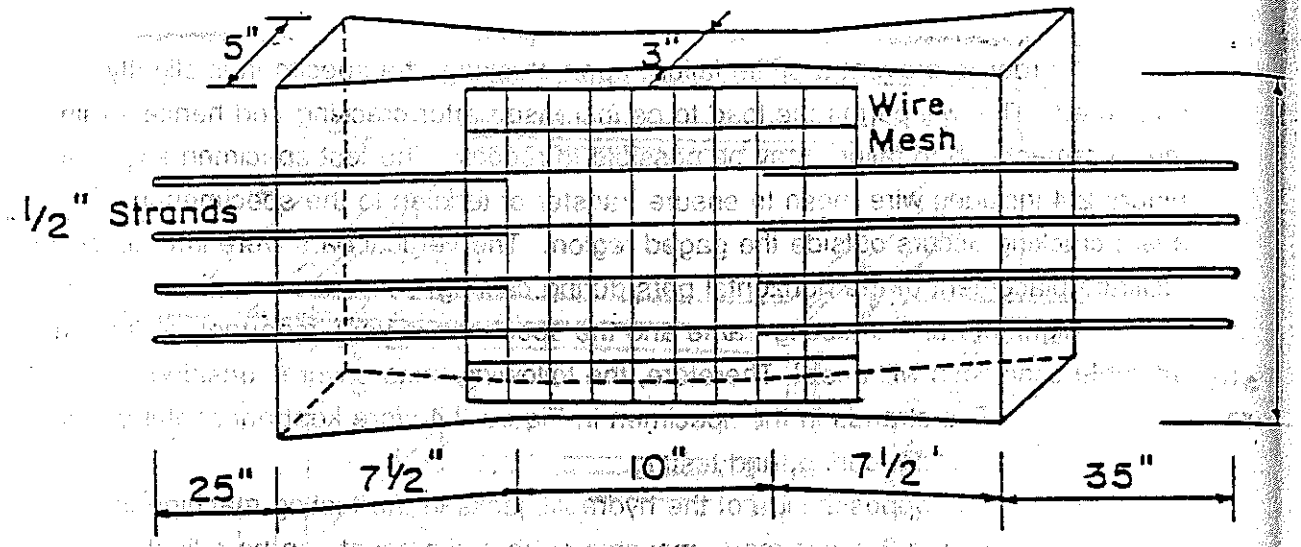

Figure 2.4
Details of the biaxial test specimen

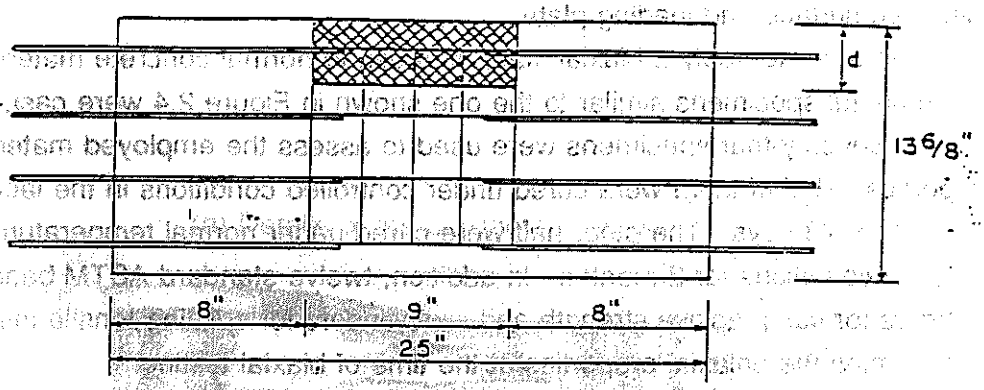

(a) Rectangular patch with various depth, d = 2", 7", and 10"

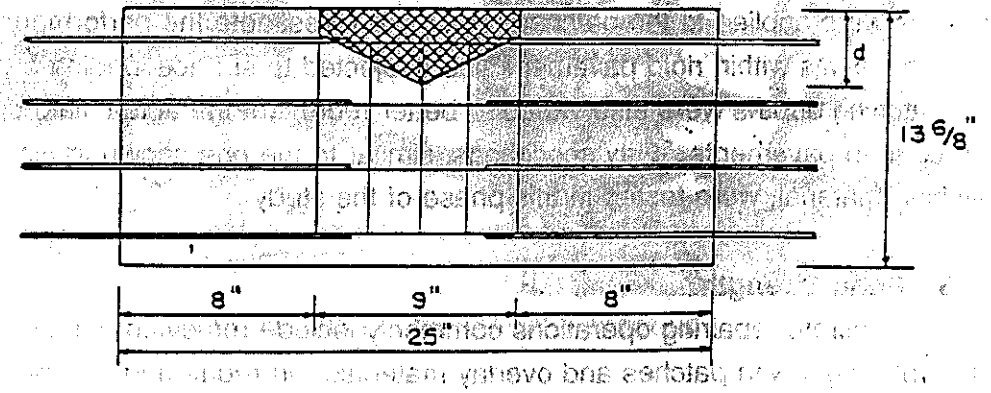

(b) Transition patch with d = 2", 7", and 10"

Figure 2.5
Patch configuration in the biaxial test specimens

Proper surface preparation is an important factor for successful bonding and should be given particular attention. Without proper preparation of the bonding surface, the other points of adhesive selection become useless. This is because a poorly prepared surface is the weak link in the bond system, regardless of the characteristics of the adhesive. A weak bond will permit neither the concrete nor the repair material to develop their full stiffness and strength under service conditions. Therefore, proper surface preparation and bonding are important factors in the success of the repair, creating a need to accurately and positively determine the quality and the strength of concrete bonding.

To test the compatibility between the repair materials and regular concrete, indirect bond tests were conducted. These tests include the split-shear test, shear test, and direct tensile test shown in Figure 2.6. The results of these tests are used to evaluate the quality and strength of the bond between the repair material and regular concrete.

In spilt-shear test, a cylinder of 3" x 6" in dimension, produced with the repair/substrate bond line at 45 degrees to the vertical, is crushed in a compression testing machine shown in Figure 2.6a. If the bond is good, the sample fails as a monolithic cylinder rather than along the bond. It should be noted that the slant shear test provides the most reliable method of evaluating the adhesion of mortars *[37]*. Extensive work has been carried out to evaluate this method *[38]*.

In the present study, twelve concrete cylinders were diamond cut at 45 degrees to their axis producing twenty-four half cylinders of parent material. The patching material was cast over the saw cut surface of the parent half cylinder. Half of them were cured under controlled conditions in the laboratory and tested after 28 days, while the other half were cured under normal temperature and moisture conditions for 90 days.

Contact surface between patch and parent material is often initially moist. In the present work, surface moisture was introduced by passing a wet rag over the surface to be patched, prior to patching.

In the direct shear test shown in Figure 2.6b, the specimen may be subject to torque based on the standard RILEM 13MR. In the present work, bond strength was measured by pushing the patching material while keeping the parent material fixed. Twenty-four (4" x 8") cylinders were cured and tested under different curing conditions and ages.

In the direct tensile test shown in Figure 2.6c, the force required to cause failure divided by the cross-sectional area of the concrete cylinder is a direct measure of the tensile strength of the material across the failure plane. Since failure occurs along the weakest plane, this test provides a quantitative measure of tensile strength, and identifies the location and nature of failure. This often provides valuable insight into specific problems, such as weak bond, poor base, or overlay material. This test

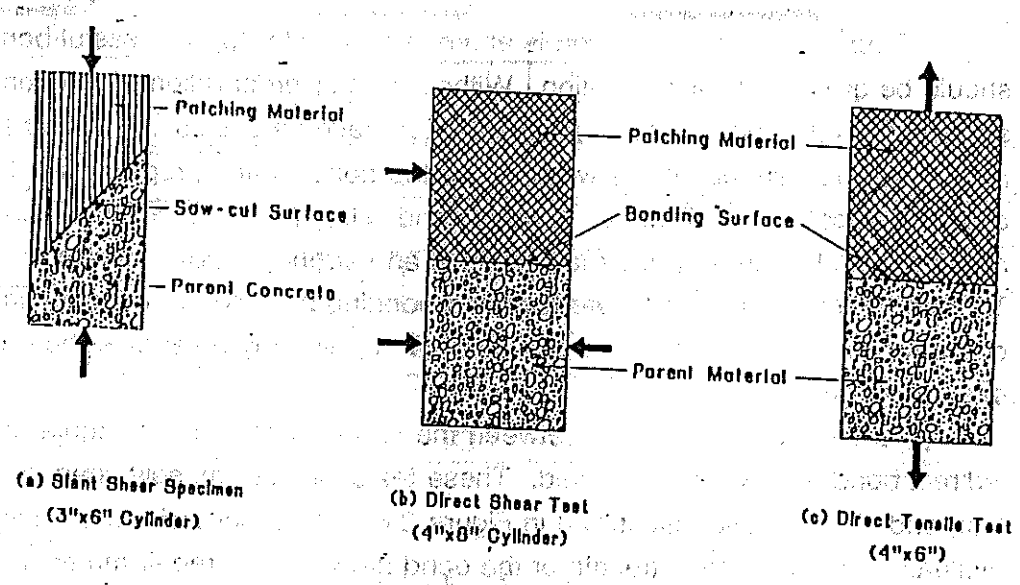

Figure 2.6
Laboratory bond strength tests

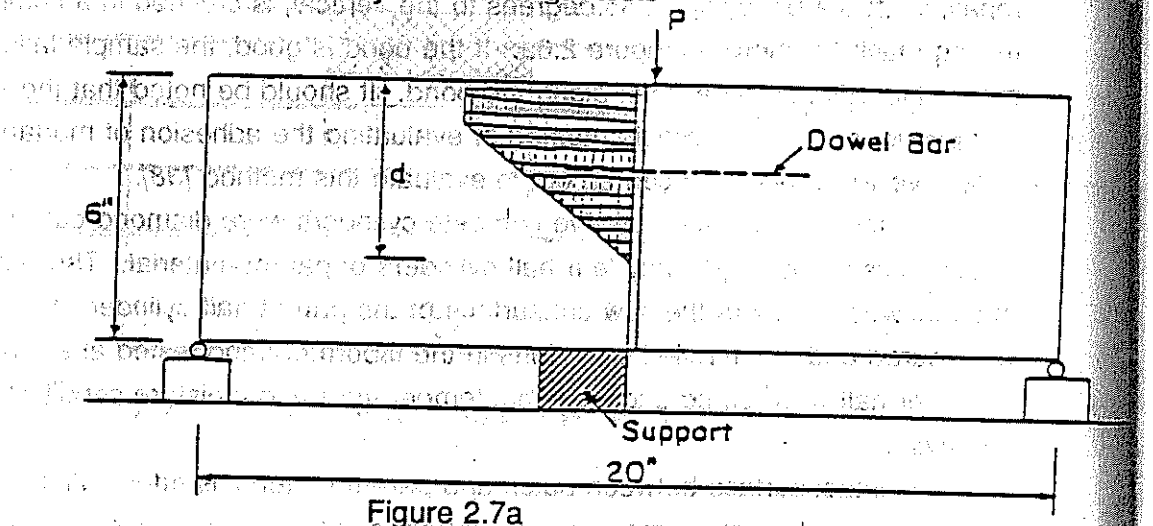

Figure 2.7a
Patch configurations in shear test of rigid joint (transition patch)

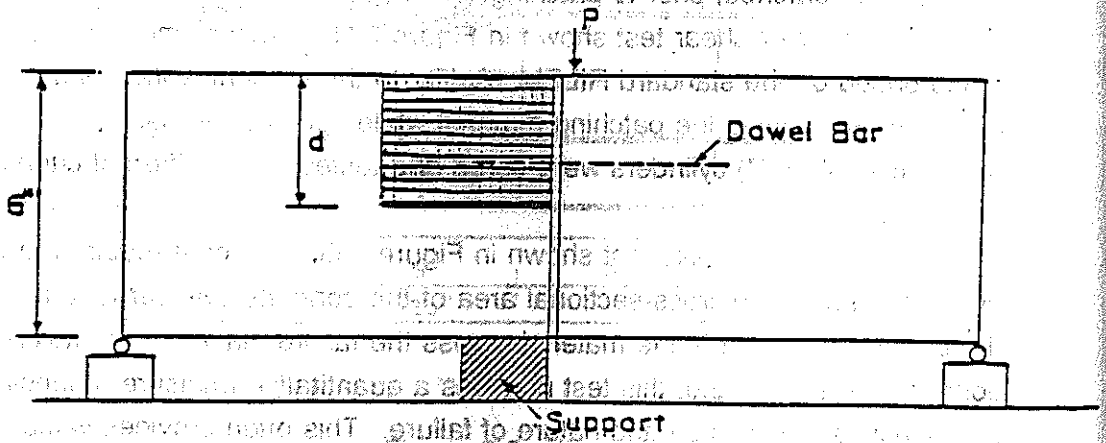

Figure 2.7b
Patch configurations in shear test of rigid joint (rectangular patch)

LIST OF TABLES (Continued)

LIST OF TABLES (Continued)

LIST OF TABLES (Continued)

LIST OF FIGURES

INTRODUCTION

In 1986 the American Association of State Highway and Transportation Officials (AASHTO) published their Guide for the Design of Pavement Structures. Significant changes were made from the 1972 AASHTO interim guide. The design and procedures for new flexible highway pavements and for overlays of hot mix asphalt (HMA) were revised and expanded. The Louisiana Department of Transportation and Development (LaDOTD) immediately began to use the AASHTO Guide as the "building block" upon which to base new LaDOTD pavement and overlay designs for both rigid and flexible pavements.

One major change occurring in the 1986 AASHTO Guide was the use of resilient modulus (M_R) to characterize the materials used in flexible pavement design and rehabilitation. M_R became the definitive characteristic of pavement layer strength. The resilient modulus is a value that, theoretically, can be determined either from testing samples of material in the laboratory or from nondestructive deflection testing (NDT) on in-service pavements. Unfortunately, by 1986 the state-of-the-art for determining M_R from either method was still in the development stages. Researchers in highway and transportation departments, in consulting firms, and in universities began a concentrated effort to determine which laboratory and field techniques could provide consistent and dependable results for this critical pavement design parameter.

With the change to resilient modulus, the use of NDT with linear elastic layer theory for determining the M_R of pavement layers began to get more serious attention. Up to this point, linear elastic techniques had been widely used to

calculate pavement stresses and strains using surface loads plus assumed layer strength characteristics, including modulus and Poisson's ratio, as program inputs. With wider use of NDT devices and the use of deflection data to estimate pavement layer M_R, many of the linear elastic computer programs, such as Chevron, Shell, and Bisar, became the "core" programs in backcalculation routines.

In general, the backcalculation programs require inputs of a surface load and deflection basin from an NDT device, along with pavement layer thicknesses and "seed" (initial estimate) moduli for each pavement layer. Using these inputs, a theoretical surface deflection basin for the given load and pavement inputs is calculated and then compared to the actual NDT deflection basin. If the differences meet certain tolerance limits, then the program stops, and the moduli are considered valid. If not the computer program adjusts the moduli, recalculates the surface deflection basin, and rechecks the basin tolerances. This iterative process continues until the required tolerances are met, and the final backcalculated moduli values are reported.

Several problems have occurred when using these newly developed programs. First, there is not a unique set, but multiple sets of layer moduli that can produce the same deflection basin. Secondly, the set of resulting layer moduli are extremely sensitive to the selection of the seed moduli. Thirdly, thin surface layers (HMA of less than 2 inches) created problems with convergence between the actual and theoretical surface deflection basins. Fourth, a rock or other very stiff layer within a 20' to 30' depth under the pavement affected the calculated deflections. Finally, there were no "correct" moduli to which the

backcalculated moduli could be compared; there was only a reasonable range of moduli against which the backcalculated values could be compared.

Researchers have spent much of the last few years modifying these programs to correct observed deficiencies. They have also compared backcalculated moduli with laboratory moduli of recompacted samples and have compared the backcalculated moduli values obtained among the many routines available. Results have been mixed leaving many researchers puzzled as to what to try next. Much work is still required before these programs are reliable and before the results can be used without a critical analysis. Meanwhile, users must carefully evaluate these backcalculation programs to determine which gives the most reasonable results for their combination of soil, pavement, and NDT device.

LITERATURE REVIEW

Resilient modulus is a fundamental material property that is similar in concept to Young's modulus of elasticity since both are measured from stress-strain data. However, it differs from the modulus of elasticity in that it is determined from the unload portion of the load pulse in a repeated-load, triaxial compression test while Young's modulus is determined from the load portion of the test. Therefore, the resilient modulus is determined using the resilient (recoverable) portion of the axial strain (1). The resilient modulus (M_R) is defined by the ratio of the repeated axial deviator stress (σ_d) to the recoverable axial strain (ϵ_a) (2):

$$M_R = \frac{\sigma_d}{\epsilon_a} = \frac{\text{load/area of the specimen}}{\text{recoverable deformation/original height}} \qquad \text{(Eq. 1)}$$

With the recent emergence of the use of resilient modulus in pavement design, NDT methods have gained popularity as an economical technique for securing material property estimates. The Falling Weight Deflectometer (FWD) is gaining popularity because it can measure the whole deflection bowl while applying loads of the same magnitude as used in design (18 kip single axle loads).

There are two distinct parts to collection and use of NDT data: 1) the mechanical functioning and reliability of the instrument, and 2) the interpretation and utilization of the measured data (3). This report deals principally with the second, use of the FWD deflection data to backcalculate resilient modulus of pavement materials.

Backcalculation is defined as the process of estimating elastic stiffness properties of pavement materials by matching a measured deflection basin with a theoretical basin calculated from a computer program which receives as input the measured deflections produced by a test load plus other information about the pavement materials such as layer thickness, Poisson's ratio, and range of allowable modulus values (3). There are a whole host of backcalculation programs discussed in the literature. Several of the most common programs are briefly discussed in the following paragraphs.

BISDEF

BISDEF, a program developed by the U.S. Army Corps of Engineers, Waterways Experiment Station, uses a deflection basin from NDT results to predict the elastic moduli of up to four pavement layers. By matching the calculated deflection basin to the measured deflection basin. The program uses an iterative process that provides the best fit between measured deflection and computed deflection basins (4).

The basic assumption of this method is that dynamic deflections correspond to those predicted from the layered elastic theory. This method uses the BISAR layered elastic program to compute the deflections, stresses, and strains of the structures under investigation (4). BISAR has a unique capability of varying the bond between layers in the pavement, i.e. variable slip between layers. However, this capability makes the program run time quite long. Additionally BISAR is also a proprietary program and can only be used by licensees.

To determine the layer moduli, the basic inputs include initial estimates of the elastic layer pavement characteristics, as well as the measured deflection basin. Inputs for each layer include:

a) Thickness of each layer,

b) Range of allowable modulus,

c) Initial estimate of modulus (seed modulus), and

d) Poisson's ratio (4).

BOUSDEF

BOUSDEF is a backcalculation program created at Oregon State University to determine in-situ pavement layer moduli using deflection data through backcalculation technique. The program was developed for use with conventional flexible pavements built on a fine grained subgrade which included a coarse grained aggregate base/subbase. The analysis methodology is based on the method of equivalent thicknesses and Boussinesq theory. BOUSDEF utilizes the seed modulus and layer thickness to determine the equivalent thickness of the pavement structure. Deflections for the given NDT load and load radius are then calculated. The calculated deflections are compared to measured deflections. If the sum of the differences is greater than the tolerance specified by the user, the program will begin iterating in an attempt to produce convergence between the calculated and measured deflections by changing the moduli before computing a new set of deflections. This iteration process continues until the sum of the deflection differences is less than the tolerance or until the maximum number of iterations has occurred. The backcalculated moduli may be used to evaluate the existing pavement structural strength and/or for use in mechanistic overlay design procedures (5).

BOUSDEF can be operated on any IBM or compatible microcomputer with a DOS version 3.1 or higher. BOUSDEF is an integrated program which includes the capability for creating, editing, and analyzing a data file (5).

CHEVDEF

CHEVDEF is similar to BISDEF except it uses CHEVRON n-layer computer program in the forward calculation scheme. CHEVDEF uses the sum of the squares of the absolute error as the convergence criterion rather than the sum of the differences as in BISDEF. This program can backcalculate reasonable modulus values for conventional flexible pavement sections, i.e., pavement sections having a layer arrangement that has decreasing stiffness with depth. However, it gives poor results for pavements having thin HMA layers or pavements with intermediate soft or hard layers such as cement stabilized bases or subbases (6 and 7).

COMDEF

COMDEF is an interactive, user-friendly, public domain FORTRAN program which backcalculates layer moduli for composite pavements based on deflections measured by a FWD. COMDEF is based on a new method which uses a matrix of precalculated solutions stored in 33 standard data base files. The method used in COMDEF is completely automated and numerically approximates the theoretical deflection basin which would be calculated by layered elastic theory. The data compression technique and interpolation routines used by COMDEF allow deflections to be calculated almost instantaneously from a relatively small data base with a high degree of accuracy. The COMDEF data base was developed for composite pavements which include portland cement concrete layers with moduli in excess of 3 million psi. As such it is not applicable to pavements included in this study (8).

ELMOD

ELMOD is a microcomputer program based on the method of equivalent thicknesses, originally developed by Odemark. This is a process where by a layered pavement structure is transformed into an equivalent Boussinesq system above the subgrade using the same process as described for BOUSDEF. ELMOD used the layer transformation approximation rather than one of numerical integration. The advantage of this approach is that nonlinear materials may be considered and the computational process is much faster than "conventional" layered elastic analysis backcalculation computer codes (9 and 10).

The basic ELMOD inputs include layer thickness and pavement surface deflections (a total of seven). The program can analyze up to a 4-layer pavement structure; it automatically calculates the subgrade nonlinear-stress relationship for each FWD drop, and it can be used to evaluate other significant factors such as remaining life and required overlay thickness (10).

The program computes moduli by using the outer deflections to first estimate the subgrade modulus. The moduli of the HMA and base courses are determined by an iterative process which uses the center deflection and the shape of the deflection basin. The subgrade modulus at the center of the loading plate is adjusted for stress level, and the outer deflections are checked. At this point a new iteration is made if needed. The program generally takes less than five seconds to run (10).

ELSDEF

ELSDEF is similar to BISDEF, except that ELSYM5 is the elastic layer program rather than BISAR. An iterative procedure is also used to determine the best fit between measured and computed deflections. The modulus adjustment procedure involves determining a relationship between log modulus and calculated deflection for each unknown modulus by varying the assumed moduli and calculating the deflections. This relationship is then used in the iteration process to find a set of moduli that produce minimum errors. Program input are similar to others using this approach, i.e., load, deflection basin data, error tolerance, layer thickness, Poisson's ratio, seed moduli, and allowable range of moduli (10).

The number of layers with unknown moduli cannot exceed the number of measured deflections. No provision is available for nonlinear material behavior, and limitations to the approach are related to this fact. The program can be run with or without a rigid base. The procedure is sensitive to the choice of seed moduli (10).

EVERCALC

EVERCALC is a mechanistic-based pavement analysis computer program that includes the Chevron N elastic layer program. This microcomputer program uses an iterative procedure of matching the measured surface deflections with the theoretical surface deflections calculated from assumed elastic moduli. The program has converged on a solution when the summation of the absolute values of the differences between the measured and calculated surface deflections falls within a preset allowable tolerance (generally 10 percent or less for a deflection

basin described by five deflections). Lower tolerance levels will produce more accurate solutions; however, the 10 percent tolerance results in modest computer run time of five minutes for a three-layer pavement (10).

The program develops estimates of initial "seed" moduli internally and backcalculates the modulus for each pavement layer. The seed moduli are estimated using internal equations, developed from regression relationships between pavement layer moduli, load, and various deflection basin parameters (10).

ISSEM4

ISSEM4 is a mechanistic-based pavement analysis computer program based on the ELSYM5 program. As in most programs, it uses an iterative procedure of matching the measured surface deflections with the surface deflections calculated from ELSYM5 using assumed elastic moduli. The program uses five deflection points in the backcalculation process for three-layer structures; however, these points are from a fitted curve of the actual deflection measurements. A typical three-layer run takes about 5 minutes on a PC (10).

LOADRATE

The LOADRATE program uses a series of regression equations between load and deflection based on results generated using ILLI-PAVE. The program was developed specifically for use with surface-treated pavements typical of secondary roads. Regression equations were developed to relate the nonlinear elastic parameters of the bulk stress model (for the base material) and the deviator

stress model (for the subgrade material) with the deflections at the load point and at some distance away from the load (6). Since the principal roadway surface type of interest in this present study is HMA, and LOADRATE was developed for surface treatments, it was not given any further consideration.

MODCOMP2

The MODCOMP2 program utilizes the Chevron elastic layer computer program for determining the stresses, strains and deformations in the pavement system. Since there is no closed-form solution for determining layer moduli from surface deflection data, an iterative approach is used that requires an input of seed moduli for each layer. The basic iterative process is repeated for each layer until the agreement between the calculated and measured deflection is within the specified tolerance or until the maximum number of iterations has been reached (4 and 10).

The program capabilities include the following:

1) Up to eight layers can be included in the pavement system.
2) The layer combinations may be linear elastic or nonlinear stress dependent.
3) The program is capable of accepting data from several typical NDT devices (e.g., FWD, Road Rater, and Dynaflect).
4) It is capable of accepting up to six load levels.

The input data required by the program are:

1) Surface deflection and radial distances of geophones from the center of the load,

2) Applied load,

3) Poisson ratio,

4) Base and subgrade soil type, and

5) Seed modulus for the pavement layers.

The computed deflections are compared with measured deflection, and the ratio of adjustment of layer is based on the magnitude of the difference in calculated deflections. This process is repeated until the difference between the computed and measured deflection is within the specific tolerance (4 and 11).

MODULUS

MODULUS is a backcalculation program that generates a data base of modulus deflections using WES5, a linear-elastic program created by the U.S. Army Corps of Engineers Waterways Experiment Station in Vicksburg, Mississippi. This program uses the Hooke-Jeeves' pattern search algorithm for minimizing the sum of the squared error between calculated and measured deflections. The algorithm is applied to a data base consisting of a large number of calculated deflections and their corresponding squared errors for various predetermined modulus combinations assigned to the pavement layers. Computation of the data base is performed automatically in MODULUS before the deflection matching process begin. Once the minimum squared error is determined from the data base by the pattern search algorithm, a 3-point Lagrange interpolation technique is used to estimate the calculated deflection basin and the corresponding layer moduli (6 and 7).

Using an IBM-AT 286 with an 8086 math co-processor chip, approximately 30 minutes is required for MODULUS to calculate and develop the data base for a four-layer pavement section; however, once the data base is computed, only one to two minutes is required to backcalculate moduli for each deflection bowl. The data base, moreover, can be saved and used repeatedly on similar pavements for analysis of other deflection data. Because of the short turn-around time to backcalculate moduli, it is now practical to perform the backcalculation analysis in the field in order to check the reasonableness of data before moving away from the test site. The program has the capability to handle both linear and nonlinear material behavior (7 and 12).

OAF

The OAF program was developed to utilize the deflection data from the FWD. The procedure requires measurement of deflections at 0, 30, 60, and 100 cm from the applied load. Backcalculation of layer moduli for a specific site requires inputting the following information into a OAF which uses the ELSYM program to calculate surface deflections:

1. Surface deflection measurements and load configurations
2. Base type
3. Layer thickness
4. Poisson's ratio for all layers, and
5. HMA modulus at field pavement test temperature (11)

Essentially, the program solves for the moduli of the various layers by attaining compatibility between measured and computed deflections (11).

SEARCH

SEARCH was developed at the Texas Transportation Institute, and uses a pattern-search technique to fit deflection basins with curves shaped like elliptic integral functions which represent solutions to the differential equations used in elastic layer theory. To account for multiple layers, a generalized form of Odemark's assumption is used to transform the thickness of all layers to an equivalent thickness of a material having a single modulus. The input data include:

1. Thickness of HMA and granular base layers
2. Force applied and radius of loading plate, and
3. Measured deflection values, and their radial distances, from center of loading plate (4)

The program searches for a set of elastic moduli that fit the measured basin to the calculated basin with the least average error. The output includes calculated moduli, computed and measured deflections, force applied, and squared error of the fitted basin (4).

WESDEF

The WESDEF computer program also utilizes WES5. WESDEF, was developed by the U.S. Army Corps of Engineers, Waterways Experiment Station. The program can calculate modulus values for one set of deflections and multiple loads. The deflection data can be entered manually by utilizing the INDEF program which accompanies the WESDEF program.

The basic assumption of WESDEF is that dynamic deflections correspond to those predicted from the same loads using static layered elastic theory. This program uses the WES5 layered elastic program to compute the deflections for the structure under investigation. The program compares computed and measured deflections and compares the differences to a 10 percent tolerance range, if not within tolerance, the program varies the layer moduli, recompute deflections and compare to measured deflections in an attempt to converge to the 10 percent tolerance range. If after three iterations the tolerance range is still greater than 10 percent, the iteration process will terminate (13).

VESYS

The VESYS program was used to develop a graphical procedure for backcalculating the pavement parameters. The VESYS model incorporates the viscoelastic and fatigue properties of the pavement materials. For the analysis of existing pavement systems, algorithms were developed that can be used with measured load deflection data and known material thickness or properties. The algorithms were developed by applying statistical regression analysis techniques to the VESYS-generated response data (11). Since the inputs required for the VESYS model are very complicated and determining the compatibilities between the properties used by the researchers and those of Louisiana materials was not possible, VESYS was determined not to be a candidate for use in this project.

COMPARISONS OF PROGRAMS

Ali and Khosla ran four different programs (ELMOD, VESYS, MODCOMP2, AND OAF) on the same sample data and compared the results to each other and to laboratory test results of pavement materials. Their findings showed both ELMOD and VESYS had great potential for pavement analysis. VESYS had the least variation between predicted and laboratory moduli values with the ratio $M_{R(lab)}/M_{R(pred)}$ ranging between 0.48 and 1.08 with most values between 0.77 and 0.97. The ratio values for ELMOD varied between 0.54 and 1.56, with most values between 0.80 and 1.26. Both MODCOMP2 and OAF predicted moduli which showed large variations from the laboratory values (11).

Lee, Mahoney, and Jackson examined the program EVERCALC and verified it in two different ways. The first verification approach was to compare theoretical and backcalculated moduli for a range of three-layer pavement systems. This was accomplished by using the Chevron N-layer elastic analysis program to generate deflection basins for specified layer moduli and thickness conditions. These comparisons showed modest differences (about 8 percent for HMA, 6 percent for the base course, and less than 2 percent for the subgrade). The largest differences for HMA were observed for thin surfaces with low stiffness. As the HMA layer thickness increased, both the base and subgrade moduli differences increased. The second verification approach was to compare backcalculated and laboratory moduli based on FWD tests and field material sampling along with appropriate laboratory testing. The results show the greatest range of differences for the HMA layers (438 percent to 1 percent difference)

followed by the base (60 percent to 0 percent) and subgrade materials (59 percent to 2 percent) (14).

Alexander, White, and Barker reported that WESDEF compared favorably (almost identical) to BISDEF for typical values for AC, PCC, and composite pavements using FWD deflection data. WESDEF matched the deflection basin about 4.5 times faster than BISDEF (13).

Tam and Brown reported that the ELMOD program can only analyze two- and three-layered structures, although a source from Dynatest has indicated that it can analyze structures with up to four layers (9).

Mahoney, Coetzee, Stubstad and Lee compared ELMOD, ELSDEF, EVERCALC, ISSEM4, and MODCOMP2 with each other and laboratory results. It is reported that the five programs showed relatively similar results but all showed greater difference compared to the laboratory results (10).

OBJECTIVES OF RESEARCH

A. Select an appropriate backcalculation procedure for estimating pavement layer resilient modulus from FWD deflection measurements.

B. Compare FWD estimated resilient modulus values with those determined from laboratory tests.

C. Develop a preliminary procedure for estimating the resilient modulus of pavement layers using deflection measurements.

SCOPE

Because of the limited time and funds available for this study, no laboratory testing of pavement materials was possible. Therefore, the evaluation of candidate programs was made using deflection data taken on a series of experimental projects built on US 71-167 in 1975-76 for which extensive material test data was available (15 and 16). Additionally, the initial selection of computer programs was made on the basis of comparisons and evaluations included in the technical literature.

To verify the use of the backcalculation approved to other pavement materials, additional field data should be collected as well as laboratory moduli determination for those pavement materials. Comparisons between moduli predicted from backcalculation procedures and moduli measured in the laboratory will indicate their applicability to other materials.

METHODOLOGY

In this study the process for selecting a computer program for backcalculation of pavement layer moduli involved several steps. First a literature survey was conducted to identify the computer programs which have shown the best promise for calculating reasonable estimates of pavement moduli. Once the programs were identified, the results from comparative studies which used more than one program were reviewed in order to develop a smaller set of candidate programs which appeared to work best, which required the minimum amount of prior information about the pavement materials, and which could be used by operators with limited experience. Based on these factors, a set of six computer programs was selected for use in this study.

After selecting the programs, a series of deflection measurements were taken by the LTRC research staff on each of the experimental base sites on US 71-167 south of Alexandria. Five deflection tests for each of four different loads were performed on each of the 18 control and test sections. These deflection data along with pavement layer data were input into each computer program and the layer moduli estimated. The average moduli were calculated two different ways: 1) calculating moduli of each layer from individual deflection basins and averaging the resulting moduli for each layer and 2) averaging all deflection basin readings for a given load and computing the moduli from this averaged basin and loading. The estimated moduli were compared to moduli determined from laboratory tests conducted as part of the experimental base project (15 and 16).

Statistical comparisons were made using analysis of variance (ANOVA) techniques and the Student-Newman-Keuls, Duncan Multiple Range, and Least Significant Difference tests. Detailed studies of the results from the 18,000 pound axle load led the authors to conclude that two programs, MODULUS and WESDEF, provided the best match-up between predicted and measured moduli.

Other factors considered in making a program selection included:

1) Seed moduli and range of moduli input requirements,
2) Adjustments for temperature effects on moduli of the HMA materials,
3) Efficiency of operations when large deflection data sets were being processed,
4) Ease of use of the program,
5) Ease of keeping the program up to date, and
6) Documentation available on the program.

Based on the above factors, MODULUS 4.0 step 3 was selected as the most appropriate for use in Louisiana. Additionally a preliminary procedure for collecting NDT data was prepared as a part of the effort. The principal objective of the field data collection effort was to provide pavement layer moduli input for use in overlay rehabilitation, and original design according to the 1986 AASHTO Design Guide.

ANALYSIS OF RESULTS

BACKCALCULATION PROGRAMS SELECTED FOR THIS STUDY

The original research plan included securing as many of the programs as possible and then using a common set of field deflection data to determine which programs performed best in backcalculating pavement layer moduli. Project staff encountered considerable difficulty both in securing copies of the computer programs and getting them to work on the project computer. Additionally the LTRC staff experienced unavoidable delays in taking delivery of the FWD and tow vehicle. As a result project staff were unable to secure deflection data in enough time to evaluate a large group of the computer programs. Therefore, the selection of candidate programs was made using results from the technical literature described in the previous sections.

Project staff initially selected six computer programs for use in the balance of the study:

1. BOUSDEF
2. ELSDEF
3. EVERCALC
4. MODCOMP2
5. MODULUS
6. WESDEF

These programs appeared to be representative of those discussed in the literature and typically used in comparisons studied. Additionally, most of the programs have been developed for and adopted for use by agencies involved in routine NDT evaluations.

The developers of each of these programs were contacted and copies were received for all but MODCOMP2. However, the project staff was unable to get ELSDEF to work on the available PC and, after considerable effort, eliminated it from the study. Several telephone calls were made to determine the status of MODCOMP2 but because of some variations in surface deflections in the vicinity of the load experienced with the CHEVRON elastic layer program, MODCOMP2 was withheld from project staff until the problems were solved. Consequently, the programs listed in Table 1 represent the four candidate backcalculation programs utilized in the balance of the project. All programs are in the public domain.

BOUSDEF is a new program based on the method of equivalent thicknesses which has not been widely tested and it is reported to have short run times. A new version of EVERCALC (EVERCALC 3.3) was just distributed in February 1992. MODULUS 4.0 was chosen because it has fared very well in comparisons both in the literature and by reputation among the pavement modulus research community. WESDEF was readily obtained from the Corp of Engineers and has been used extensively in their pavement evaluation work, and fared well when predicted moduli were compared with laboratory determined moduli.

Table 1.

Backcalculation Computer Programs

Program Name	Layered Elastic Program	Number of Layers	Stiff Layer	Creator	Ref.
BOUSDEF	Method of Equiv-alent Thick-nesses	5	NO	(for) Oregon DOT	5
EVERCALC 3.3	CHEVNL	5	YES	(for) Washington State DOT	17
MODULUS 4.0	WES5	4	YES	Texas Transportation Institute	18
WESDEF	WES5	5	YES	U.S. Army Corps of Engineers	19

DESCRIPTION OF TEST SITE AND LABORATORY DATA

This project utilized a series of test sections located in central Louisiana, between the communities of Meeker and Chambers in Rapides Parish as shown in Figure 1. The test sections are located on a portion of US 71-167 which accommodates a moderate volume of mixed vehicular traffic. The terrain at the site is generally flat with poor drainage and the subgrade material is a relatively uniform, fine-grained soil. The average daily air temperature at the test site ranged from 39°F to 84°F and the annual rainfall ranges from 55 to 60 inches (15).

The test site contained eighteen sections; fourteen test sections and four control sections arranged as shown in Figure 2. The control sections were used as control sections in the previous study by Hadley (15); however, in this research study the control sections were treated the same as the test sections. Included in the cross sections are three different base types (black base, soil cement, and cement stabilized sand-clay-gravel) of several thicknesses, and two hot mix asphalt (HMA) surface thicknesses. Each section is approximately 550 feet long with a 50 feet transition zone between adjacent sections. Construction of the test sections began in 1975 and was completed 1976 (15). All sections were recently overlaid with a 3-inch layer of HMA.

The properties of each test section material were measured in the laboratory as part of a previous LTRC research project and reported by Hadley (15). The average of the laboratory values were determined in order to compare the computer backcalculated values obtained from each computer program to the

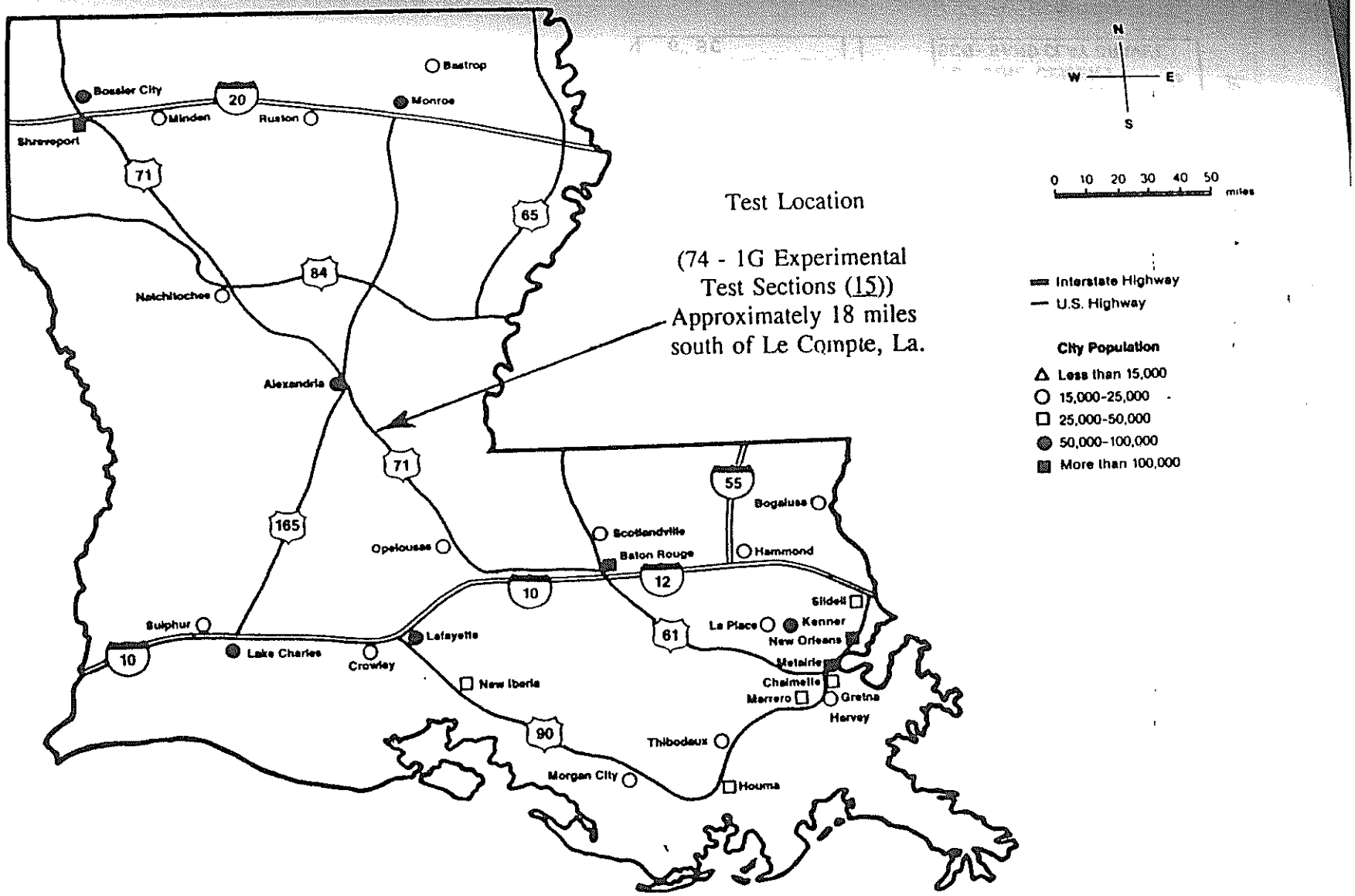

Figure 1. Location of experimental base test sections

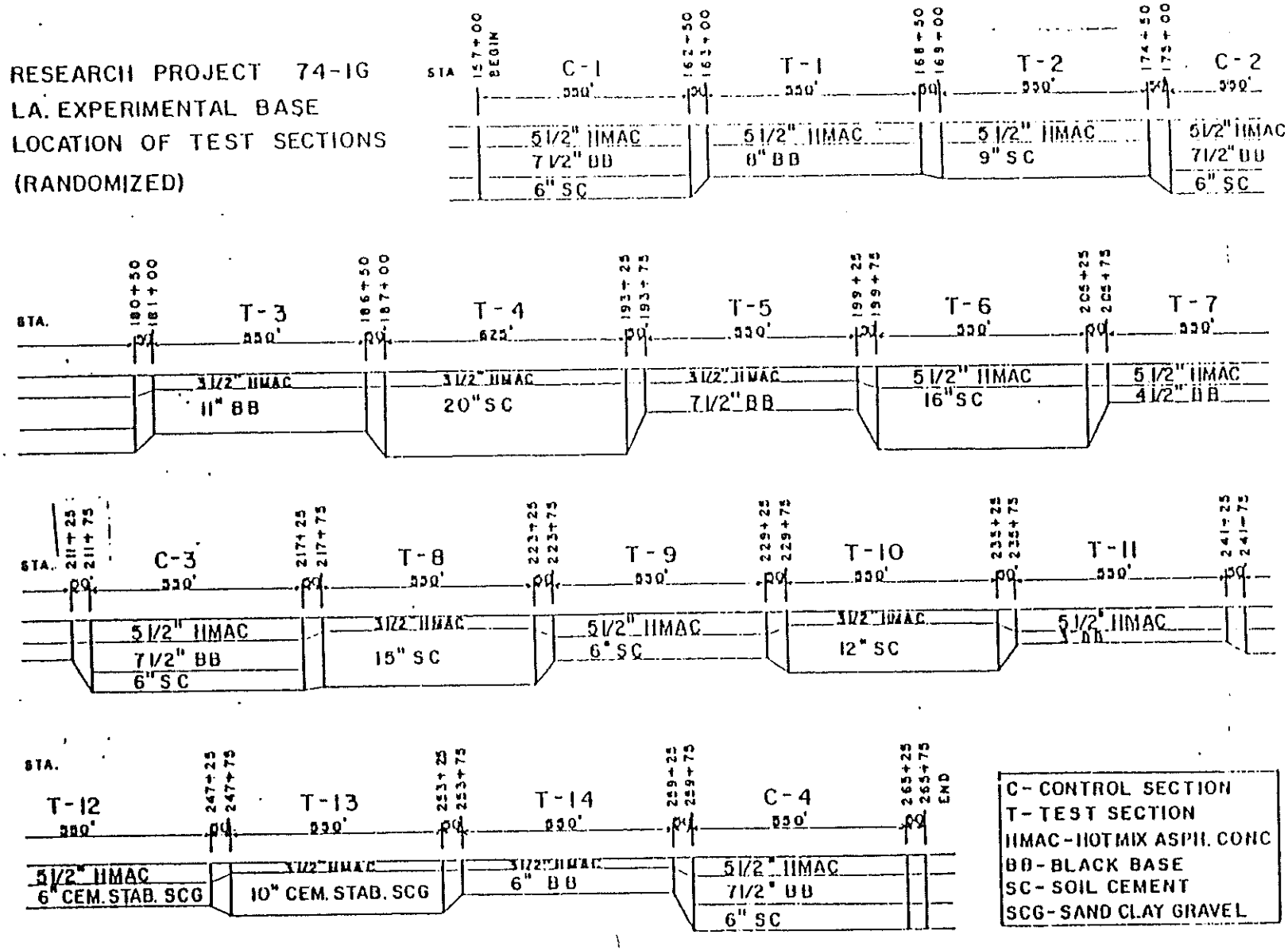

Figure 2. Experimental base pavement cross sections in the laboratory.

laboratory determined values, in order to assess the ability of each program to estimate the measured moduli.

The average layered modulus (in psi) values from Hadley (15) are given in Table 2. Hadley determined the properties of the surface and base materials using the indirect tensile test. Values used in this report were determined by first calculating the mean and standard deviation of all the data; next the outliers were removed using a 5 percent significance level; the mean was recalculated using the remaining data. Properties of the subgrade soil were determined using a tri-axial resilient modulus test. Values used in this report were determined in the manner described for surface and base materials. The individual test values were extracted from Tables 46-50, 52, and 56 of reference 15. The resilient modulus values from field cores taken from each of the materials are summarized in Volume 2-Appendix 1.

Poisson's ratio for the materials is shown in Table 3. These values were determined from laboratory tests on field cores secured after construction using the material described in reference 15.

FEATURES TO BE CONSIDERED DURING THE SELECTION PROCESS

When selecting a backcalculation program several features should be considered. To begin with, it is important to determine how extensively the program has been used in past research studies and, if possible, how well the backcalculated moduli from a program compare with moduli values determined.

Table 2.

Average Laboratory Modulus Values for Layers 2, 3, and 4 As Secured From Hadley (15)

Section	Layer 1[a]	Layer 2	Layer 3	Layer 4
C-1[b]	500000	540000	371400	6175
C-2	500000	540000	449100	6384
C-3	500000	540000	477500	8769
C-4	500000	540000	378600	13074
T-1[c]	500000	563000	494500	6546
T-2	500000	563000	449400	7229
T-3	500000	563000	494500	11367
T-4	500000	563000	594000	12851
T-5	500000	563000	494500	11282
T-6	500000	563000	560900	8397
T-7	500000	563000	494500	7479
T-8	500000	563000	616000	9620
T-9	500000	563000	408300	13415
T-10	500000	563000	564000	14710
T-11	500000	563000	494500	12812
T-12	500000	563000	500000	11266
T-13	500000	563000	500000	11827
T-14	500000	563000	494500	14257

[a]The modulus values for layer 1 (overlay) were not determined in the laboratory, but were assumed to be reasonable values.
[b]C-1 indicates control section 1 as shown in Figure 2.
[c]T-1 indicates test section 1 as shown in Figure 2.

Table 3.
Poisson's Ratio for Each Material As Determined From Test On Field Cores (16)

Material	Poisson's Ratio
HMA	0.35
Soil Cement	0.18
Sand Clay Gravel	0.10
Subgrade	0.49

It is also desirable to determine how often the program predicts moduli that are out of a reasonable range for the material being evaluated.

Finally, the program requirements, ease of use of the program, and the required technical expertise of the operator are important also. Included in this last group of factors is the basic mathematical theory used in the program, type and size of computer required, length of run time for the program to generate output, availability and ease of understanding the user's guide, and availability of help from the developers of the program.

DETERMINATION OF SEED MODULI

The range of typical modulus values expected for various pavement materials has to be determined and input for some of the computer programs. These initial estimates of moduli are called the seed moduli. Range of the seed moduli for the pavement layers were estimated in the following manner. The range of test results for the HMA material tested by Hadley (16) was from 100,000 psi to 1,200,000 psi for a standard reference temperature of 77°F. Since the FWD data were performed at temperatures other than 77°F, the HMA seed moduli had to be corrected for temperature. The temperature correction was secured from a semi-log plot of "stiffness correction factor" vs temperature shown in Figure 3 (18). The seed modulus for a particular test was estimated by multiplying the correction factor derived from Figure 3 by the range of moduli secured from Hadley's laboratory data.

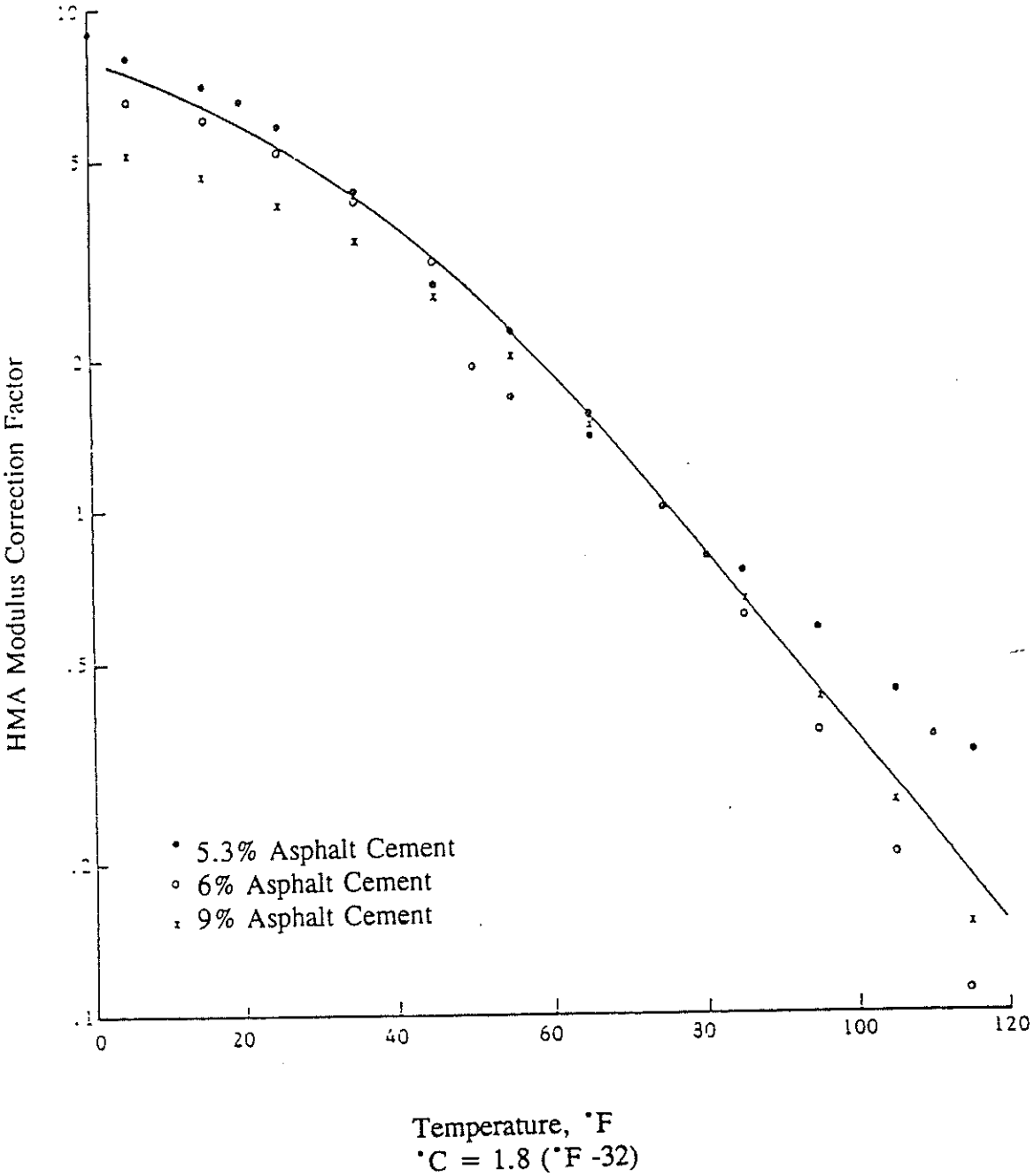

Figure 3. Relationship selected for modifying HMA modulus as a function of temperature

The range of moduli for the cement stabilized layers was estimated to be from 100,000 psi to 1,000,000 psi with Hadley's mean laboratory value used as the seed modulus. The range of moduli for the subgrade was estimated to be from 1,000 psi to 25,000 psi, with the seed modulus being the mean laboratory value. Volume 2 -- Appendix 2 contains a procedure for estimating seed moduli for various layers that was secured from reference 19 and 20. This procedure can be used for pavements where the pavement properties are unknown. The procedure was checked for the experimental test sections and appears to work well, except for cement stabilized bases, where the estimated values were found to be too small when compared to Hadley's laboratory results for the cement stabilized materials.

PROGRAM OPERATION TO ESTIMATE M_R

Each of the four computer programs required the same types of input data and each creates an output file of backcalculated moduli. A brief description of the operation of each program is included in the following paragraphs. The program and option designations used in this portion of the project are defined below:

Program:

1 = MODULUS step 2.

2 = MODULUS step 3.

3 = EVERCALC with no rigid layer.

4 = EVERCALC with rigid layer.

5 = EVERCALC with rigid layer and high water table.

6 = WESDEF

7 = BOUSDEF

Program 1, MODULUS step 2, is designed for a user who is familiar with material information but who has limited experience with modulus backcalculation techniques. For this option the user selects the material types, thicknesses for the pavement layers, and pavement temperature at time of testing, and the program assigns the range of acceptable moduli and Poisson's ratio values to be used in the analysis. MODULUS is a menu driven program. To begin the program, the following inputs for the data input option of the program are required:

- file name,
- highway and location,
- station number where the tests were performed,
- number of deflection bowls included in the data set,
- load applied to pavement,
- lane tests were performed in, and
- deflection reading for each sensor.

Once the input file has been generated and saved, the backcalculation step in the program can be run. This step requires that the input file name and the data set

be defined by indicating beginning and ending stations, then it is necessary to select Step 2) "input material types." Now the program requires:

- load plate radius,
- number of sensors and their distance from the center of the plate,
- surface thickness,
- aggregate type,
- average or range of values for the HMA modulus adjusted for temperature at time of test,
- HMA temperature at time of deflection testing, the program automatically adjusts the moduli to standard temperature of 77°F,
- base and subbase type and thickness, and
- subgrade type.

Now the program backcalculates the modulus value for each layer of the pavement. Once the program has completed the backcalculation process, the output is stored and can be printed. The run time for this program is approximately two minutes on a 386, 40 megahertz IBM PC or compatible computer.

Program 2, MODULUS step 3, is designed for the more knowledgeable user. Program 2 has the same input option as program 1. After the input has been entered and saved, the backcalculation option can be executed. As for program 1, the operator must enter the input file name and define the data set with beginning and ending station, then it is necessary to select Step 3) "Run a Full Analysis." In this option the user supplies all of the input parameters needed to perform the analysis. The user has full control over all of the inputs used in the analysis. This is in contrast to MODULUS step 2 where the computer program assigns layer moduli and Poisson's ratios using typical values for similar

materials as defined by staff at TTI. For step 3 the program requires the following input:

- load plate radius,
- number of sensors and their distance from the center of the plate,
- thickness of each pavement layer,
- range of moduli values for each pavement layer,
- Poisson's ratio for each pavement layer, and
- seed modulus and Poisson's ratio for the subgrade.

Now the program backcalculates the modulus value for each layer in the pavement structure and stores the output which can be printed. MODULUS step 3 takes approximately 2.5 minutes on a 386, 40 megahertz IBM PC or a compatible computer.

Program 3 is EVERCALC without a rigid layer and is also menu driven. To begin option 1) "Edit General Data File" must be selected to begin preparing the input file:

- file name,
- number of layers,
- units (english or metric),
- load plate radius,
- number of sensors and their distance from the center of the load plate,
- temperature correction option,
- method of temperature measurement (direct or Southgate method),
- method of estimating seed moduli (internal equations or engineering judgment),
- stiff layer option,
- maximum number of iterations before terminating the run,
- deflection tolerance in percent, and
- modulus tolerance in percent.

For this option of EVERCALC, "no" was selected for the stiff layer option. Program developers suggest that the maximum number of iterations be set at 3,

5, or 10 (all are considered acceptable) and that the deflection tolerance range from 1 to 10 percent. After the general data file has been generated and saved, step 2) "Enter Deflection Data Interactively" is selected for each pavement cross section. In this step the following input is required:

- file name for each layer,
- Poisson's ratio for each layer at standard temperature of 77°F,
- seed modulus for each layer at standard temperature of 77°F,
- modulus range,
- station number where test was performed,
- thickness for each layer,
- number of deflection data sets,
- temperature of the pavement at the test site, the program automatically adjusts moduli to standard conditions,
- load applied to pavement, and
- deflection at each sensor.

Once this file is saved, the program goes back to the main menu and step 3) "Perform Backcalculation" can be selected. In this step, the program backcalculates the modulus for each layer and saves it in an output file. The run time for the EVERCALC program is approximately 1.5 minutes on a 386, 40 megahertz IBM PC or compatible computer.

Program 4, EVERCALC run with a rigid layer, is run just like program 3 except in the general data file the stiff layer option is indicated by a "yes" and in step 2 the stiff layer modulus value and Poisson's ratio must be input. The developers recommend that the stiff layer modulus value be 10 times the modulus value for the subgrade (17). This version of EVERCALC also takes approximately 1.5 minutes on a 386, 40 megahertz IBM PC or compatible computer.

Program 5, EVERCALC run with a rigid layer and a high water table, is run just like program 4 except that the developers suggest that the stiff layer modulus value be reduced to 2 or 3 times the modulus value for the subgrade (2). This version of EVERCALC also takes approximately 1.5 minutes on a 386, 40 megahertz IBM PC or compatible computer.

Program 6, WESDEF, is not menu driven. Data is input through a program called INDEF with the following input required:

- file name,
- number of sensors and their distance from the center of the load plate,
- deflection for each sensor,
- number of loads per deflection bowl,
- load applied to the pavement,
- load plate radius,
- number of pavement layers,
- layer type,
- seed moduli and range for each layer,
- layer thickness, and
- slip condition (adhesion between the layers, ranges from full adhesion to full slip).

After the input information is entered and stored, the INDEF program can be exited and the WESDEF program can be executed. After identifying an output file name, the WESDEF program can compute the backcalculated modulus values. The WESDEF program takes approximately 0.5 minutes on a 386, 40 megahertz IBM PC or compatible computer. However, only one deflection basin at a time can be input into the program. For a second deflection basin, INDEF must be called, the input entered for the second basin and then WESDEF is run. To evaluate an extensive set of deflection data is a tedious job using the WESDEF program.

Program 7, BOUSDEF, is menu driven and requires the following input:

- input file name,
- number of layers,
- thickness of each layer,
- Poisson's ratio of each layer,
- seed moduli and range for each layer,
- density of each layer,
- load plate radius,
- number of sensors and their distance from the center of the load plate,
- load applied to pavement,
- deflection at each sensor,
- deflection error tolerance in percent, and
- maximum number of iterations.

Once the input file is stored, the backcalculation step of the program can be executed. The program predicts modulus values one load at a time, and requires that the key-board operator be present throughout the program run to finish its backcalculation technique. The program does not automatically create an output file and therefore the final results must be printed, using the print screen key on the computer before continuing with the next deflection basin. This program takes approximately 0.5 minutes on a 386, 40 megahertz IBM PC or compatible computer.

PROCEDURE FOR STATISTICAL ANALYSIS

In this project all statistical work was performed by the Statistical Analysis System (SAS) computer package which can perform regression procedures, analysis of variance, and many other statistical operations. The analysis of variance (ANOVA) procedure was utilized during this project to develop

information with which means can be tested to determine if one set of observations are significantly different from another. ANOVA calculations are recorded in an ANOVA table similar to that shown below.

Source	DF	SS	MS	F-value
Model	Df_m	SSM	MSM	F
Error	Df_e	SSE	MSE	
Corrected Total	Df_{ct}	SST		

The output table has the following column titles: source, degrees of freedom (df), sum of squares (SS), mean squares (MS), and F-value. The source column includes model, error, and corrected total categories. The degrees of freedom section includes the degrees of freedom for each of the three categories listed in the source column. The sum of squares column includes the sum of squares results for each of the three source categories. The mean squares column includes the mean squares of the model and error, the values for these two are calculated by dividing the SS by the df for the respective categories. The F-value is calculated by dividing the mean square of model (MSM) by the mean square of error (MSE) and this calculated value is compared with a tabulated F-values for the number of degrees of freedom as the model and the error terms to determine whether the source elements are significant or not.

In an attempt to determine which of the backcalculation programs produced average moduli most like the laboratory determined values, three

significance tests were utilized; 1) Student-Newman-Keuls (SNK) Test for Variance, 2) Duncan's Multiple Range Test, and 3) Least Significant Difference (LSD) Test. All three tests use results from the ANOVA procedure.

Student-Newman-Keuls test is a good test because it allows investigation of all possible pairs of means in a sequential manner, has very good power, and keeps the level of significance constant for investigation of all pairs of means. The SNK test procedure is as follows. First arrange the means in rank position from largest to smallest.

RANK NUMBER	1	2	3	4
GROUP NAME	B	D	C	A
GROUP MEAN	8.7	6.8	5.7	5.0

Then prepare a table of differences between means from the largest differences (column K) to the smallest (column K-2) in all possible pairs forming a triangular arrangement. The differences for the first row are computed by subtracting from the largest mean (1) each of the other smaller means: 1-4, 1-3, 1-2 which correspond to the means for groups B-A, B-C, and B-D. The second row is computed by subtracting from the next largest mean (2) each of the other smaller means: 2-4, 2-3 which correspond to the means for groups D-A and D-C beginning with the largest difference for the K^{th} column. The third row is computed by subtracting from the next largest mean (3) each of the smaller means: 3-4 which correspond to the means for group C-A.

	k	k-1	k-2
	4	3	2
1	B-A	B-C	B-D
2	D-A	D-C	
3	C-A		

Next a list of the least significant ranges is calculated for each of the columns K, K-1, and K-2 using the following procedure:

$$R_k = q_\alpha(k,df)S_y \quad \text{(Eq. 2a)}$$

$$R_{k-1} = q_\alpha(k-1,df)S_y \quad \text{(Eq. 2b)}$$

$$R_{k-2} = q_\alpha(k-2,df)S_y \quad \text{(Eq. 2c)}$$

where:

$q_\alpha(k,df)$ = upper percentage point for Studentized range for desired α (found in statistics tables).

α = Level of significance.

k = Number of means evaluated.

df = Degrees of freedom from error from the ANOVA table.

S_y = Standard error of the mean $(MSE/n)^{1/2}$.

MSE = Mean square of error from the ANOVA table.

The next step is to compare the values in the triangular table to the calculated value for R_k. Look at each diagonal element and compare R_k to the values in the column for k. If any value in the diagonal element is larger than

the calculated value, R_k, then the two means are significantly different. Repeat the comparison for R_{k-1} and the differences in the diagonal element k-1 and for R_{k-2} and diagonal element k-2 (22).

Duncan's Multiple Range Test is a test that determines if a group's mean is significantly different from each other. The test is performed by taking all of the sample means (k), arranging them in increasing order of magnitude, and then calculating the differences between the adjacent sample means. Next, the existence of significant variation between each of the two groups of (k-1) adjacent ordered means is checked. The range of group one is computed by subtracting the first mean (the smallest) from the (k-1) mean, this value is compared to a standardized R_s value (defined later). If the standardized value is less than the calculated range then the first mean and the (k-1) mean are significantly different. The same procedure is repeated for the range of group 2, the second mean in order of magnitude is subtracted from the k^{th} mean (the largest). If a set does not give a significant result, it is concluded that the variability of means within that group of (k-1) is random and no further testing for differences within that group of (k-1) means is warranted. This result is indicated in the table of means by underlining with a common line the range of means that produced the not significant result. If there is a significant difference between the means, all the sets of (k-2) adjacent ordered means in the block are examined, and so on. This procedure is illustrated in the following section (23).

Group Means A B C D E

(k = 5)

where A is the smallest and E is the largest.

In the (k-1) step the interval for testing is 5-1=4, therefore mean A is compared to mean D and mean B is compared to mean E as these 2 sets are the only sets with a difference of 4. (D - A) and (E - B) are calculated and compared to the calculated R_g value. If (D - A) is larger than R_g then all means from A through D are significantly different and it is time to repeat the process but using (k-2) and an updated value for R_g. If (D-A) is smaller than R_g then there is no significant difference between the means from A through D, and no other tests are required for means A through D.

At each stage, the test consists of comparing the range of the group of adjacent means under study with a critical limit, R_g, which is calculated as:

$$R_g = C(g,\nu,\alpha)(MSE / n)^{1/2} \qquad \text{(Eq. 3)}$$

where

$C(g,\nu,\alpha)$ = a constant found in statistical tables,

g = number of groups,

ν = degrees of freedom for error, from ANOVA table,

α = significance level,

MSE = mean square of error, from ANOVA table,

n = number of observations in group.

Least Significant Difference (LSD) is a measure of how far apart the group means need to be to show significance. Significance can be determined if the difference between group means is greater than the LSD value.

$$LSD = (t_{\alpha,\, DFE})(S)(2/n)^{1/2} \qquad \text{(Eq. 4)}$$

where α = significance level,

DFE = degrees of freedom for error, from ANOVA table,

$(t_{\alpha,\, DFE})$ = t-table value,

S = root mean square of error = $(MSE)^{1/2}$, from ANOVA table,

n = number of data per group.

These tests were selected because they represent the most commonly used tests in statistical research. Three tests were used because multiple comparisons using any one of the three tests, such as used in this project, are not faultless indicators; therefore three were used to see if any of the three would indicate significant differences from the different types of tests. However, it is important to note that when multiple comparisons are interpreted, failure to reject the hypothesis that two or more means are equal should not lead to the conclusion that the population means are in fact equal. Failure to reject the null hypothesis implies only that the difference between population means, if any, is not large enough to be detected with the given sample size (24).

STATISTICAL COMPARISONS OF MODULI

The deflection data collected by LTRC staff from the KUAB Falling Weight Deflectometer for each section is included in Volume 2 -- Appendix 3. Each section was tested at five different locations within the 500 feet length and at each test location four different loads were applied. The loads ranged from approximately 3,500 up to 14,000 pounds which correspond to axle loads of 7,000 to 28,000 pounds. Measured deflections from each load were input into each of the programs in order to backcalculate the layer modulus values for each pavement layer.

Initially, all of the load and deflection data were included in a single analysis and interpretation was found to be very difficult. All of the predicted moduli were significantly different from the laboratory data, primarily because of the stress sensitivity of some pavement layers. This can be expected since the laboratory moduli were developed for an 18 kip load stress level; therefore it was more appropriate to compare laboratory data with predicted data from the 9 kip wheel load.

Therefore, since the 18 kip single axle load is the design load for highway pavements, the project staff decided to concentrate on results with that load to determine if any of the backcalculation programs appeared to be superior to the others. This decision decreased the number of deflection basins to one per location, or five per section. Each program was run using both these individual deflection basins, which were evaluated for each section, and an average of the five deflection basins for each section with the average deflection basin used as

input for each program. These average values are included in Volume 2 -- Appendix 4, and the computer generated moduli generated from both individual and average deflections are shown in Volume 2 -- Appendix 5.

When performing a statistical evaluation of the results from the programs, the sections were grouped by similar characteristics, i.e, the sections with black base layers were grouped together, the sections with a soil cement base were grouped together, and the sections with a cement stabilized sand clay gravel base were grouped together. Also sections with a soil cement base were analyzed separate from the control sections since the control sections had an unusually thick HMA bases (after combining the old surface and old base into one layer). Since Hadley's laboratory data showed the stabilized sand clay gravel and the soil cement material had virtually the same modulus value, these two base types were combined into one group, and analyzed both with and without the control sections. All of the above mentioned groupings were also evaluated using average moduli estimated from both individual and averaged deflections.

A comparison between predicted moduli and measured laboratory moduli that showed no statistical difference is denoted in the output Tables 4-10 by "no significant difference." Comparisons that were significantly differnt are denoted in the output tables by a blank. The statistical analysis output data have been summarized for each computer program to show for each pavement layer which base type results are not significantly different from the laboratory values and which statistical test produced the not significantly different result. The summary from this series of SAS output are contained in Tables 4-10 (the actual SAS

Table 4.

Results of Significance Test Which Compared The Various Material Moduli Predicted From Program 1 With The Laboratory Measured Moduli for Pavements With Different Bases

BASE TYPE	LAYER 1	LAYER 2	LAYER 3	LAYER 4
BLACK BASE[1]	1,2,3[2]			
AVG.[3] BLACK BASE	1,2,3			
SOIL CEMENT[1]	1	1,2,3		
AVG. SOIL CEMENT	1,2,3	1,2,3		
SOIL CEMENT[1] NO CONTROL	1,2,3		1	
AVG.[3] SOIL CEMENT NO CONTROL	1,2,3		1,2,3	
CEMENT TREATED SAND CLAY GRAVEL[1]	1		1,2,3	
AVG.[2] CEMENT TREATED SAND CLAY GRAVEL	1,2,3		1,2,3	
SOIL CEMENT AND CEMENT TREATED SAND CLAY GRAVEL[1]				
AVG.[3] SOIL CEMENT AND CEMENT TREATED SAND CLAY GRAVEL	1,2,3	1,2,3		
SOIL CEMENT AND CEMENT TREATED SAND CLAY GRAVEL[1] NO CONTROL	1			
AVG.[3] SOIL CEMENT AND CEMENT TREATED SAND CLAY GRAVEL NO CONTROL	1,2,3		1,2,3	

1. Moduli backcalculated from individual deflection basins.

2. Number Key
   1 = No significant difference from Student-Newman-Keuls test.
   2 = No significant difference from Duncan Multiple Range test.
   3 = No significant difference from Least Significant Difference test.

3. Moduli backcalculated from the average of five deflection basins.

Table 5.

Results of Significance Test Which Compared The Various Material Moduli Predicted From Program 2 With The Laboratory Measured Moduli for Pavements With Different Bases

BASE TYPE	LAYER 1	LAYER 2	LAYER 3	LAYER 4
BLACK BASE[1]	1,2,3[2]	1,2,3		
AVG.[3] BLACK BASE	1,2,3			1
SOIL CEMENT[1]	1,2,3	1,2,3		
AVG. SOIL CEMENT	1,2,3	1,2,3	1,2,3	
SOIL CEMENT[1] NO CONTROL	1,2,3		1,2,3	
AVG.[3] SOIL CEMENT NO CONTROL	1,2,3		1,2,3	1,2,3
CEMENT TREATED SAND CLAY GRAVEL[1]	1,2,3		1,2,3	
AVG.[2] CEMENT TREATED SAND CLAY GRAVEL	1,2,3		1,2,3	1,2,3
SOIL CEMENT AND CEMENT TREATED SAND CLAY GRAVEL[1]	1,2,3	1,2		
AVG.[3] SOIL CEMENT AND CEMENT TREATED SAND CLAY GRAVEL	1,2,3	1,2,3	1,2,3	
SOIL CEMENT AND CEMENT TREATED SAND CLAY GRAVEL[1] NO CONTROL	1,2,3		1,2	
AVG.[3] SOIL CEMENT AND CEMENT TREATED SAND CLAY GRAVEL NO CONTROL	1,2,3		1,2,3	1

1. Moduli backcalculated from individual deflection basins.

2. Number Key
   1 = No significant difference from Student-Newman-Keuls test.
   2 = No significant difference from Duncan Multiple Range test.
   3 = No significant difference from Least Significant Difference test.

3. Moduli backcalculated from the average of five deflection basins.

Table 6.

Results of Significance Test Which Compared The Various Material Moduli Predicted From Program 3 With The Laboratory Measured Moduli for Pavements With Different Bases

BASE TYPE	LAYER 1	LAYER 2	LAYER 3	LAYER 4
BLACK BASE[1]	1,2,3[2]			
AVG.[3] BLACK BASE	1,2,3			
SOIL CEMENT[1]				
AVG. SOIL CEMENT	1	1,2,3	1,2,3	
SOIL CEMENT[1] NO CONTROL	1		1,2,3	
AVG.[3] SOIL CEMENT NO CONTROL	1,2,3		1,2,3	
CEMENT TREATED SAND CLAY GRAVEL[1]	1		1,2,3	
AVG.[2] CEMENT TREATED SAND CLAY GRAVEL	1,2		1,2,3	
SOIL CEMENT AND CEMENT TREATED SAND CLAY GRAVEL[1]				
AVG.[3] SOIL CEMENT AND CEMENT TREATED SAND CLAY GRAVEL	1,2,3	1,2,3	1,2,3	
SOIL CEMENT AND CEMENT TREATED SAND CLAY GRAVEL[1] NO CONTROL	1,2,3		1,2,3	
AVG.[3] SOIL CEMENT AND CEMENT TREATED SAND CLAY GRAVEL NO CONTROL	1,2,3		1,2,3	

1. Moduli backcalculated from individual deflection basins.

2. Number Key
   1 = No significant difference from Student-Newman-Keuls test.
   2 = No significant difference from Duncan Multiple Range test.
   3 = No significant difference from Least Significant Difference test.

3. Moduli backcalculated from the average of five deflection basins.

Table 7.

Results of Significance Test Which Compared The Various Material Moduli Predicted From Program 4 With The Laboratory Measured Moduli for Pavements With Different Bases

BASE TYPE	LAYER 1	LAYER 2	LAYER 3	LAYER 4
BLACK BASE[1]	1,2,3[2]			
AVG.[3] BLACK BASE	1,2,3	1,2,3		
SOIL CEMENT[1]	1,2,3			
AVG. SOIL CEMENT	1,2,3	1,2,3	1,2,3	
SOIL CEMENT[1] NO CONTROL	1,2,3		1	
AVG.[3] SOIL CEMENT NO CONTROL	1,2,3		1,2,3	
CEMENT TREATED SAND CLAY GRAVEL[1]	1,2,3		1,2,3	
AVG.[2] CEMENT TREATED SAND CLAY GRAVEL	1		1,2,3	
SOIL CEMENT AND CEMENT TREATED SAND CLAY GRAVEL[1]	1,2,3	1,2,3		
AVG.[3] SOIL CEMENT AND CEMENT TREATED SAND CLAY GRAVEL	1,2,3	1,2,3	1,2	
SOIL CEMENT AND CEMENT TREATED SAND CLAY GRAVEL[1] NO CONTROL	1,2,3			
AVG.[3] SOIL CEMENT AND CEMENT TREATED SAND CLAY GRAVEL NO CONTROL	1,2,3		1,2,3	

1. Moduli backcalculated from individual deflection basins.

2. Number Key
   1 = No significant difference from Student-Newman-Keuls test.
   2 = No significant difference from Duncan Multiple Range test.
   3 = No significant difference from Least Significant Difference test.

3. Moduli backcalculated from the average of five deflection basins.

Table 8.

Results of Significance Test Which Compared The Various Material Moduli Predicted From Program 5 With The Laboratory Measured Moduli for Pavements With Different Bases

BASE TYPE	LAYER 1	LAYER 2	LAYER 3	LAYER 4
BLACK BASE[1]	1,2,3[2]			
AVG.[3] BLACK BASE	1,2,3	1		
SOIL CEMENT[1]	1,2,3	1,2,3		
AVG. SOIL CEMENT	1,2,3	1,2,3	1,2,3	
SOIL CEMENT[1] NO CONTROL	1,2,3		1	
AVG.[3] SOIL CEMENT NO CONTROL	1,2,3		1,2,3	
CEMENT TREATED SAND CLAY GRAVEL[1]	1,2,3		1,2,3	
AVG.[2] CEMENT TREATED SAND CLAY GRAVEL	1		1,2,3	
SOIL CEMENT AND CEMENT TREATED SAND CLAY GRAVEL[1]	1,2,3	1,2,3		
AVG.[3] SOIL CEMENT AND CEMENT TREATED SAND CLAY GRAVEL	1,2,3	1,2,3	1,2,3	
SOIL CEMENT AND CEMENT TREATED SAND CLAY GRAVEL[1] NO CONTROL	1,2,3		1	
AVG.[3] SOIL CEMENT AND CEMENT TREATED SAND CLAY GRAVEL NO CONTROL	1,2,3		1,2,3	

1. Moduli backcalculated from individual deflection basins.

2. Number Key
   1 = No significant difference from Student-Newman-Keuls test.
   2 = No significant difference from Duncan Multiple Range test.
   3 = No significant difference from Least Significant Difference test.

3. Moduli backcalculated from the average of five deflection basins.

Table 9.

Results of Significance Test Which Compared The Various Material Moduli Predicted From Program 6 With The Laboratory Measured Moduli for Pavements With Different Bases

BASE TYPE	LAYER 1	LAYER 2	LAYER 3	LAYER 4
BLACK BASE[1]				
AVG.[3] BLACK BASE	1,2,3[2]			
SOIL CEMENT[1]	1,2,3	1,2,3		1,2,3
AVG. SOIL CEMENT	1,2,3	1,2,3	1,2,3	1,2,3
SOIL CEMENT[1] NO CONTROL	1		1	1,2,3
AVG.[3] SOIL CEMENT NO CONTROL	1,2,3		1,2,3	1,2,3
CEMENT TREATED SAND CLAY GRAVEL[1]	1,2,3		1,2,3	1,2,3
AVG.[2] CEMENT TREATED SAND CLAY GRAVEL	1,2,3		1,2,3	1,2,3
SOIL CEMENT AND CEMENT TREATED SAND CLAY GRAVEL[1]	1,2,3	1,2,3		
AVG.[3] SOIL CEMENT AND CEMENT TREATED SAND CLAY GRAVEL	1,2,3	1,2,3	1,2,3	1,2,3
SOIL CEMENT AND CEMENT TREATED SAND CLAY GRAVEL[1] NO CONTROL	1		1	1,2,3
AVG.[3] SOIL CEMENT AND CEMENT TREATED SAND CLAY GRAVEL NO CONTROL	1,2,3		1,2,3	1,2,3

1. Moduli backcalculated from individual deflection basins.

2. Number Key
   1 = No significant difference from Student-Newman-Keuls test.
   2 = No significant difference from Duncan Multiple Range test.
   3 = No significant difference from Least Significant Difference test.

3. Moduli backcalculated from the average of five deflection basins.

Table 10.

Analysis of Significance Test Which Compared The Various Material Moduli Predicted From Program 7 With The Laboratory Measured Moduli for Pavements With Different Bases

BASE TYPE	LAYER 1	LAYER 2	LAYER 3	LAYER 4
BLACK BASE[1]	1,2[2]			
AVG.[3] BLACK BASE	1,2,3			
SOIL CEMENT[1]	1,2,3			
AVG. SOIL CEMENT	1,2,3	1,2,3	1,2	
SOIL CEMENT[1] NO CONTROL	1		1,2,3	
AVG.[3] SOIL CEMENT NO CONTROL	1,2,3		1,2,3	
CEMENT TREATED SAND CLAY GRAVEL[1]	1,2,3		1,2,3	
AVG.[3] CEMENT TREATED SAND CLAY GRAVEL			1,2,3	
SOIL CEMENT AND CEMENT TREATED SAND CLAY GRAVEL[1]	1,2,3			
AVG.[3] SOIL CEMENT AND CEMENT TREATED SAND CLAY GRAVEL	1,2,3	1,2,3	1,2	
SOIL CEMENT AND CEMENT TREATED SAND CLAY GRAVEL[1] NO CONTROL	1		1,2,3	
AVG.[3] SOIL CEMENT AND CEMENT TREATED SAND CLAY GRAVEL NO CONTROL	1,2,3		1,2	

1. Moduli backcalculated from individual deflection basins.

2. Number Key
   1 = No significant difference from Student-Newman-Keuls test.
   2 = No significant difference from Duncan Multiple Range test.
   3 = No significant difference from Least Significant Difference test.

3. Moduli backcalculated from the average of five deflection basins.

output is included in Volume 2 -- Appendix 6). In order to more easily digest these results a summary table has been prepared to show the number of results which were not significantly different results by layer and by program. This analysis is described in the next section.

When attempting to evaluate all the programs to determine which one appears to work best for Louisiana materials, three things were considered; 1) results from the statistical analysis which determined for each program the number of times that calculated moduli results for each layer were not significantly different from the laboratory moduli determined by Hadley (15); 2) the percentage of times that the predicted modulus values go to either the upper or lower limit of the moduli range during the iterations in the backcalculation process; and 3) the capabilities and ease of use of each program.

Results of the Statistical Analysis of Modulus Results

In the statistical analysis, the backcalculated modulus for each layer was compared to the laboratory value determined for that material by Hadley (15). If the difference between the backcalculated and measured moduli was not significant, the program which generated the modulus from deflection data was judged to be an adequate prediction of modulus. Using the deflection data on all test sections, the results from the statistical analysis are summarized in Table 11 which was prepared from the data contained in Tables 4-10 showing by sections which layers had

Table 11.

Number of Section Types By Layer Where the Moduli Predicted From FWD Deflections Were Not Significantly Different From Measured Laboratory Moduli

Program	Layer 1	Layer 2	Layer 3	Layer 4
1	11	3	5	0
2	12	5	8	4
3	11	2	8	0
4	12	4	7	0
5	12	5	8	0
6	11	4	8	9
7	11	2	8	0

predicted moduli not significantly different from laboratory moduli for each program. In all cases a 5 percent level of significance was used. Based on the moduli results from program 1 as shown in Table 11:

a) The predicted moduli for layer 1 were not significantly different from the measured laboratory moduli for 11 of the 12 test sections.

b) The predicted moduli for layer 2 were not significantly different from the measured laboratory moduli for only three of the 12 section types. For the remaining nine sections types, the predicted moduli were significantly different from the laboratory values.

c) The predicted moduli for layer 3 were not significantly different from the measured laboratory moduli for only five of the 12 sections types. For the remaining seven sections, the predicted moduli were significantly different from the laboratory values.

d) For the subgrade moduli from program 1, all predicted moduli for the 12 section types were significantly different from the laboratory values.

The remaining six programs can be analyzed in the same manner as program 1 by examining the data in Table 11.

From Table 11, four of the programs appear to more accurately predict moduli than the rest. The programs with the larger overall numbers recorded in Table 11 are 2, 4, 5, and 6, with 2 and 6 having the largest numbers of non-significant results. The next section contains a program to program comparison of the output from these four.

(2 vs 4) -- For layers 2 and 3 program 2 has one more section where the predicted moduli are not significantly different from the lab data than does program 4, and for the subgrade program 2 has four sections where the predicted moduli are not significantly different from the laboratory data while program 4 has none (Table 11). Output from program 4 is not significantly different from the lab data for the average of all the black bases for layer 2 (Table 7) while output from program 2 is significantly different (Table 5). However, output from program 2 for individual deflection basins is not significantly different from the lab data for both black base and soil cement for layer 2 (Table 5) while outputs from program 4 are significantly different (Table 7).

(2 vs 5) -- For layers 1, 2, and 3 program 2 has the same number of section types where the predicted moduli are not significantly different from the lab values as program 5, however, for layer 4 (subgrade) program 2 has four sections showing results that are not significantly different while program 5 has none (Table 11). Results from programs 2 and 5 flip flop when comparing black base results from individual deflections, and average deflections. Output from program 2 has layer 2 for the black base section being not significantly different (Table 5) while program 5 does show significance (Table 8). However, output from program 5 is not significantly different for layer 2 for the average black base sections (Table 8), while program 2 does show significance (Table 5).

(2 vs 6) -- For layers 1 and 2 program 2 has one more section where the predicted moduli are not significantly different from the lab moduli than does program 6 (Table 11). Both programs have eight of the 12 layer 3 section types being not significantly different from the measured laboratory moduli, while for layer 4 the predicted moduli for the subgrade is not significantly different for five more section types for program 6 than for program 2. For layer 2 black base materials, program 2 shows non-significant results (Table 5), while program 6 does not (Table 9). For the following section types, program 6 predicts subgrade modulus not significantly different from lab data (Table 9) while, program 2 shows them being significantly different (Table 5): average of soil cement, soil cement no control, sand clay gravel, average of soil cement and sand clay gravel, and soil cement and sand clay gravel no control.

(4 vs 5) -- For layer 1 both programs have the same number of not significantly different results. Program 5 has one more section being not significantly different than program 6 for both layers 2 and 3. For layer 4 neither program has any not significant values. Output from program 5 has a not significantly different value for layer 2 of the soil cement section (Table 8) while output from program 4 does not (Table 7). Program 5 also has a not significant result for layer 3 of the soil cement and sand clay gravel no control section (Table 8), while program 4 does not (Table 7).

(4 vs 6) -- For layer 1 program 4 has one more section being not significantly different than program 6. Both programs have four of the 12 layer 2 section types being not significantly different from the measured laboratory moduli, while for layer 4, program 6 has one more section being not significantly different than program 4 for layer 3, and nine more for layer 4. Output from program 4 has layer 1 of the black base section type showing not significantly different results (Table 7), while output from program 6 does not (Table 9). For layer 2 program 4 has the average black base section type being not significantly different (Table 7), while program 6 is significantly different (Table 9). Also for layer 2, program 6 has the soil cement section type being not significantly different (Table 9), while program 4 is significantly different (Table 7). Program 6 has the soil cement section type for layer 3 being not significantly different (Table 9), while program 4 is significantly different (Table 7).

(5 vs 6) -- For layers 1 and 2 program 5 has one more section type where the predicted moduli are not significant different from the lab data than does program 6, but the same number of not significantly different values for layer 3 (Table 11). Program 6 has nine section types being not significantly different for layer 4 (Table 9) while program 5 has none (Table 8). Program 5 has layer 2 of the black base section type and layer 3 of the average black base section type being not significant (Table 8), while program 6 does not (Table 21).

After noting the above comparisons, programs 2 and 6 (MODULUS Step 3 and WESDEF) appear to more adequately predict values comparable with laboratory results more often than the others.

Percentage at Limit

It is also important to determine the number of times that a computer program reaches the limit of the moduli range in an attempt to converge on a solution. When a program goes to a limit before converging, the predicted moduli may be suspect since the program tried to go beyond the limits of the moduli range. These limits are set at a reasonable range to give the program considerable flexibility in converging on a solution, however, when the predicted values are at a limit the results may be questioned. Output from the statistical analysis shows which programs predicted moduli that were not significantly different from the measured laboratory moduli. These two types of information have been summarized in Tables 12-23 by type of base material and pavement layer by indicating with 1) an asterisk (*) if the moduli predicted by the program are significantly different (not desirable) from the laboratory measured moduli, and 2) by a number, if the predicted moduli are not significantly different (desirable) from the laboratory measured moduli, which represents the percent of time that the predicted modulus is at either the upper or lower limit of the allowable range input by the user or as calculated internally by the program. Tables 24 and 25 contain a summary of Tables 12-23 for the percentages of predicted moduli values that are at either the upper or lower limit for each program.

Table 12.

Significance Test Results and Percent of Values at Either the Upper or Lower Modulus Limit for Black Base Section Results for Each Program From Individual Deflection Basins

Test	Program	Percent of Values at Limit			
		Layer 1	Layer 2	Layer 3	Layer 4
SNK	1	1.1[1]	*	*	*
SNK	2	14.4	26.7	*	*
SNK	3	40.0	*	*	*
SNK	4	22.2	*	*	*
SNK	5	28.9	*	*	*
SNK	6	*	*	*	*
SNK	7	51.1	*	*	*
DUNCAN	1	1.1	*	*	*
DUNCAN	2	14.4	26.7	*	*
DUNCAN	3	40.0	*	*	*
DUNCAN	4	22.2	*	*	*
DUNCAN	5	28.9	*	*	*
DUNCAN	6	*	*	*	*
DUNCAN	7	51.1	*	*	*
LSD	1	1.1	*	*	*
LSD	2	14.4	26.7	*	*
LSD	3	40.0	*	*	*
LSD	4	22.2	*	*	*
LSD	5	28.9	*	*	*
LSD	6	*	*	*	*
LSD	7	*	*	*	*

* Means there is a significant difference between program predicted and laboratory measured moduli.

[1] Numbers in the column is the percent of values at either an upper or lower modulus limit for results showing no significant difference between predicted and laboratory measured moduli.

Table 13.

Significance Test Results and Percent of Values at Either the Upper or Lower Modulus Limit for Black Base Section Results for Each Program From Averaged Deflection Basins

TEST	Program	Percent of Values at Limit			
		Layer 1	Layer 2	Layer 3	Layer 4
SNK	1	1.1[1]	*	*	*
SNK	2	14.4	*	*	0
SNK	3	40.0	*	*	*
SNK	4	22.2	38.9	*	*
SNK	5	28.9	27.8	*	*
SNK	6	28.9	*	*	0
SNK	7	51.1	*	*	*
DUNCAN	1	1.1	*	*	*
DUNCAN	2	14.4	*	*	*
DUNCAN	3	40.0	*	*	*
DUNCAN	4	22.2	38.9	*	*
DUNCAN	5	28.9	*	*	*
DUNCAN	6	28.9	*	*	0
DUNCAN	7	51.1	*	*	*
LSD	1	1.1	*	*	*
LSD	2	14.4	*	*	*
LSD	3	40.0	*	*	*
LSD	4	22.2	38.9	*	*
LSD	5	28.9	*	*	*
LSD	6	28.9	*	*	0
LSD	7	51.1	*	*	*

* Means there is a significant difference between program predicted and laboratory measured moduli.

[1] Numbers in the column is the percent of values at either an upper or lower modulus limit for results showing no significant difference between predicted and laboratory measured moduli.

Table 14.

Significance Test Results and Percent of Values at Either the Upper or Lower Modulus Limit for Soil Cement Section Results for Each Program From Individual Deflection Basins

Test	Program	Percent of Values at Limit			
		Layer 1	Layer 2	Layer 3	Layer 4
SNK	1	1.1[1]	8.8	*	*
SNK	2	14.4	26.7	*	*
SNK	3	*	*	*	*
SNK	4	22.2	*	*	*
SNK	5	28.9	27.8	*	*
SNK	6	28.9	42.2	*	*
SNK	7	51.1	*	*	*
DUNCAN	1	*	8.8	*	*
DUNCAN	2	14.4	26.7	*	*
DUNCAN	3	*	*	*	*
DUNCAN	4	22.2	*	*	*
DUNCAN	5	28.9	27.8	*	*
DUNCAN	6	28.9	42.2	*	*
DUNCAN	7	51.1	*	*	*
LSD	1	*	8.8	*	*
LSD	2	14.4	26.7	*	*
LSD	3	*	*	*	*
LSD	4	22.2	*	*	*
LSD	5	28.9	27.8	*	*
LSD	6	28.9	42.2	*	*
LSD	7	51.1	*	*	*

* Means there is a significant difference between program predicted and laboratory measured moduli.

[1] Numbers in the column is the percent of values at either an upper or lower modulus limit for results showing no significant difference between predicted and laboratory measured moduli.

Table 15.

Significance Test Results and Percent of Values at Either the Upper or Lower Modulus Limit for Soil Cement Section Results for Each Program From Averaged Deflection Basins

Test	Program	Percent of Values at Limit			
		Layer 1	Layer 2	Layer 3	Layer 4
SNK	1	1.1[1]	8.8	*	*
SNK	2	14.4	26.7	38.9	*
SNK	3	40.0	34.4	48.9	*
SNK	4	22.2	38.9	62.2	*
SNK	5	28.9	27.8	48.9	*
SNK	6	28.9	42.2	55.6	0
SNK	7	51.1	42.2	54.4	*
DUNCAN	1	1.1	8.8	*	*
DUNCAN	2	14.4	26.7	38.9	*
DUNCAN	3	*	34.4	48.9	*
DUNCAN	4	22.2	38.9	62.2	*
DUNCAN	5	28.9	27.8	48.9	*
DUNCAN	6	28.9	42.2	55.6	0
DUNCAN	7	51.1	42.2	54.4	*
LSD	1	1.1	8.8	*	*
LSD	2	14.4	26.7	38.9	*
LSD	3	*	34.4	48.9	*
LSD	4	22.2	38.9	62.2	*
LSD	5	28.9	27.8	48.9	*
LSD	6	28.9	42.2	55.6	0
LSD	7	51.1	42.2	*	*

* Means there is a significant difference between program predicted and laboratory measured moduli.

[1] Numbers in the column is the percent of values at either an upper or lower modulus limit for results showing no significant difference between predicted and laboratory measured moduli.

Table 16.

Significance Test Results and Percent of Values at Either the Upper or Lower Modulus Limit for Soil Cement (No Control) Section Results for Each Program From Individual Deflection Basins

Test	Program	Percent of Values at Limit			
		Layer 1	Layer 2	Layer 3	Layer 4
SNK	1	1.1[1]	*	22.2	*
SNK	2	11.1	*	27.8	*
SNK	3	25.6	*	26.7	*
SNK	4	17.8	*	42.2	*
SNK	5	16.7	*	27.8	*
SNK	6	26.7	*	36.7	0
SNK	7	41.1	*	34.4	*
DUNCAN	1	0.0	*	*	*
DUNCAN	2	11.1	*	27.8	*
DUNCAN	3	*	*	26.7	*
DUNCAN	4	17.8	*	*	*
DUNCAN	5	16.7	*	*	*
DUNCAN	6	*	*	*	0
DUNCAN	7	*	*	34.4	*
LSD	1	0	*	*	*
LSD	2	11.1	*	27.8	*
LSD	3	*	*	26.7	*
LSD	4	17.8	*	*	*
LSD	5	16.7	*	*	*
LSD	6	*	*	*	0
LSD	7	*	*	34.4	*

* Means there is a significant difference between program predicted and laboratory measured moduli.

[1] Numbers in the column is the percent of values at either an upper or lower modulus limit for results showing no significant difference between predicted and laboratory measured moduli.

Table 17.

Significance Test Results and Percent of Values at Either the Upper or Lower Modulus Limit for Soil Cement (No Control) Section Results for Each Program From Averaged Deflection Basins

Test	Program	Percent of Values at Limit			
		Layer 1	Layer 2	Layer 3	Layer 4
SNK	1	0[1]	*	22.2	*
SNK	2	11.1	*	27.8	0
SNK	3	25.6	*	26.7	*
SNK	4	17.8	*	42.2	*
SNK	5	16.7	*	27.8	*
SNK	6	26.7	*	36.7	0
SNK	7	41.1	*	34.4	*
DUNCAN	1	0	*	22.2	*
DUNCAN	2	11.1	*	27.8	0
DUNCAN	3	25.6	*	26.7	*
DUNCAN	4	17.8	*	42.2	*
DUNCAN	5	16.7	*	27.8	*
DUNCAN	6	26.7	*	36.7	0
DUNCAN	7	41.1	*	34.4	*
LSD	1	0	*	22.2	*
LSD	2	11.1	*	27.8	0
LSD	3	25.6	*	26.7	*
LSD	4	17.8	*	42.2	*
LSD	5	16.7	*	27.8	*
LSD	6	26.7	*	26.7	0
LSD	7	41.1	*	34.4	*

* Means there is a significant difference between program predicted and laboratory measured moduli.

[1] Numbers in the column is the percent of values at either an upper or lower modulus limit for results showing no significant difference between predicted and laboratory measured moduli.

Table 18.

Significance Test Results and Percent of Values at Either the Upper or Lower Modulus Limit for Cement Treated Sand Clay ---Gravel Section Results for Each Program From Individual Deflection Basins

Test	Program	Percent of Values at Limit			
		Layer 1	Layer 2	Layer 3	Layer 4
SNK	1	1.1[1]	*	40.9	*
SNK	2	14.4	*	38.9	*
SNK	3	40.0	*	48.9	*
SNK	4	22.2	*	62.2	*
SNK	5	28.9	*	48.9	*
SNK	6	28.9	*	55.6	0
SNK	7	51.1	*	54.4	*
DUNCAN	1	*	*	40.9	*
DUNCAN	2	14.4	*	38.9	*
DUNCAN	3	*	*	48.9	*
DUNCAN	4	22.2	*	62.2	*
DUNCAN	5	28.9	*	48.9	*
DUNCAN	6	28.9	*	55.6	0
DUNCAN	7	51.1	*	54.4	*
LSD	1	*	*	40.9	*
LSD	2	14.4	*	38.9	*
LSD	3	*	*	48.9	*
LSD	4	22.2	*	62.2	*
LSD	5	28.9	*	48.9	*
LSD	6	28.9	*	55.6	0
LSD	7	51.1	*	54.4	*

* Means there is a significant difference between program predicted and laboratory measured moduli.

[1] Numbers in the column is the percent of values at either an upper or lower modulus limit for results showing no significant difference between predicted and laboratory measured moduli.

Table 19.

Significance Test Results and Percent of Values at Either the Upper or Lower Modulus Limit for Cement Treated Sand Clay Gravel Section Results for Each Program From Averaged Deflection Basins

Test	Program	Percent of Values at Limit			
		Layer 1	Layer 2	Layer 3	Layer 4
SNK	1	1.1[1]	*	40.9	*
SNK	2	14.4	*	38.9	0
SNK	3	40.0	*	48.9	*
SNK	4	22.2	*	62.2	*
SNK	5	28.9	*	48.9	*
SNK	6	28.9	*	55.6	0
SNK	7	*	*	54.4	*
DUNCAN	1	1.1	*	40.9	*
DUNCAN	2	14.4	*	38.9	0
DUNCAN	3	40.0	*	48.9	*
DUNCAN	4	*	*	62.2	*
DUNCAN	5	*	*	48.9	*
DUNCAN	6	28.9	*	55.6	0
DUNCAN	7	*	*	54.4	*
LSD	1	1.1	*	40.9	*
LSD	2	14.4	*	38.9	0
LSD	3	*	*	48.9	*
LSD	4	*	*	62.2	*
LSD	5	*	*	48.9	*
LSD	6	28.9	*	55.6	0
LSD	7	*	*	54.4	*

* Means there is a significant difference between program predicted and laboratory measured moduli.

[1] Numbers in the column is the percent of values at either an upper or lower modulus limit for results showing no significant difference between predicted and laboratory measured moduli.

Table 20.

Significance Test Results and Percent of Values at Either the Upper or Lower Modulus Limit for Soil Cement and Cement Treated Sand Clay Gravel Section Results for Each Program From Individual Deflection Basins

Test	Program	Percent of Values at Limit			
		Layer 1	Layer 2	Layer 3	Layer 4
SNK	1	*[1]	*	*	*
SNK	2	14.4	26.7	*	*
SNK	3	*	*	*	*
SNK	4	22.2	38.9	*	*
SNK	5	28.9	27.8	*	*
SNK	6	28.9	42.2	*	*
SNK	7	51.1	*	*	*
DUNCAN	1	*	*	*	*
DUNCAN	2	14.4	26.7	*	*
DUNCAN	3	*	*	*	*
DUNCAN	4	22.2	38.9	*	*
DUNCAN	5	28.9	27.8	*	*
DUNCAN	6	28.9	42.2	*	*
DUNCAN	7	51.1	*	*	*
LSD	1	*	*	*	*
LSD	2	14.4	*	*	*
LSD	3	*	*	*	*
LSD	4	22.2	38.9	*	*
LSD	5	28.9	27.8	*	*
LSD	6	28.9	42.2	*	*
LSD	7	51.1	*	*	*

* Means there is a significant difference between program predicted and laboratory measured moduli.

[1] Numbers in the column is the percent of values at either an upper or lower modulus limit for results showing no significant difference between predicted and laboratory measured moduli.

Table 21.

Significance Test Results and Percent of Values at Either the Upper or Lower Modulus Limit for Soil Cement and Cement Treated Sand Clay Gravel Section Results for Each Program From Averaged Deflection Basins

Test	Program	Percent of Values at Limit			
		Layer 1	Layer 2	Layer 3	Layer 4
SNK	1	1.1[1]	8.8	*	*
SNK	2	14.4	26.7	38.9	*
SNK	3	40.0	34.4	48.9	*
SNK	4	22.2	38.9	62.2	*
SNK	5	28.9	27.8	48.9	*
SNK	6	28.9	42.2	55.6	0
SNK	7	51.1	42.2	54.4	*
DUNCAN	1	1.1	8.8	*	*
DUNCAN	2	14.4	26.7	38.9	*
DUNCAN	3	40.0	34.4	48.9	*
DUNCAN	4	22.2	38.9	62.2	*
DUNCAN	5	28.9	27.8	48.9	*
DUNCAN	6	28.9	42.2	55.6	0
DUNCAN	7	51.1	42.2	54.4	*
LSD	1	1.1	8.8	*	*
LSD	2	14.4	26.7	38.9	*
LSD	3	40.0	34.4	48.9	*
LSD	4	22.2	38.9	*	*
LSD	5	28.9	27.8	48.9	*
LSD	6	28.9	42.2	55.6	0
LSD	7	51.1	42.2	*	*

* Means there is a significant difference between program predicted and laboratory measured moduli.

[1] Numbers in the column is the percent of values at either an upper or lower modulus limit for results showing no significant difference between predicted and laboratory measured moduli.

Table 22.

Significance Test Results and Percent of Values at Either the Upper or Lower Modulus Limit for Soil Cement and Cement Treated Sand Clay Gravel (No Control) Section Results for Each Program From Individual Deflection Basins

Test	Program	Percent of Values at Limit			
		Layer 1	Layer 2	Layer 3	Layer 4
SNK	1	0[1]	*	*	*
SNK	2	11.1	*	27.8	*
SNK	3	25.6	*	26.7	*
SNK	4	17.8	*	*	*
SNK	5	16.7	*	27.8	*
SNK	6	26.7	*	36.7	0
SNK	7	41.1	*	34.4	*
DUNCAN	1	*	*	*	*
DUNCAN	2	11.1	*	27.8	*
DUNCAN	3	25.6	*	26.7	*
DUNCAN	4	17.8	*	*	*
DUNCAN	5	16.7	*	*	*
DUNCAN	6	*	*	*	0
DUNCAN	7	*	*	34.4	*
LSD	1	*	*	*	*
LSD	2	11.1	*	*	*
LSD	3	25.6	*	26.7	*
LSD	4	17.8	*	*	*
LSD	5	16.7	*	*	*
LSD	6	*	*	*	0
LSD	7	*	*	34.4	*

* Means there is a significant difference between program predicted and laboratory measured moduli.

[1] Numbers in the column is the percent of values at either an upper or lower modulus limit for results showing no significant difference between predicted and laboratory measured moduli.

Table 23.

Significance Test Results and Percent of Values at Either the Upper or Lower Modulus Limit for Soil Cement and Cement Treated Sand Clay Gravel (No Control) Section Results for Each Program From Averaged Deflection Basins

Test	Program	Percent of Values at Limit			
		Layer 1	Layer 2	Layer 3	Layer 4
SNK	1	0[1]	*	22.2	*
SNK	2	11.1	*	27.8	0
SNK	3	25.6	*	26.7	*
SNK	4	17.8	*	42.2	*
SNK	5	16.7	*	27.8	*
SNK	6	26.7	*	36.7	0
SNK	7	41.1	*	34.4	*
DUNCAN	1	0	*	22.2	*
DUNCAN	2	11.1	*	27.8	*
DUNCAN	3	25.6	*	26.7	*
DUNCAN	4	17.8	*	42.2	*
DUNCAN	5	16.7	*	27.8	*
DUNCAN	6	26.7	*	36.7	0
DUNCAN	7	41.1	*	34.4	*
LSD	1	0	*	22.2	*
LSD	2	11.1	*	27.8	*
LSD	3	25.6	*	26.7	*
LSD	4	17.8	*	42.2	*
LSD	5	16.7	*	27.8	*
LSD	6	26.7	*	26.7	0
LSD	7	41.1	*	*	*

* Means there is a significant difference between program predicted and laboratory measured moduli.

[1] Numbers in the column is the percent of values at either an upper or lower modulus limit for results showing no significant difference between predicted and laboratory measured moduli.

Table 24.

Frequency and Percentage of Times the Predicted Moduli Was At a Limit, When Control Sections Were Included

Program	Layer 1		Layer 2		Layer 3		Layer 4	
	# at limit	% at limit	# at limit	% at limit	# at limit	% at limit	# at limit	% at limit
1	1	1.1	8	8.8	36	40.0	0	0.0
2	13	14.4	24	26.7	35	38.9	0	0.0
3	36	40.0	31	34.4	49	48.9	1	1.1
4	20	22.2	35	38.9	56	62.2	0	0.0
5	26	28.9	25	27.8	44	48.9	0	0.0
6	26	28.9	38	42.2	50	55.5	0	0.0
7	46	51.1	38	42.2	49	54.4	12	13.2

Table 25.

Frequency and Percentage of Times Predicted Moduli Was At a Limit, When Control Sections Were Not Included

Program	Layer 1		Layer 2		Layer 3		Layer 4	
	# at limit	% at limit	# at limit	% at limit	# at limit	% at limit	# at limit	% at limit
1	0	0.0	4	4.4	16	22.2	0	0.0
2	10	11.1	18	20.0	25	27.8	0	0.0
3	23	25.6	27	30.0	24	26.7	0	0.0
4	16	17.8	20	22.2	38	42.2	0	0.0
5	15	16.7	17	18.9	25	27.8	0	0.0
6	24	26.7	30	33.3	33	36.7	0	0.0
7	37	41.1	33	36.7	31	34.4	4	4.4

Results from Tables 24 and 25 indicate that predicted moduli for programs 1 and 2 were at a limit less than the other programs. However, when looking at the previous step where the programs were compared by number of not significantly different output values, it was observed that programs 2 and 6 gave the best results compared to the rest. When comparing the results from Table 24 for programs 2 and 6 it can be seen that program 2 goes to the limit 58 percent less for layer 1, 40 percent less for layer 2 and 24 percent less for layer 3 than for program 6. Table 25 shows a similar trend with both programs going to limits less when the control sections are eliminated from the analysis. Only program 1 consistently performed better than program 2 in going to the limit a smaller number of times. However, based on the results from Table 11, program 2 is superior to program 1 in backcalculating moduli that are not significantly different from the laboratory determined moduli.

Capabilities and Ease of Program Use

Now comparing the two best programs, 2 and 6, one very important difference between the two is that with MODULUS multiple deflection bowls can be run at the same time, while WESDEF can only evaluate one deflection bowl per run. Secondly, the MODULUS program comes with an extensive user's manual while the projects staff received no formal user's manual with WESDEF. Additionally, the authors are of the opinion that updates to MODULUS will be well documented and easily obtained since it has been adopted for use in the

Strategic Highway Research Program (SHRP) Long Term Pavement Performance (LTPP) program. Finally, the WESDEF output values were at either the upper or the lower limits of the moduli range more often than the output from MODULUS.

COMPARISONS OF RESULTS FROM AVERAGE DEFLECTIONS vs INDIVIDUAL DEFLECTIONS

When considering the procedure to be used in collecting field data for use in backcalculation of moduli to be used in pavement design, the engineer is faced with a decision as to whether to 1) take individual deflection basins and backcalculate moduli from each or, 2) make multiple drops at each location, average the deflections and use the average deflection basin to backcalculate moduli.

In an attempt to determine which of these procedures is superior, the project staff first backcalculated moduli from each deflection basin as shown in Volume 2 -- Appendix 5. Each of the five deflection basins taken on each section for the 18,000 pound axle load were then assumed to be replicate drops even though each was taken from a different location. The average deflection basin was generated by averaging the five readings at each sensor and then using that average basin as input for each program. Project investigators recognize that the variation among these five drops at five different locations should exceed the variation that would occur if the five drops had occurred at the same location.

Therefore calculating the average in this manner should be a worst case test to determine if the moduli from the average deflection basin was superior to the moduli from individual deflection basins. The data which forms the basin for this comparison are found in Tables 12-23.

The comparisons between the averaged deflection data and the individual deflection data can be made by studying the data in adjacent sets of tables: for example, to compare the moduli results from individual and average deflection basins for the black base type pavements the reader is directed to Tables 12 and 13; for soil cement base type pavements see Tables 18 and 19; and for the combination of soil cement and cement stabilized sand clay gravel see Tables 20 and 21. These tables contain the significant test results for all seven programs. However since programs 2 and 6 have been identified as the best candidates for potential use in Louisiana, results for each base type for programs 2 and 6 have been summarized in Table 26. The comparison data in Table 26 is arranged in each block of the table so that the results from individual deflection basins are shown to the left of the slash and the results from the average deflection basin are on the right of the slash. Results form each different base type is also separated in the table. A careful review of the data in Table 26 will show that for the soil cement, cement stabilized sand clay gravel and the combination of all cement stabilized bases the moduli predicted from the average basin was always superior to the moduli predicted form the individual basins for both programs 2 and 6. That is to say, there are fewer asterisks on the right side of the slash than on the left side of the slash. The only base type that did not show uniform improvement when using the average deflection basin to calculate moduli was the black base

and specifically layer 2 using program 2. The authors have no reasonable explanation for this occurrence. Because of the improvements in the prediction of moduli for layers 3 and 4 that arise from using the average deflection basin, the authors recommend that backcalculated moduli be predicted from an average deflection basin rather than from individual deflection basins. Since the thrust of this investigation has been directed toward developing information for use in pavement design using the 1986 AASHTO Design Guide, the researchers suggest that deflection data be secured using only the 9,000 pound load which corresponds to an 18,000 pound single axle load and that the deflection from five replicate drops be averaged as input into program 2, MODULUS 4.0 step 3. Moduli predicted from this procedure can then be plotted along the highway section to determine where any subsections need to be divided up for individual designs.

SUMMARY

After analyzing the programs on the three different levels presented in this chapter, it appears that program 2 (MODULUS 4.0) is the best choice for use in Louisiana. It was observed in the significance comparison that programs 2 and 6 were about the same with program 2 being a little better for layers 1 and 2, while program 6 was a little better for layer 4. The next level of comparison, number of times a predicted value went to the limit, showed program 2 to be much better than program 6. Finally, in the third level of comparison,

capabilities and ease of use; it can be seen that program 2 is superior to program 6 in both capabilities and ease of use.

CONCLUSIONS

As stated in the results, MODULUS 4.0 run utilizing step 3 the "Run a Full Analysis" option (step 2) appears to be the best choice for use in the state of Louisiana. It was observed to be one of two programs to give the best comparison between predicted and laboratory moduli values than the other five programs in the statistical analysis. Also it was judged to be the best program in the other two analysis, number of times the predicted value went to the limit, and the capabilities and ease of use.

For MODULUS 4.0, the statistical analysis showed the moduli values predicted from the average deflection data to be better estimates of laboratory moduli than those predicted from the individual deflection data for all base types except for layer 2 of some sections with a black base. The results indicate that moduli predicted from an average deflection basin calculated from five individual deflection basins from a 9,000 pound load produced better estimate of laboratory moduli than moduli predicted from individual deflection basins.

Future users of the MODULUS 4.0 program should be reminded, however, that results from program must be evaluated using sound engineering judgement. Because the modulus values approached the limits of reasonable values for 14.4 percent of the deflection bowls for layer 1, 26.8 percent for layer 2, and 38.9 percent for layer 3 and that layer 4 compared favorably to laboratory test data in only 33 percent of the section types, one must conclude that the method may not always produce reasonable results. Good engineering judgement must be applied to recognize these output which might be questionable. Such

cases may require that the deflection data be looked at, that checks be made on cross-section elements, or that the deflection survey be repeated.

A limitation of this analysis of programs is that the backcalculated moduli are compared to laboratory moduli which were assumed to be the correct values. Current testing underway as part of the Strategic Highway Research Program indicates that there can be significant variability in M_R values measured in the laboratory. However, improvements in the testing procedure and equipment have been and continue to be realized in this area, so that confidence in future comparisons such as these will continue to grow as these improvements are made and as experience is gained.

RECOMMENDATIONS

The authors recommend that the program MODULUS 4.0 be used to predict moduli from the FWD data, and that the average of five deflection basins be used to estimate the moduli of the pavement layers. The users manual for MODULUS 4.0 is included in Volume 2 -- Appendix 7. However, future studies are necessary to further evaluate the validity of using MODULUS 4.0.

A. MODULUS 4.0 should be evaluated with a wider variety of pavement structures and subgrade types that are spread throughout the State of Louisiana to provide a broader assessment than was possible in this project.

B. The deflection data from the FWD should be taken repeatedly (at least five drops) for the same point at many different points per section. This will enable researchers to evaluate and determine the "optimum" number of drops and test locations needed to properly evaluate a pavement.

C. Only the design load (approximately 9,000 pounds for a wheel load on an 18 kip single axle load) needs to be applied unless the stress sensitivity of the pavement materials is of interest.

D. Laboratory tests, using the improvements continually being realized in M_R laboratory testing, should be conducted in conjunction with the field testing to provide a wider basis of comparison between backcalculated and laboratory measured M_R values. Since LTRC currently has a project underway to develop

Table 26.
Comparisons of Results from Programs 2 and 6 Showing the Effects of Using Individual and Average Deflections On Significance Test Results and Percent of Moduli Values at Either the Upper or Lower Limit for Both Test Sections and Control Sections

Test	Program	Base Type	Layer 1	Layer 2	Layer 3	Layer 4
			Percent of Values at Limit			
SNK	2	Black	14.4[1]/14.4[2]	26.7/*[3]	*/*	*/0
	6		*/28.9	*/*	*/*	*/0
Duncan	2		14.4/14.4	26.7/*	*/*	*/*
	6		*/28.9	*/*	*/*	*/0
LSD	2		14.4/14.4	26.7/*	*/*	*/0
	6		*/28.9	*/*	*/*	*/0
SNK	2	Soil Cement	14.4/14.4	26.7/26.7	*/38.9	*/0
	6		28.9/28.9	42.2/42.2	*/55.6	*/0
Duncan	2		14.4/14.4	26.7/26.7	*/38.9	*/*
	6		28.9/28.9	42.2/42.2	*/55.6	*/0
LSD	2		14.4/14.4	26.7/26.7	*/38.9	*/*
	6		28.9/28.9	42.2/42.2	*/55.6	*/0
SNK	2	Cement Stabilized Sand Clay Gravel	14.4/14.4	*/*	38.9/38.9	*/*
	6		28.9/28.9	*/*	55.6/55.6	0/0
Duncan	2		14.4/14.4	*/*	38.9/38.9	*/0
	6		28.9/28.9	*/*	55.6/55.6	0/0
LSD	2		14.4/14.4	*/*	38.9/38.9	*/0
	6		28.9/28.9	*/*	55.6/55.6	0/0
SNK	2	Soil Cement and Cement Stabilized Sand Clay Gravel	14.4/14.4	26.7/26.7	*/38.9	*/*
	6		28.9/28.9	42.2/42.2	*/55.6	*/0
Duncan	2		14.4/14.4	26.7/26.7	*/38.9	*/*
	6		28.9/28.9	42.2/42.2	*/55.6	*/0
LSD	2		14.4/14.4	26.7/26.7	*/38.9	*/*
	6		28.9/28.9	42.2/42.2	*/55.6	*/0

[1] First number is percent of moduli at upper or lower limit as calculated from individual deflection basins.

[2] Second number is percent of moduli at upper or lower limit as calculated from average deflection basins.

[3] * means there is a significant difference between program predicted and laboratory measured moduli.

laboratory procedures for measuring M_R, this recommendation is a logical extension of that work.

REFERENCES

1. Elliott, R.P. and S.I. Thornton, "Resilient Modulus and AASHTO Pavement Design," Transportation Research Record 1196, Transportation Research Board, Washington, D.C., 1988, pp 116-124.

2. Yoder, E.J. and M.W. Witczak,Principles of Pavement Design, Second Edition, John Wiley and Sons, New York, NY, 1975, p. 262.

3. Jung, F.W.,"Nondestructive Testing: Interpretation of Deflection Bowl for Falling Weight Deflectometer Tests on Flexible Pavements," Journal of Testing and Evaluation, Vol. 17, No. 6, American Society for Testing Material, Philadelphia, PA, Nov. 1989, pp. 333-343.

4. Rwebangira, T., R.G. Hicks, and M.Truebe, "Sensitivity Analysis of Selected Backcalcultion Procedures," Transportation Research Record 1117, Transportation Research Board, Washington, D.C., 1987, pp. 25-37.

5. BOUSDEF User's Guide, Oregon Department of Transportation, Eugene, OR.

6. Chua, K.M., "Evaluation of Moduli Backcalculation Programs for Low-Bolume Roads," Nondestructive Testing of Pavements and Backcalculation of Moduli, ASTM STP 1026, A.J. Bush III and G.Y. Baladi, Eds., American Society for Testing and Materials, Philadelphia, PA, 1989, pp. 398-414.

7. Lytton, R.L., F.P.Germann, Y.J. Chou and S.M. Stoffels, "Determining Asphaltic Concrete Pavement Structural Properties by Nondestructive Testing," Transportation Research Board, Washington, D.C., June 1990.

8. Anderson, M., "A Data Base Method for Backcalculation of Composite Pavement Layer Moduli," Nondestructive Testing of Pavements and Backcalculation of Moduli, ASTM STP 1026, A.J. Bush III and G.Y. Baladi, Eds., American Society for Testing and Materials, Philadelphia, PA, 1989, pp. 201-216.

9. Tam, W.S. and S.F. Brown, "Back-Analyzed Elastic Stiffnesses: Comparison Between Different Evaluation Procedures," Nondestructive Testing of Pavements and Backcalculation of Moduli, ASTM STP 1026, A.J. Bush III and G.Y. Baladi, Eds., American Society for Testing and Materials, Philadelphia, PA, 1989, pp. 189-200.

10. Mahoney, J.P., N.F. Coetzee, R.N. Stubstad, and S.W. Lee, "A Performance Comparison of Selected Backcalculatio Computer Programs," Nondestructive Testing of Pavements and Backcalculation of Moduli, ASTM STP 1026, A.J. Bush III and G.Y. Baladi, Eds., American Society for Testing and Materials, Philadelphia, PA, 1989, pp. 452-467.

11. Ali, N.A. and N.P. Khosla, "Determination of Layer Moduli Using a Falling Weight Deflectometer," Transportation Research Record 1117, Transportation Research Board, Washington, D.C., 1987, pp. 1-10.

12. Germann, F.P. and R.L. Lytton, "Temperature, Frequency and Load Level Correction Factors for Backcalculated Moduli Values," Nondestructive Testing of Pavements and Backcalculation of Moduli, ASTM STP 1026, A.J. Bush III and G.Y. Baladi, Eds., American Society for Testing and Materials, Philadelphia, PA, 1989, pp. 431-451.

13. Van Cauwelaert, F.J., D.R. Alexander, T.D. White, and W.R. Barker,"Multilayer Elastic Program for Backcalculatio Layer Moduli in Pavement Evaluation," Nondestructive Testing of Pavements and Backcalculation of Moduli, ASTM STP 1026, A.J. Bush III and G.Y. Baladi, Eds., American Society for Testing and Materials, Philadelphia, PA, 1989, pp. 171-188.

14. Lee, S.W., J.P. Mahoney, and N.C. Jackson, "Verification of Backcalculation of Pavement Moduli," Transportation Research Record 1196, Transportation Research Board, Washington, D.C., 1988, pp. 85-95.

15. Hadley, W.O., "Materials Characterization and Inherent Variation Analysis - Fundamental Material Properties of Construction Materials," Report 78-1, Materials Research Laboratory, Louisiana Tech University, Ruston, Louisiana, January 1983.

16. Hadley, W.O., "Materials Characterization and Inherent Variation Analysis - Fundamental Material Properties of Construction Materials," Report 78-2, Materials Research Laboratory, Louisiana Tech University, Ruston, Louisiana, January 1983.

17. EVERCALC User's Guide, Version 3.3, Washington State Department of Transportation, Olympia, WA, 1992.

18. Roberts, F.L., T.W. Kennedy, and G.E. Elkins,"Material Properties to Minimize Distress In Zero-Maintenance Pavements," Report No. FHWA-RD-80, Austin Research Engineers, Austin, Texas, 1980.

19. Chou, Y.J., J. Uzan, and R.L. Lytton, "Backcalculation of Layer Moduli from Nondestructive Pavement Deflection Data Using the Expert System Approach," Nondestructive Testing of Pavements and Backcalculation of Moduli, ASTM STP 1026, A.J. Bush III and G.Y. Baladi, Eds., American Society for Testing and Materials, Philadelphia, PA, 1989, pp. 341-354.

20. Thompson, M.R., "ILLI-PAVE Based NDT Analysis Procedures," Nondestructive Testing of Pavements and Backcalculation of Moduli, ASTM STP 1026, A.J. Bush III and G.Y. Baladi, Eds., American Society for Testing and Materials, Philadelphia, PA, 1989, pp. 487-501.

21. Phone conversation with Joe P. Mahoney, University of Washington, Seattle, WA,July 1992.

22. Anderson, V.L. and R.A. McLean, Design of experiments, A Realistic Approach, Marcel Dekker, Inc., New York, NY, 1974; pp. 10-12.

23. Kotz, S. and N.L. Johnson, Encyclopedia of Statistical Sciences, Volume 2, John Wiley and Sons, Inc, New York, NY, 1982, pp.424-425.

24. SAS User's Guide: Statistics, SAS Institute Inc., 1982 Edition, Cary, NC, 1982.

This public document is published at a total cost of $ 1,125.36 . One Hundred Twenty (120) copies of this public document were published in this first printing at a cost of $ 555.36 . The total cost of all printings of this document including reprints is $ 1,125.36 . This document was published by Louisiana State University, Graphic Services, 3555 River Road, Baton Rouge, Louisiana 70802, to report and publish research findings of the Louisiana Transportation Research Center as required in R.S.48:105. This material was printed in accordance with standards for printing by State Agencies established pursuant to R.S.43:31. Printing of this material was purchased in accordance with the provisions of Title 43 of the Louisiana Revised Statutes.

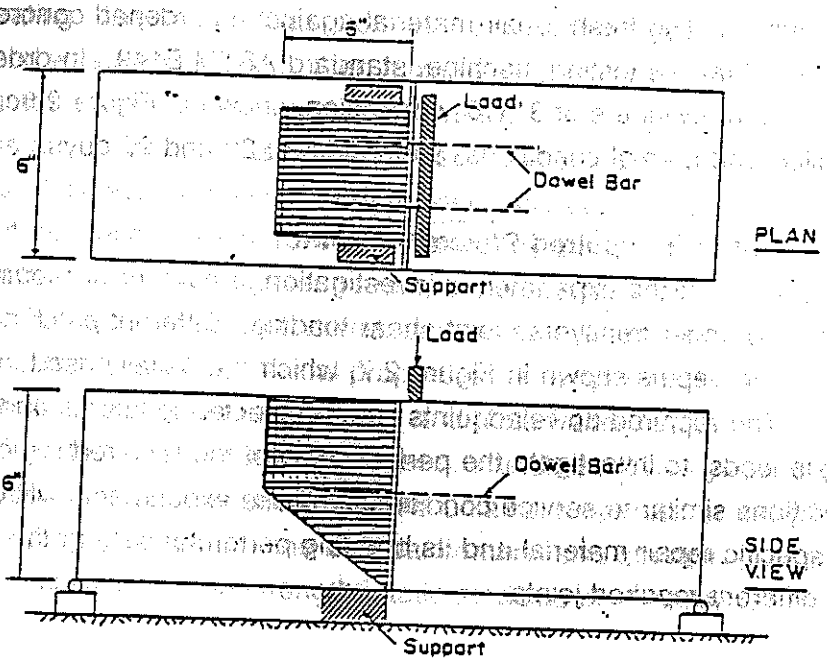

Figure 2.7c
Shear test of a repaired joint

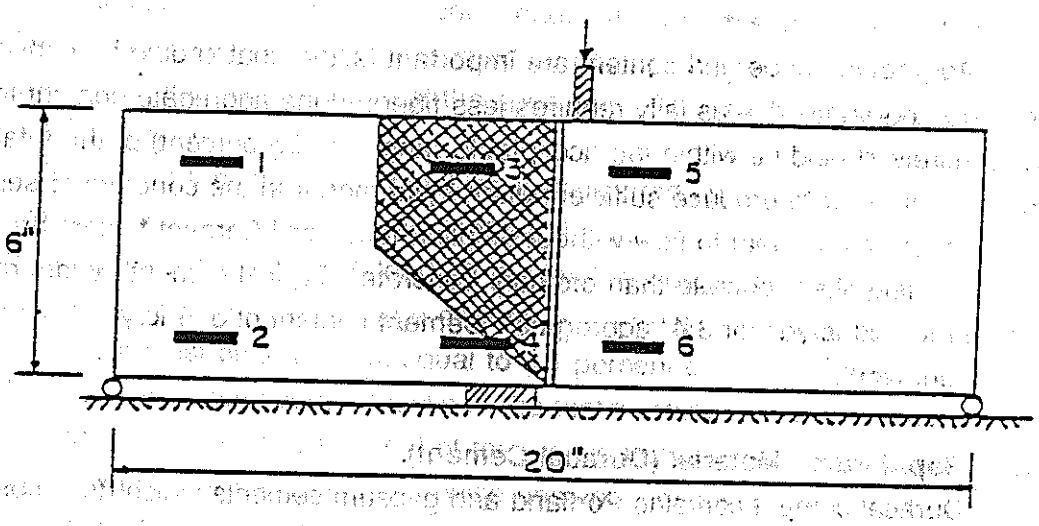

Figure 2.7d
Locations of the strain gages attached to a repaired joint specimen

generally involves casting fresh repair material against a hardened concrete and pulling in standard tensile testing machine, standard ASTM E149. In order to carry out this test, twenty-four cylinders of 3" x 6" dimension, shown in Figure 2.6c, were cured under controlled and normal conditions, and tested at 28 and 90 days.

2.4.4 Shear Test of a Repaired Pavement Joint

In this phase of the experimental investigation, a number of repaired pavement joints were tested under transverse joint shear loading. Different patching configurations and depths shown in Figure 2.7, which are usually used in the field, were studied. The repaired doweled joints were subjected to lateral loads, simulating the traffic axle loads, to investigate the performance of the repaired region under loading conditions similar to service conditions. These experiments will determine the merits of a specific repair material and its bonding performance with the surrounding concrete in different repaired joints.

2.4.5 Steel Fiber Concrete

The content of the fibers for a given concrete depends primarily on the material properties that need to be improved and to what level. The upper limit of fiber content is dictated by the effect that the fiber has on the workability. On the other hand, the steel fiber content should not be below the lower limit in order to get the acceptable benefit gained from the presence of the fiber. In the present work, 88 lb/yd^3 of XOREX steel fiber of 2-inch length and 57 aspect ratio (length/diameter) was added to the concrete producing acceptable workability of the steel fibrous concrete. The volume of the fiber was 0.67 percent.

Aggregate shape and content are important factors that should be considered. The large aggregate size usually requires less fibers. Fine aggregate content for steel fiber concrete should be within the acceptable range (45-55 percent) of the total aggregate in order to produce sufficient quantity of mortar in the concrete to separate the fibers and allow them to flow without tangling together. Cement factors are usually higher for steel fiber concrete than ordinary concrete. Typical cement factors range from 550 to 700 lb/yd^3 for 3/4" aggregate. Cement content of 576 lb/yd^3 was used in the present work.

2.4.6 Rapid Patch Material (Duracal Cement)

Duracal cement contains Portland and gypsum cements which develops high, early strength, and expands slightly. It can be used neat or aggregated. In the present work, the proportions of Duracal cement to sand weight was 1:1 as recommended by the manufacturer.

A horizontal shaft mortar mixer was used in mixing the rapid patch material. Mixing was done by pouring in water and then adding one-half of the sand while the

operating. Dry cement was then added to sand and water and finally the g sand was added. It was then mixed until it was lump-free, but not for more ve minutes. The mix was used immediately.

Unless a special test is specified, Duracal cement will set in approximately 20 minutes. It should be noted that dirty water and equipment will accelerate this al to set, and acceleration from dirty conditions can cause problems.

For each material investigated herein, experimental specimens similar to the shown in Figure 2.2 were cast, cured, and tested. Thirty specimens were used to ss the employed materials' biaxial properties. The specimens were cured under rolled conditions in the laboratory room and tested after 7 days.

In addition to the biaxial test specimens, standard ASTM cylinders and beams ast, cured, and tested to determine the uniaxial properties at the time of biaxial ng. These properties include the uniaxial compressive strength (f_c'), flexural nsile strength, splitting tensile strength, static modulus of elasticity (E), and Poisson's o (v).

4.7 Test Procedure: Procedure for the Biaxial Testing of Brittle Repair Materials

Apparatus

1. Testing Machine: The testing machine employed consists of the standard universal testing machine producing compression and a set up of hydraulic jacks in the orthogonal direction, as shown in Figure 2.3, producing tensile loading.
   The university testing machine should be of a type having sufficient capacity and capable of providing continuous loading without shocks.
2. The university testing machine should be equipped with a circular bearing block bearing on the upper surface of the specimen. The bottom bearing block is not used in this test.
3. If the load of a compression machine is registered on a dial, the dial shall be provided with a graduated scale that can be read to at least the nearest 0.1 percent of the full scale load. If the load is indicated in digital form, the numerical display must be large enough to be read easily and the numerical increment must be of at least equal to 0.1 percent of the full scale load.
4. The position of the hydraulic jacks in the testing frame should be made movable to adjust the alignment of the testing frame and the specimen. This alignment is very important, otherwise unstable conditions may arise.
5. The testing set-up is equipped with three steel bearing blocks (each one inch thick) together with the circular bearing block of the universal testing machine which is aligned at the center of the steel plates. These plates are placed on the upper surface of the specimen in order to ensure transfer of a uniform compression load to the specimen.

2.5 TEST RESULTS

The investigation employed a Portland cement concrete of standard mix for both the parent material and the patched material. The standard mix consisted of ASTM Type I Portland cement with weight proportions of cement-to-sand-to-coarse aggregate of 1:2:3.6. Cement content was 576 lb/yd^3 (344 kg/m^3), and the water-cement ratio was 0.42. The maximum coarse aggregate size was 3/4". The concrete was air entrained with air content as measured by the pressure method (ASTM C231), ranging from 4.6 to 5.3 percent by volume. Slump ranged from 2 to 3 in. (50 to 75 mm). Unit weight of the fresh concrete ranged from 142.6 to 144.8 lb/ft^3 (2300 to 2335 kg/m^3).

During the investigation, 30 batches of concrete mix were used. Since concrete properties vary from one batch to another, it is expected to get slightly different properties from each batch. In order to obtain average properties, the specimens of each test were distributed over these batches. Properties of the fresh concrete of each batch are tabulated in Table A.1 (Appendix A). The difference between the maximum and the minimum value of each property was compared with the precision recommended by ASTM C192 and are shown in Table A.2.

By comparing the precision of the obtained values with the ASTM standard in Table A.2, it can be concluded that the results of slump, air content, and unit weight of these batches are acceptable. Thus, the specimens made from these batches met the standard procedure and provide satisfactory and consistent results.

In the following sections, we will discuss the test results of the properties of the hardened concrete.

2.5.1 Uniaxial Strength of Concrete

Results of compressive strength of patch material (normal concrete) are tabulated in Tables A.3 and A.4. Two groups of (6 x 12 in.) cylinders were tested. The first group was tested in order to obtain the uniaxial properties of the patch material, while the second group was used as the control group in testing the material under the biaxial state of stress. The average values of concrete compressive strength at 28 days and 3 months are 4700 psi and 5400 psi, respectively. The specimens that were tested after 28 days were cured under room temperature conditions, while the specimens that were tested after three months were cured under normal temperature and moisture. Hence the deviation in the results of a concrete strength of three months is due to randomness of the environment.

Some of the cylindrical concrete specimens were used to determine the values of the modulus of elasticity E, and Poisson's ratio ν. Based on ASTM C469, the values of these properties are tabulated in Table A.5. The average values of the modulus of elasticity E, and Poisson's ratio ν were obtained, 5.0 x 10^6 psi and 0.16, respectively.

In investigating the tensile properties of brittle material, the most popular method used to determine tensile strength is the split-cylinder (Brazilian) indirect tension test. The popularity of this test may be because it is easy to perform and uses the same cylindrical specimen and testing equipment that are used in compression tests. The flexural test is also an indirect tensile strength test, however, it does not measure tensile strength but measures the modulus of rupture.

In the present study, tensile properties of brittle repair material were obtained by two types of tests: splitting tensile strength, and a flexural test using simple beam with third-point loading. The results of splitting-cylinder test are tabulated in Table A.6 with average values of 368 psi of 28 days and 382 psi of 90 days. Flexural beam tests gives results on modulus of rupture as shown in Tables A.7 and A.8. The average value of the modulus of rupture was obtained 625 psi and 700 psi of concrete beams after 28 and 90 days, respectively. Load-deflection response of concrete beam under flexural testing is shown in Figure 2.8 and tabulated in Tables A.9 and A.10. It should be noted that the concrete of 28 days was cured under control temperature and moisture, while the 90-day concrete was cured under environmental conditions. The concrete at 90 days is stiffer than the concrete beam at 28 days. This is clear by comparing the results shown in Figure 2.8.

Generally, in indirect tensile strength tests such as the split-cylinder and the beam flexural test, the actual state of stress in the test specimen is unknown and cannot be accurately predicted from the applied load. By the proposed set-up in Figure 2.3 used in the present study, it was possible to load the specimen in direct tension. In this case, the stress is uniformly distributed over the test cross section. In addition, the special shape specimen shown in Figure 2.4 assures that failure occurs sufficiently far from the ends of the specimen. The stress-strain relations for uniaxial tension of the concrete specimen are tabulated in Tables A.11 to A.14 and shown in Figures 2.9 to 2.14. The results of the present study were compared with the available previous work. A comparison with the stress-strain relation of uniaxial tension proposed by Gopalartnam and Shah *[39]* is shown in Figure 2.9 and with the curve proposed by Meier, et al. *[40]* is shown in Figure 2.10. From these figures, good agreement was achieved, and it can be concluded that the proposed set-up and specimen shape together with the approach may be used to study the behavior of brittle material subjected to biaxial tension-compression.

Testing of brittle material, as concrete, in tension poses the problem of inability to obtain post-peak response. The stress-strain curve obtained by Meier, et al. *[40]* did not possess any descending branch because of their test technique. In the present study, it was not difficult to get some of the descending branch.

From the stress-strain relation of uniaxial tension of concrete shown in Figure 2.9 it can be shown that the strain at failure (300 μstr.) is almost twice as large as the

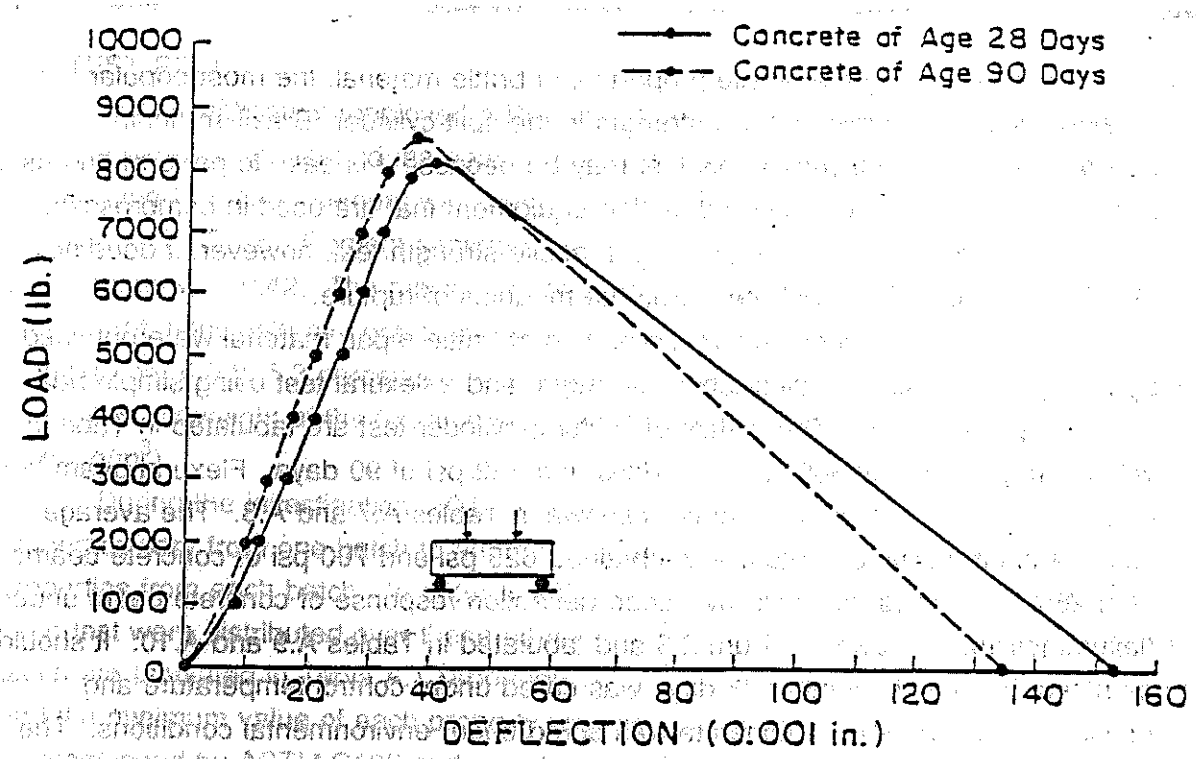

Figure 2.8
Load-deflection relation of plain concrete under flexural

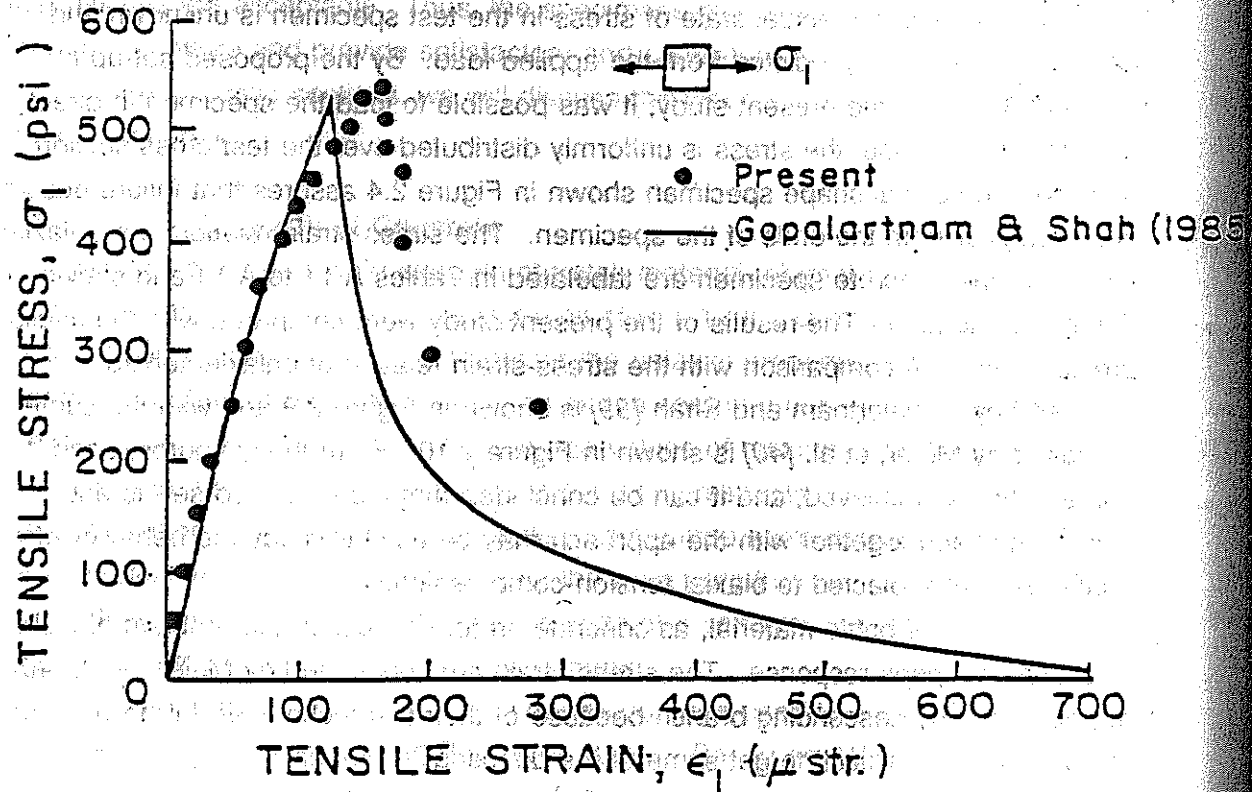

Figure 2.9
Stress-strain for concrete subjected to uniaxial tension

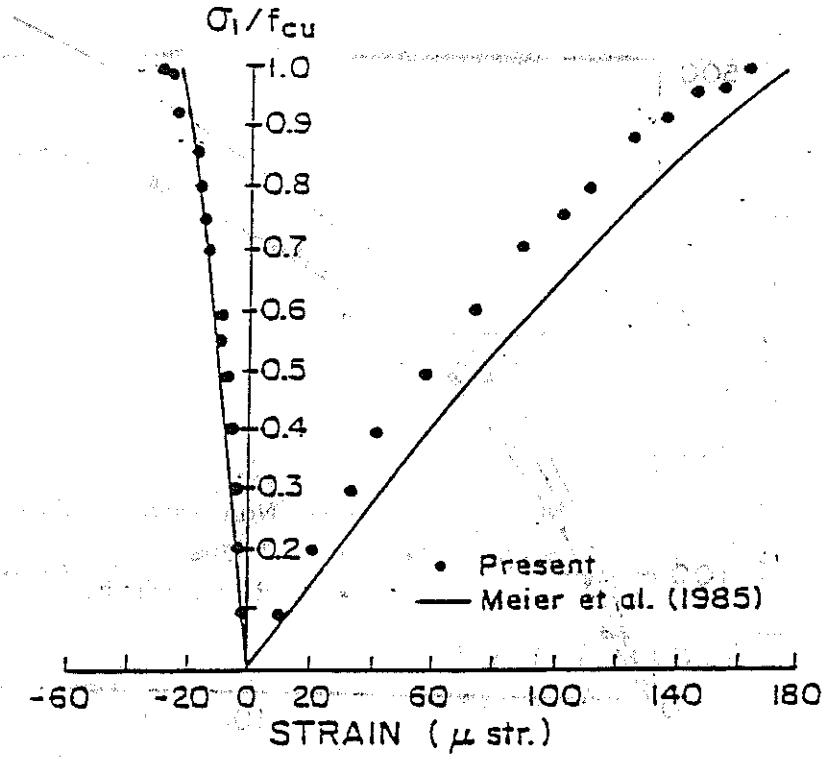

Figure 2.10

Stress-strain response for concrete under uniaxial tension

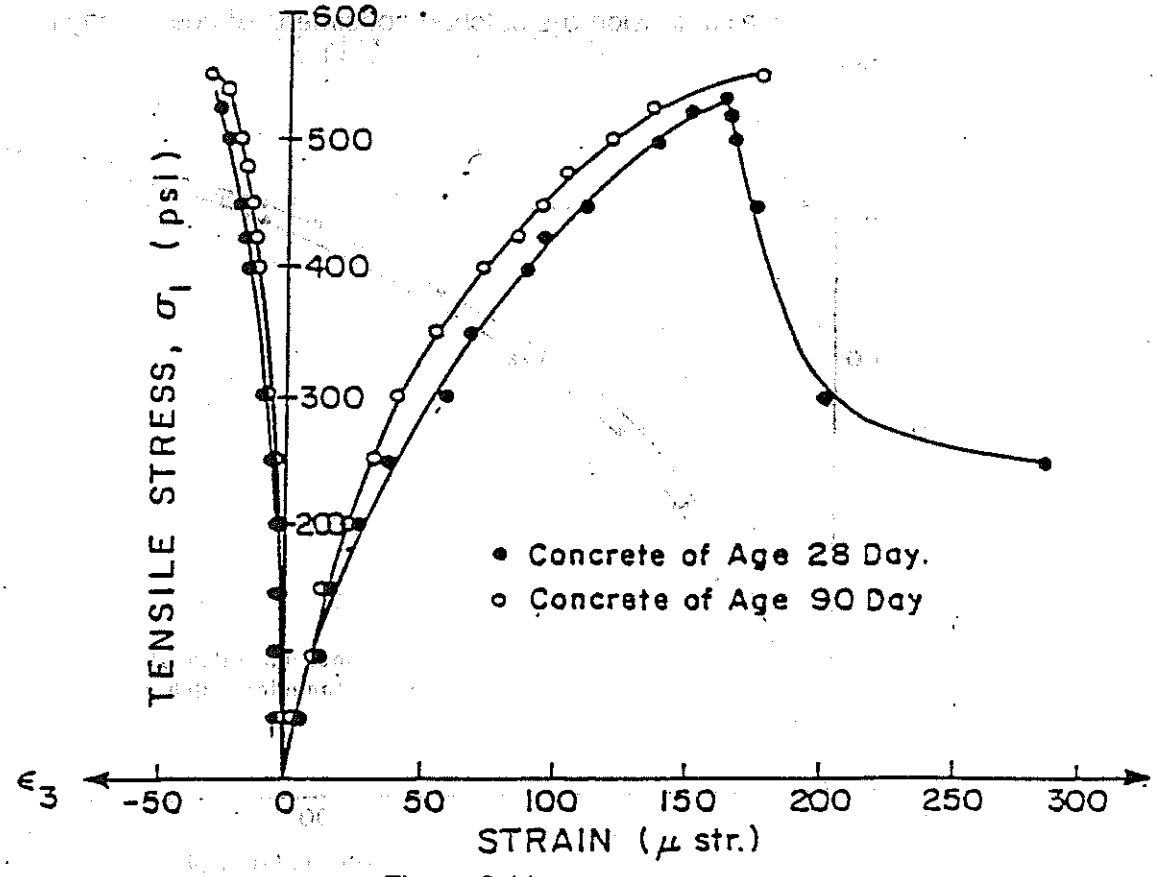

Figure 2.11

Stress-strain of concrete of different age in uniaxial tension

[illegible] who show that the failure strain is twice the strain at peak stress.

Uniaxial direct tension tests were conducted for 18 specimens. These specimens constituted four groups. Two of these groups are concrete specimens of 28 and 90 days. The other two are patched concrete specimens of 28 and 90 days. One specimen from each group was tested with strain gages attached. Figure 2.11 shows the stress-strain relations of concrete of age 90 days subjected to uniaxial tension and compared with the stress-strain relations of concrete of age 28 days. The results are tabulated in Table A.12. The behavior of patched specimens of age 28 and 90 days subjected to uniaxial tension are tabulated in Tables A.13 and A.14 and shown in Figures 2.12 and 2.13. The effect of the environmental condition and patching material can be seen from Figure 2.14.

In the experiments performed on the patched specimens, two different patch shapes were tested. The first type consists of a transition patch shape while the second type consists of a rectangular patch. The testing program was performed on each type using three different depths of the patch material, namely, 2, 7, and 10 inches.

In testing these patched specimens under uniaxial tension, it was noticed that the 2 inch depth-patched specimens for both types failed under tensile failure, while all the other specimens failed by bond failure.

The stress-strain relationships of the 2 inch depth patch specimens subjected to uniaxial tension are tabulated in Table A.13 and shown in Figure 2.12. From this figure, it can be shown that both the peak stress and the corresponding strain are larger in the case of transition patched specimen than the rectangular patched specimen.

Compression tests under a monotonically increasing compressive stress were conducted for 21 specimens distributed over four groups of tests. Some of these specimens were tested with strain gages attached. The results of these tests are shown in Tables A.15 to A.19 and drawn in Figures 2.15 to 2.19.

Figure 2.15 shows the relationship of stress to strain for plain concrete under uniaxial compression loading. The peak stress, f_{cu}, of the uniaxial rectangle strength is 3055 psi for this specimen. However, the average value of uniaxial compressive strength from rectangular cross sections was obtained 3170 psi. In Figure 2.15, the principal strains ε_1 and ε_3 are in the direction of the principal stresses σ_1 and σ_3, respectively.

The stress-strain behavior (Figure 2.15) is almost linear when the stress is less than 35 percent of the ultimate stress. At this stress level, it is called the elastic limit *[10]* or discontinuous point *[13]*. It should be noted that this point is equivalent to the initial yield point in the theory of plasticity. It is a well known fact that in uniaxial compression test, the microcracks develop parallel to the axis of loading. In the

compressive strength.

Stress-strain response of concrete at 90 days is shown in Figure 2.16. The effect of patched shape and depth is shown in Figures 2.17 to 2.19.

Two different types of patched specimens were tested under uniaxial compression. The first type consists of transition patch, the second type consists of rectangular patch. Both types were tested using three different depths, namely 2, 7, and 10 inches.

In subjecting these patched specimens to uniaxial compression, it was noticed that a single hair crack appeared at the bonding surface at very low loads, but it did not cause failure. Compression failure was the mode of failure of this test. The stress-strain relationships of the patched specimens subjected to uniaxial compression were measured and tabulated in Tables A.17 and A.18. Figures 2.17 (a,b,c), 2.18 and 2.19 show these relationships.

In Figure 2.17(a), stress-strain relationships for transition patched subjected to uniaxial compression, the peak stress and the corresponding strain were increased by decreasing the patch depth. The same conclusion can be made for the rectangular patch, as shown in Figure 2.17(b).

In a comparison between the transition patch and rectangular patch, both types were tested under uniaxial compression using fixed patch depth (d = 7 inches). The stress-strain relationships of this set were drawn in Figure 2.18. It can be shown that the specimen of transition patch is stiffer than the rectangular one.

Finally, it should be noted that the stress-strain curves obtained in the present investigation were similar to shape in both uniaxial compression and tension in comparison with other investigations.

2.5.2. Biaxial State of Stress

Since patched material is subjected to a biaxial state of stress, testing under uniaxial stress conditions may lead to a poorer performance. The remedy is a better representative testing of the material for a more realistic formulation of its response in the structure. This is done by subjecting the material to biaxial state of stress. Details of patched material behavior under a biaxial state of stress will be discussed here.

Seventy-four specimens, shown in Figures 2.4 and 2.5, were distributed over four groups of tests: (1) plain concrete of age 28 days, (2) plain concrete at 90 days, (3) patched specimens at 28 days, and (4) patched specimens at 90 days. Patched specimens include two different configurations, partial and transition, with three different depths each. All these specimens were subjected to a biaxial state of stress. Some of them were tested using strain gages attached.

The series of ultimate strength tests were performed using a sequential loading path rather than proportional loading, in which the compressive stress was applied first to a prescribed level relative to the uniaxial compressive strength and then held constant followed by tensile stress along another axis of the specimen until failure occurred. The loading path used here is shown in Figure 2.20. The reason why we select this type of loading is to adequately investigate the shape of the failure envelope in the tensile-compressive region. Previous investigations *[10], [43]* indicated that the failure-envelope of the tension-compressive region contains some inflection points which represent a transition from tensile mode of failure at a lower compressive stress level to compressive failure at higher compressive stress levels.

The material investigation undertaken with the new device dealt with the strength and stress-strain behavior of both plain concrete and patched concrete under biaxial tensile-compressive loading. In order to verify the apparatus capabilities, standard uniaxial cylinder compression and split-cylinder tests were conducted as a prelude to the investigation. The uniaxial compression and tensile strengths of plain concrete at 28 days, as measured by these tests, were 4700 psi (32.4 MPa) and 365 psi (2.5 MPa), respectively. These results are markedly different from the uniaxial compressive and tensile strength as measured in the new device. The compressive and tensile strengths obtained in the new set-up were 3170 psi (21.9 MPa) and 535 psi (3.7 MPa), respectively.

The ultimate strength data of the concrete subjected to biaxial tension-compression are summarized in the form of biaxial stress envelopes as shown in Figures 2.21 to 2.24, and tabulated in Tables A.20 to A.23. The effect of environmental conditions and patching on ultimate strength are shown in Figures 2.22 to 2.24, in which the stresses are nondimensionalized by dividing them with the uniaxial compressive rectangular strength of plain concrete. The average compressive rectangular strength, f_{cu}, was (- 3170 psi) at 28 days. From the ultimate strength envelope obtained in this investigation, the effect of the principal stress ratio on the ultimate strength is evident in these figures. It can be seen that, depending on the principal stress ratio (σ_1/σ_3), the ultimate strength in biaxial tension-compression is smaller than in uniaxial compression.

In order to verify the capabilities of the new device, the experimental data obtained here are compared with previous investigations *[11], [40]* and shown in Figure 2.21. It can be concluded that a good agreement was achieved.

The influence of patch shape and depth were studied by testing concrete specimens of two different patch shapes namely rectangular and transition shape. Each shape includes three depths 2, 7, and 10 inches. Specimens with a transition patch were stronger than specimens with a rectangular patch. Within each patch, strength was decreased as depth was increased from 2 to 7 to 10 inches. The effect of patch shape and depth on uniaxial strength reduction is shown in the following table.

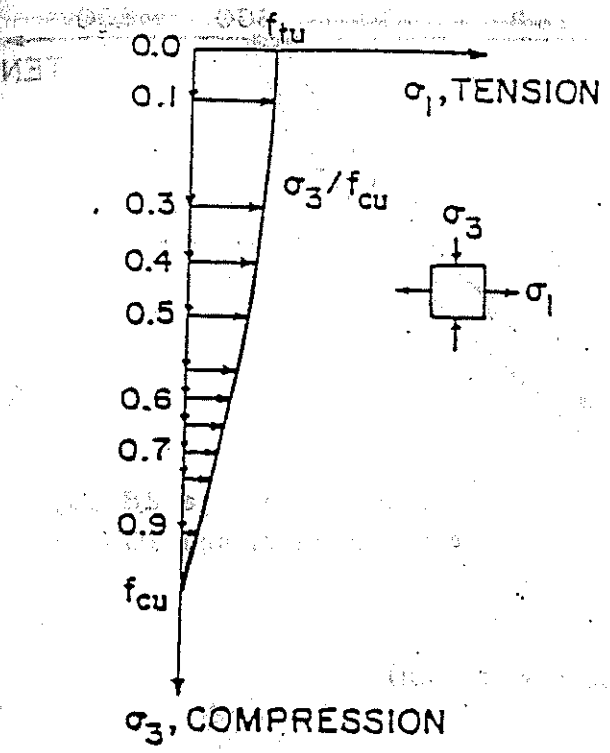

Figure 2.20
Stress paths in the biaxial stress plane

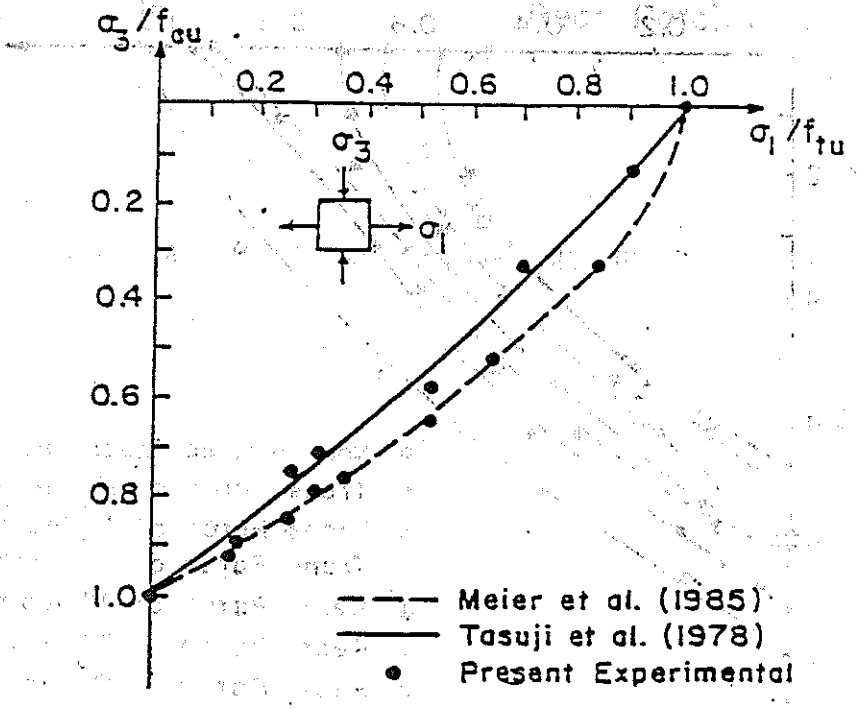

Figure 2.21
Ultimate strength envelop of biaxial tension-compression

	d=2"	d=7"	d=10"	d=2"	d=7"	d=10"
σ_3	2950	2665	2550	2860	2570	2350
σ_1	435	350	270	415	315	235
σ_3/f_{cu}	0.93	0.84	0.80	0.9	0.81	0.73
σ_1/f_{tu}	0.87	0.70	0.54	0.83	0.63	0.47

f_{cu} and f_{tu} are the uniaxial compressive and tensile strength of the non-patched rectangular specimens which are equal to 3170 and 500 psi, respectively.

Table A.24 and Figure 2.25 show the stress-strain relationship for concrete subjected to biaxial loading at different stress ratios. Comparison with Chen and Chen *[20]* and Tasuji, et al. *[11]* shows good agreement with the present experimental investigation.

Figure 2.26 shows the effect of principal stress ratio (σ_1/σ_3) for plain concrete at 28 days. When tensile stress σ_1 was introduced, both peak stress and corresponding strain decreased. The material became more brittle and a lower load was required to produce self-propagation microcracks under tension-compression biaxial than under uniaxial compression.

From these figures, in which the typical relationships of stress-strain for the various ratios of biaxial tension-compression are shown, the compressive strain corresponding to peak stress of uniaxial compression was about -2000 microstrain and the average value of the corresponding tensile strain was about +530 microstrain. In biaxial tension-compression, the average value at the peak stress of both the principal compressive strain and the principal tensile strain decreased as the applied tensile stress increased. In uniaxial tension, shown in Figure 2.9, the average value of the principal tensile strain at the ultimate stress (ε_1) was about +160 microstrain.

The stress-strain relations of the concrete subjected to biaxial tension-compression is shown in Figure 2.26. They all have similar shapes for different σ_1/σ_3 ratios. It can be seen that for a given value of the axial stress (σ_3), the strain in the corresponding direction ε_3 is increased by increasing the tensile stress. For example, for the ratio (σ_1/σ_3) = - 0.034, the increase in strain, ε_3, compared with uniaxial is about 63 percent at 65 percent of uniaxial ultimate load.

The stress-strain relationship of concrete at 90 days subjected to different ratios of biaxial tension-compression is tabulated in Table A.25 and shown in Figure 2.27. The effect of patching shape and depth is shown in Tables A.26 and A.27 and Figures 2.28 to 2.30.

Two different sets of patched specimens were tested under biaxial tension-compression state of loading. The first set consists of a transition patch of two

subjected to different stress ratios, namely, σ_1/σ_3 = - 0.22, - 0.28, and - 0.38.

The stress-strain relationships of these two sets are shown in Figure 2.28. This figure shows the comparison between the response of the transition patched specimens and the response of the rectangular patched specimen when subjected to a biaxial state of stress with σ_1/σ_3 = - 0.28. Figure 2.29 shows the behavior of the transition patch when subjected to three different stress ratios, namely, - 0.22, -0.28, and - 0.38.

In the biaxial test of both transition and rectangular patched specimens, it was observed that for a patch depth of 7 inches, three different modes of failure occurred depending on the stress ratios. Tensile failure was observed when the ratio of the tensile stress to compressive stress (σ_1/σ_3) was between 1/15 and 1/2. When the stress ratio was smaller than 1/15, compression failure was dominant. For ratios higher than 1/2, the bond mode of failure was observed.

Figures 2.31 to 2.33 show photographs of failure patterns of plain and patched concrete under uniaxial and biaxial loading. Tensile splitting is the dominant failure mode in both uniaxial and biaxial states of stress, with the fracture surface perpendicular to the direction of the maximum tensile strain. The failure surface in all specimens tested here show that there are no cracks that passed directly through the coarse aggregate. This is perhaps because the aggregate used in this study forced the cracks to go around.

Under uniaxial compression, fracture occurred by the formation of cracks parallel to the applied load and orthogonal to the unloaded surface of the specimen. Under uniaxial tension, failure was by the formation of a single crack perpendicular to the direction of the maximum tensile stress.

Under a biaxial state of stress, concrete cracks or crushes at tensile or compressive stress levels smaller than uniaxial cracking, f_{tu}, or uniaxial crushing, f_{cu}. In the present tests, under combined tension and compression, a single continuous crack normal to the maximum tensile strain direction was formed except for ratios of the tensile stress to compressive stress smaller than 0.05, for which several cracks were observed and crushing fracture occurred. In the experiments conducted by Kupfer, et al. *[10]* when the ratio of the applied tensile to compressive stress was more than 0.07, a cracking mode of failure was observed in the specimens. For smaller ratios, a crushing mode was dominant. This supports the observation made in the present investigation.

material is essential and the strength of the repair material should be similar to that of the parent material.

A number of tests are in use to evaluate bonding. The tests used here include the slant shear test, direct tensile test, and direct shear test. The results of these tests were used to evaluate the quality and strength of the bond.

In the slant shear test (Figure 2.6a), the bond between repair material and parent material is evaluated by crushing the cylinder in a compression testing machine and recording the failure load. In the present study, the slant-shear test was conducted using 3 x 6 in cylinders with a 45 degree cut, although, ASTM C882 specifications require a 30 degree slant, but this is technically impractical for a 3 x 6 in cylinder. Results of the slant shear tests are tabulated in Tables A.28 and A.29 and shown in Figure 2.34. Slant shear strength was expressed as the failure load divided by the nominal cylinder cross-section. This strength provides a comparative measure of shear bond, and the failure modes are also of interest. The failure modes are given in Table A.30(a) and some examples are shown in Figure 2.35. All the specimens tested under direct shear were failed by bond failure, while the specimens tested under direct tension show three different failure modes as shown in Table A.30(b) and Figure 2.35.

2.5.4 Shear Test of a Repaired Pavement Joint

In the final phase of the testing program, a number of repaired pavement joints were tested under transverse joint shear loading. Two different patching configurations, transition patch and rectangular patch, were examined. Each patching configuration consists of three different patch depths 2, 4, and 6 inches, as shown in Figure 2.7.

In this testing program, the repaired doweled joints were subjected to lateral loads, shown in Figure 2.7, simulating the traffic axle loads. These experiments were made in order to determine the merits of the repair material and its bonding performance with the surrounding concrete. The performance of the repaired region under loading conditions similar to service conditions was investigated in this phase of the test program.

The repaired doweled joints were subjected to lateral loads up to failure, and the ultimate load was recorded. Shear stress due to the peak load was calculated at the interface of the parent material and the repair material. Failure loads and shear stresses are tabulated in Tables A.31 and A.32.

Some of the repaired doweled joints were tested with strain gages attached. This set consists of specimen without patch, specimen with full depth of transition

The specimens with strain gages attached were subjected to lateral load up to failure. The response of these specimens to the applied load is tabulated in Tables A.33 and A.34 and drawn in Figures 2.36 and 2.37. It should be noted that the strain recorded in these figures is the strain that was measured at point number 4, as shown in Figure 2.7.

From Figure 2.36, it can be seen that there is no significant difference in the response of the transition and the rectangular patch. However, comparing the response of the patched specimen and the response of the plain specimen, the area under the curve of the patched specimen is almost 40 percent of the area under the curve of the plain specimen.

It was observed that all the specimens tested in this test program were failed by bracking mode failure. A single crack was started at the bottom fiber of the specimen under the applied load, then the crack tended to change direction going toward the interface of the parent and the patch material.

2.5.5 Test Results of Fiber Concrete and Duracal Cement

In the present work, a Portland cement concrete was used for both the ordinary concrete and the steel fiber concrete. Concrete was air entrained. The air content, slump, and unit weight of both materials are tabulated in Table A.35. It can be seen that the workability as measured by slump is less in the steel fibrous concrete than in the ordinary concrete. The third employed material (rapid patch material) set quickly and therefore, it was not possible to measure slump, air content, and unit weight of the material.

The small tensile strength of concrete has prompted researchers' concern for increasing its resistance to crack propagation. One way to increase the resistance is by reinforcement. Once the tensile strength of concrete is exceeded, cracks will initiate and consequently steel will resist the entire tension. Therefore, the significant contribution of the reinforcement comes after the crack is initiated. This is true in reinforcing concrete with continuous steel bars. However, Romualdi and Mandel *[44]* tested mortar reinforced with randomly distributed steel fibers. They obtained the same results as with continuous wires, namely, that for spacing less than 0.4 in (1.02 cm), the tensile strength is proportional to the inverse square root of fiber spacing. However, their spacing-strength relationship was obtained by using two types of testing methods, splitting tests and flexural tests.

Since Romualdi and Batson *[45]* explored the idea of steel fiber, great progress has been made on steel fiber reinforced concrete. However, the majority of the progress has been concentrated on uniaxial tensile or flexural behavior. To investigate the influence of fibers on crack initiation of the repair material in the present work,

2.5.5.1 Flexural Properties

Three materials were tested for flexural strength. This group of tests include plain concrete, steel fiber concrete, and rapid patch material. For each material, 6 x 6 x 20 in (15 x 15 x 50 cm) beams were cast. The specimens were allowed to set during the following 24 hours, and then the molds were stripped and the specimens placed in the curing room (as per ASTM C511) for seven days.

In the first series of this group of tests, concrete beams reinforced with a 2 in. length of Xorex steel fiber (57 aspect ratio and 0.67 percent volume of mild carbon steel) were tested in flexure in a three-point loading and with a span of 18 in. Fibers had cross-sectional dimension of 0.03 and 0.05 in. in equivalent diameters and a tensile a strength of approximately 140 ksi.

Figure 2.38 shows the effects of adding steel fiber on the flexural strength and toughness of concrete beams reinforced with Xorex steel fiber. It can be seen that adding steel fiber to concrete increases both the flexural strength and toughness. However, the increase in toughness was more significant and higher than the increase in strength. Similar results have also been obtained by the U.S. Army Corps of Engineers (1965). They found that adding 2 percent of chopped steel of tensile strength 375 ksi to concrete increases the 28-day flexural strength twice. The increase in toughness was considerably larger. Shah and Rangan *[46]* have supported this result. They found that incorporating a low-carbon, smooth steel fiber of tensile strength of 120 ksi increases the toughness as much as 20 times for 1.25 percent of fibers, while for the same volume of fibers, the increase in strength was less than two times. In the present investigation, it was found that adding a 2 inch length of mild-carbon steel fiber of tensile strength 140 ksi to concrete increases the flexural strength 14 percent, while the increase in toughness was 24 times. The results of these properties for the three materials are tabulated in Table A.36.

Figure 2.39 shows the load-deflection curves for the employed materials. The area under the complete load-deflection curve was taken as a measure of toughness or resistance against crack propagation. Duracal cement material was higher in strength and more ductile than plain concrete.

2.5.5.2 Tensile Properties

In addition to the flexural beam test, a splitting test was conducted on the three employed materials. The results of this test are tabulated in Table A.37. The splitting test was used to measure the ductility. This is because the finite measure in the ductility cannot be reported due to lack of information, especially in the falling branch

cracks in the planer surface.

The flexural test as well as the splitting test give only an indirect indication about the tensile properties. Therefore, direct uniaxial tensile tests were carried out. Two specimens shown in Figure 2.2 from each employed material were cast, cured, and tested in uniaxial tension after seven days. Results are shown in Table A.38. During loading, longitudinal and lateral strains were continuously recorded. The tensile stress-strain relation is shown in Figure 2.40 for both fiber reinforced concrete and plain concrete. A higher ultimate strength and larger strain occur at the ultimate load for the specimens which are reinforced by the steel fiber. It was observed that the addition of steel fiber to the concrete had no effect on the elasticity limit of the stress-strain behavior. Similar observations have been reported by Haynes *[47]* in this experimental test on 1.5 x 6 x 22 inch beams of fiber concrete, in which brass coated steel fibers of a volume equal to 4.6 percent were used. They found that the stress-strain relationship up to the proportional limit of fiber concrete was the same as that of control concrete, although the flexural strength was approximately twice as large. McKee *[48]* also found that the stress-stain relationship of concrete reinforced with steel fiber up to 3 percent of volume is the same as for plain concrete up to about 80 percent of the ultimate load.

The increase in ultimate strength and ductility of fiber concrete subjected to tensile load may be due to the interface bond (shearing stress) between the fiber and the matrix, in which some of the tensile forces go to the matrix while the balance is taken by the fiber. Shah and Rangan *[46]* observed that during tensile testing of fiber concrete, a crack appeared and the load dropped by a certain amount. The remaining load, after the formation of crack, indicated the resistance of steel fiber against the crack propagation. This may be due to the bond which is responsible for the transmission of force into the uncracked elements of the matrix after cracking has occurred. Therefore, the composite does not necessarily fail once the cracks appeared because the bond at the interface transfers the forces that cannot be carried by the cracked part of the matrix.

In order to study the tensile properties of the rapid patch material, specimens of Duracal cement were cast, cured, and tested in uniaxial tension after seven days. The tensile stress-strain relationship is shown in Figure 2.41 and tabulated in Table A.39 as a comparison with both fiber concrete and plain concrete. It can be seen that Duracal cement material behaves similarly as plain and fiber concrete.

2.5.5.3 Compression Properties

Fiber concrete and plain concrete specimens similar to the one shown in Figure 2.2 were tested in uniaxial compression. The fiber concrete specimens were

in Figure 2.42. The following conclusions can be drawn from these figures:

1. The addition of steel fibers has no significant effect on the stress-strain curve up to approximately 50 percent of the peak stress of plain concrete.
2. The addition of fibers increases the ductility of concrete.

The extensive tests of Newman *[49]* show that concrete subjected to uniaxial compression exhibits cleavage failure while concrete subjected to confining compression failed by faulting failure (shear failure). When adding fibers to concrete, it can be assumed that the effect of fiber is equivalent to providing a small confining compression in the unloaded direction. With this confining pressure, the failure mode will be changed from splitting to faulting.

From the above argument, it can be concluded that the increase in ductility of fiber concrete may be due to the increased resistance against crack propagation.

The compressive test of fiber concrete in the present work demonstrated that there was little effect on the compressive strength. Table A.40 shows that there was an increase in the compressive strength of about 5 percent due to the addition of fibers.

The experiments *[10]*, *[35]*, *[36]* have shown that plain concrete fails by tensile splitting when subjected to uniaxial compression. This proves that failure of concrete when subjected to uniaxial compression is governed by the tensile property, and that compressive strength should be increased by adding the steel fibers. On the other hand, the strength of concrete under triaxial compression is considerably higher than that under uniaxial or biaxial compression. Hence, adding steel fibers (equivalent to small confining pressure) will change the failure mode, and will increase the ultimate strength. However, the increase of ultimate strength is small in uniaxial compression because the equivalent confining pressure in the unloading direction is small.

In order to investigate the response of Duracal cement material to uniaxial compression, two specimens of this rapid patch material were cast, cured for seven days, and then tested. The stress-strain curve is shown in Figure 2.43 and tabulated in Table A.41 with the stress-strain relation of the plain and the fiber concrete. It can be shown that concrete is stiffer than Duracal.

For all employed materials tested in the present work, the average compressive strength as measured in the new test set-up was less than the cylinder compressive strength found by the ASTM compression cylinder (tabulated in Table A.37). The difference could be due to a difference in size, shape, and boundary conditions. In the ASTM cylinder test, the loading system produces uniform displacement. On the other hand, in this work five one inch plates were placed at the bottom and top of the specimens in which full contact of loading was achieved, and hence, uniform stress was produced. In addition, the friction between the steel plate and the concrete

plates of teflon, one of each, at the top and bottom of the specimen in order to minimize lateral confinement due to friction. The uniform stress without lateral constraints produced a lower measured compressive strength.

2.5.5.4 Biaxial Tension-Compression

Repaired material is subjected mainly to a biaxial tension-compression state of stress. Tests under uniaxial stress conditions may lead to a poorer performance. The remedy is a better representative testing of the material. This can be done by subjecting the material to a biaxial state of stress.

In the present investigation, 30 specimens, shown in Figure 2.2, were distributed over three groups of tests: (1) plain concrete, (2) fiber reinforced concrete, and (3) Duracal cement material. All these specimens were subjected to a biaxial state of stress after seven days of curing. The material investigated with the new device dealt with the material strength and stress-strain behavior. In order to verify the apparatus capabilities, ASTM standard uniaxial cylinder compression and splitting tensile tests were conducted as a prelude to the investigation. The results of these tests were markedly different from the uniaxial compressive and tensile strengths measured in the new device, as shown in Table A.42.

The ultimate strength data of the employed materials subjected to biaxial tension-compression are summarized in the form of biaxial stress envelops as shown in Figure 2.44, and tabulated in Table A.43. The ultimate strength envelopes in Figure 2.44 show that for all employed materials, depending on the principal stress ratio (σ_1/σ_3), the ultimate strength in biaxial tension-compression is smaller than in uniaxial compression. It should be noted that all the stresses in Figure 2.44 are non-dimensionalized by the uniaxial compressive rectangular strength of plain concrete. The average compressive strength of plain concrete is (- 2645 psi) after seven days.

Generally, fiber concrete possesses higher strength than plain concrete. However, the effect of adding fiber is different in the uniaxial state of stress than the biaxial tension-compression. As shown in Figure 2.44, the increase in strength due to fiber addition is about 9 percent at stress ratio of $\sigma_1/\sigma_3 = -0.08$. In contrast, the increase in strength is up to 20 percent in uniaxial tension and up to 5 percent in uniaxial compression.

As shown in Figure 2.44, Duracal cement material behaves similarly to concrete for high stress ratio of tension to compression, while in compression, Duracal cement is stronger than both plain and fiber concrete.

A comparison of the biaxial stress-strain relationship of the three employed materials is shown in Figure 2.45. It should be noted that plain and fiber concrete

...results of these tests are tabulated in Table A.44.

2.5.5.5 Failure Modes

It is known that microcracks in plain concrete subjected to tension, fle... compression are started significantly prior to the maximum load. In investiga... effect of fiber addition on crack initiation, previous studies *[31]* stated that the... deflection curves for flexural as well as the stress-strain relationship in tensio... compression show that the point where the nonlinearity started can be consid... an indication of crack initiation.

In the present study, when plain concrete was subjected to uniaxial co... sion, cracks in the direction of loading were observed, and the specimens fail... tensile splitting. Unlike plain concrete, in uniaxial compression testing of fiber... concrete, fracture occurred by the formation of many inclined cracks known as... faulting failure. The present observation of failure type supported the theoreti... of Horri and Nemat-Nasser *[50]* who showed that the different loading conditi... the reason for the different failure modes of brittle materials. For example, wh... material is subjected to uniaxial loading, the microcracks gradually develop in... direction of the load, which causes splitting failure. However, when small con... pressure (fiber in our case) is applied together with loading, the growth of micr... will slow down and the material will fail by interconnecting inclined cracks alon... zone that causes faulting or shear failure.

2.6 CONCLUSIONS AND RECOMMENDATIONS

2.6.1 Conclusions

An investigation has been presented on the performance of repair mat... such as plain concrete, fiber concrete, and Duracal cement, as they respond i... repaired regions of rigid pavements. Based on consideration of the test result... described herein, the following conclusions can be drawn concerning the beha... brittle repair materials:

1. The availability of a biaxial testing set-up for simultaneously app... tensile and compressive loads with a minimum of boundary con... and for making accurate measurements, has been shown to pro... better understanding by which the strength and behavior of brit... materials can be fully investigated. The test results show the ca... ties of the biaxial tensile-compressive experimental technique...

2. In uniaxial compression and tension, the compressive strain and the tensile strain at peak load are about -2000 and +160 microstrain, respectively. The peak stress in tension is 15 percent of the peak stress in compression.

3. The uniaxial tensile strength of concrete can be satisfactorily predicted by the expression $8\sqrt{f'_c}$ where f'_c is the uniaxial compressive cylinder strength in psi. The tensile strain at failure is almost twice as large as the tensile strain at the peak of uniaxial tensile stress.

4. In uniaxial compression, the stress-strain behavior is almost linear when the stress is less than 35 percent of the ultimate stress. Small cracks parallel to the axis of loading appear on the specimens at a stress level of 80 percent of the ultimate load.

5. The nonlinearity of the tensile stress-strain relations indicate that some inelastic deformation occurs under tensile loading. The pre-peak stress-strain curve is relatively more nonlinear in compression than in tension.

6. Test results show that the strength of concrete under combined tension and compression is lower than the strength under uniaxial loading. The strength decrease is dependent on the principal stress ratio, i.e., the strength decreases as the applied tensile stress increases.

7. For different biaxial stress ratios (σ_1/σ_3), the stress-strain curves possess the same general shape. However, both peak stress and corresponding strain decreased as the tensile stress (σ_1) increased.

8. The biaxial tension-compression test program presented herein is simple. The results are in agreement with previous investigations.

9. For all uniaxial and biaxial tests, failure occurs by tensile splitting, with the fracture surface orthogonal to the direction of the maximum tensile strain.

10. Under combined tension and compression, a single continuous crack normal to the maximum tensile strain direction was formed except for ratios of the tensile stress to compressive stress smaller than 0.05 for which crushing fracture occurred.

11. The bond strength tests used in this study include the slant shear, direct tension, and direct shear tests. These tests are required to determine the bond strength and quality of the bonding system.

12. Addition of steel fiber to concrete increases both flexural strength and toughness. However, the increase in toughness was more significant and much higher than the increase in strength.

13. Duracal cement material has higher flexural strength and is more ductile than plain concrete but less ductile than fiber concrete.

14. Adding steel fibers increases both the tensile peak stress and the corresponding strain.
15. The addition of steel fiber to concrete had no effect up to the elastic limit of the tensile stress-strain behavior.
16. In uniaxial compression, the increase in strength due to the addition of steel fibers is insignificant. Duracal cement was stronger in compression in comparison with plain and fiber concrete.
17. For all three employed materials, depending on the principal stress ratio (σ_1/σ_3), the ultimate strength in biaxial tension-compression is smaller than in uniaxial compression.
18. Generally, fiber concrete possesses higher strength and ductility than plain concrete. However, the effect of adding fiber is different in the uniaxial state of stress than the biaxial tension-compression.
19. Duracal cement material behaves similar to concrete at a high stress ratio of biaxial tension-compression.
20. Plain concrete subjected to uniaxial compression and biaxial tension-compression failed by tensile splitting. Fiber concrete failed by faulting or shear failure.

2.6.2 Recommendations

1. For more practical and realistic applications, modifying the available biaxial test set-up proposed here to be used for multiaxial cyclic loading is recommended.
2. The biaxial stress-strain response and the biaxial ultimate strength criterion for concrete in the form of a simple stress envelope is recommended for design purposes.
3. For a better understanding of the effect of adding steel fiber to plain concrete, investigate the behavior of fiber concrete reinforced with different volume percent of steel fibers.
4. To improve properties of Duracal cement material, it is recommended that the cement material be reinforced with the available fibers.

Chapter 3

ANALYSIS OF JOINTED CONCRETE PAVEMENTS

INTRODUCTION

The main reason for not understanding the nature of failure in jointed concrete pavements is the inherent variability of the parameters involved, namely, the material behavior, the support, and loading conditions. Any analytical model developed for studying a problem of this nature must be capable of simulating these conditions as realistically as possible. The behavior of concrete is highly complex. Concrete is a heterogeneous, multi-phase, nonlinear, and time-dependent material. It has widely different strengths in tension and compression. The important nonlinearities associated with concrete are as follows:

(1) Concrete is a heterogeneous material consisting of hard aggregate inclusions in a relatively soft mortar matrix, which consists of fine aggregates and cement gel. Voids and cracks at the initial stage cannot be avoided. Loading causes propagation of cracks and alters the structural response.

(2) Concrete has different strengths in tension and compression, its tensile strength is about a tenth of its compressive strength. Cracking in tension leads to stress-induced anisotropy.

(3) The constitutive relationship of concrete is complex. The main cause of the nonlinearity is microcracking, which is a random and discrete process. Post-peak strain softening under tension and compression is a peculiar behavior of concrete. Multiaxial load response is complex, involving hydrostatic pressure sensitivity, inelastic volume changes, dilatancy, and load path dependency.

(4) Failure criteria are complex and depend on several parameters.

(5) Time-dependent behavior adds to the complications. Shrinkage due to loss of water and creep under sustained loading are present. In addition, there is a gain in strength with age.

(6) The distribution of local strength in concrete is random. There is a relatively high variation of strength and other properties for identical specimens tested under similar conditions.

(7) Addition of steel reinforcements and dowels cause additional nonlinearities through interface behavior. Bond-slip and tension stiffening effects are inherently nonlinear phenomena.

(8) Behavior of concrete under repeated loads and load reversals is rather complex and is not thoroughly understood.

over-design procedures in spite of which, failures are still observed. Classical analytical procedures cannot suffice for analyzing concrete structures. The only method presently capable of realistically considering most of the nonlinearities and complexities of concrete behavior is the nonlinear finite element method. Hence, it is proposed to develop a nonlinear finite element procedure to analyze jointed concrete pavements in this study. The effect of the various support conditions and loading conditions will also be considered. The study of the effect of different rehabilitation measures was also proposed. It was necessary to develop and implement a three-dimensional nonlinear finite element program. The input parameters necessary for the material model are calibrated based on existing and new specially-conducted test results. With such analyses the effect of the various parameters involved can be studied in isolation.

The following stages are involved in the development of the analytical/numerical procedures:

- formulation of a material model for concrete
- analytical modelling of interface behavior between dowel bars and concrete and also between repair material and old concrete
- simulation of subgrade conditions and the effect of curling of slabs
- simulation of full and partial depth patches and the effect of the patching procedure on stress distribution in jointed pavement slabs

3.2 BACKGROUND AND OBJECTIVES

3.2.1 Background

Westergaard *[51]* was the first to develop analytical expressions for stresses and deformations of pavements based on the theory of plates on elastic foundation. Bradbury *[52]* analyzed an infinitely long beam resting on elastic supports and used this analysis to compute stresses in dowels and concrete. Later, Frieberg *[53]* simulated dowel embedment in concrete through an infinitely long beam on elastic supports. Holl *[54]* and Hogg *[55]* presented analyses of thin plates on elastic foundation which was considered as a semi-infinite elastic solid. Kushing and Fremont *[56]* developed a method for evaluating load transfer across a doweled joint. Burmister *[57], [58]* developed methods for analysis of multilayered elastic systems. Later, they published *[58]* influence charts as design-aids based on a two layer rigid soil base system. Picket and Ray *[59]* developed influence charts to compute the stresses under a pavement subjected to general loading arrangements. Niu and Picket *[60]* studied the effect of a single crack on the stress distribution in a concrete pavement.

The development of the finite element method as a powerful analytical tool and the availability of computers led to a number of analytical studies of concrete

pavements. In some of these analyses, the pavement system has been simulated by means of plate elements on idealized Winkler subgrade *[64], [65], [66], [67], [68]* whereas some others assumed the subgrade to be a semi-infinite elastic medium *[69], [70], [71]*. Majidzadeh *[67]* has described a mechanistic approach to analyze and design rigid concrete pavements including the effects of dowels, loss of subgrade support, and curling of slabs due to temperature. A computer program developed for this purpose was also described. Currently, several computer programs are available for the analysis of pavements. Some of the most popular ones are described here.

ILLI-SLAB: This computer program, developed at the University of Illinois *[63]*, assumes a Winkler subgrade supporting plate elements representing the pavement. The stiffness of the Winkler springs can be varied from point to point. The dowel bars are considered to be linearly elastic and are placed at the neutral axis of the plates. These bars are assumed to be capable of transferring shear and moments across the joint. The dowel bars and the surrounding concrete elements are linked through dowel-concrete interface spring elements which are also utilized to simulated dowel looseness. Equivalent springs simulate the effects of aggregate interlock and keyways. The model has also been extended to consider a variety of loading and support conditions which includes an elastic solid option for the subgrade.

JSLAB: This program was employed by Tayabji and Colley *[72]* to analyze jointed pavements subjected to axle loads and thermal stresses. The effect of nonuniformly spaced dowels was also studied. The program employs rectangular plate elements for concrete, a beam element for dowels, and spring elements for subgrade and aggregate interlock. The wheel loads are applied as concentrated loads at the nodes of finite elements. Variable support conditions and loss of support can also be simulated. The pavement can consist of up to nine slabs and up to two layers. However, temperature warping and curling can be considered for a single layer system only.

WESLIQUID and WESLAYER *[73]*: These programs, developed by the US Army Engineer Waterways Experiment station, are based on the original work of Huang and Wang *[62], [74]*. WESLIQUID employs a thin plate element for slab and Winkler spring elements for subgrade. The other effects considered are linear temperature gradients, full or partial contact between a slab and subgrade, and moment and shear transfer at joints. The last effect is modeled through specified transfer coefficients based on shear and moment transfer efficiency factors. Program WESLAYER is developed assuming the subgrade to be an elastic foundation capable of sustaining shear and normal reactions.

FEACONS: A group of researchers at the University of Florida *[66], [68], [75]* described the development of a finite element program for analysis of concrete pavements. The program employed the plate element for concrete and Winkler spring element for subgrade. The weight of the slabs was considered. Load transfer at the

joints was considered through the introduction of shear and rotational springs. Thermal stresses were included and loss of support was simulated. A nonlinear subgrade response was considered. The effect of inplane stresses was considered through a second analysis using a plane stress element. An extension to consider skew joints *[68]* was also developed. Parametric studies with variation in the subgrade, rotational and shear stiffnesses, and temperature differentials, were conducted. Slab corner stresses in case of skewed joints were found to be higher than the case of normal joints. Armaghani *[66]* reported that the nighttime temperature differential is the most critical condition for stresses in concrete pavements, particularly due to the fact that most of the heavy traffic travels during the night.

Saxena and Dounias *[70]* analyzed continuously reinforced concrete pavements by employing a three-dimensional finite element program. Both the slab and the subgrade were simulated using solid finite elements. An interface element was used between the pavement and subgrade to consider frictional effects. Deflection along the surface was obtained by employing coarse mesh, whereas a finer mesh was used to compute stresses. A heat transfer analysis was performed to obtain the distribution of temperature that was used in stress analysis. Mechanical effects of the load and the environmental effect of the temperature were superimposed to obtain the net effects.

3.2.2 Objectives and Scope

A review of available computer programs indicated that most of the programs employ plate elements for modeling the pavement. One of the main disadvantages of these models is their inability to consider the effect of the direct stress due to load and the stresses around the dowels. Particularly, concrete around the dowels is highly stressed, and local yielding, crushing, and cracking of concrete are encountered. These lead to a loss of dowel support after a number of repetitions of load, thus reducing the joint efficiency. Some researchers have employed commercial three-dimensional programs. These programs, besides being expensive, are available in compiled form only, and hence, cannot be modified for specialized purposes such as the simulation of cracking and other distresses in patched concrete pavements. Because of these considerations, a special purpose three-dimensional nonlinear finite element program was developed during the course of this study.

The program employs a special constitutive model for characterizing the response of concrete. The parameters required for using this constitutive model have hitherto been obtained from sophisticated testing techniques. In the experimental phase of this study, simple testing procedures using the available equipment have been developed to obtain the necessary data. These procedures have been shown to be capable of reproducing the results obtained from more sophisticated tests.

The main objectives of this study are:

1. To develop a specialized finite element computer program for analyzing jointed concrete pavements
2. to be capable of simulating jointed rigid pavement distresses due to loss of support, concrete deterioration due to fatigue, looseness of dowels, etc.
3. to be able to consider the development and propagation of cracks in pavements and inelastic deformations of concrete
4. to include the effects of night-time and day-time curling and warping of slabs
5. to be able to analyze full and partial depth patched slab sections, and to study the effect of patching on the response, deflections, and stress levels in pavements
6. to include the strains due to shrinkage in the analyses
7. In this investigation, examples of full three-dimensional analyses of pavements and repair sections under combinations of self weight, wheel loads, and temperature are presented and discussed. The study is only of an exploratory nature. It does not include parametric studies on the various pavement configurations and different loading conditions. It also does not cover the distresses due to blow-up which may need a geometric nonlinearity modeling capability.

To be of real value to practicing engineers, the program will have to be used to analyze different pavement configurations on a case by case study, and the results of such an analysis could be employed fruitfully in arriving at alternative rehabilitation procedures.

In this study, a complete distress simulation capability has been built into a three-dimensional analysis program for the first time; and it is expected that analyses using this program will enable better understanding of pavement behavior, which can lead to proper guidelines for evaluation of different materials and repair procedures in rehabilitating rigid-jointed pavements.

3. ELEMENTS OF CONCRETE PAVEMENT

The main features of a jointed concrete pavement are:

1. A slab cast in portland cement concrete
2. A subgrade, cemented, bonded, or unbonded
3. Joints - Doweled or undoweled
4. Shoulders - concrete or asphalt
5. Reinforcement

A typical section of a concrete pavement is shown in Figure 3.1

1. To develop a specialized finite element computer program for analyzing jointed concrete pavements
2. to be capable of simulating jointed rigid pavement distresses due to loss of support, concrete deterioration due to fatigue, looseness of dowels, etc.
3. to be able to consider the development and propagation of cracks in pavements and inelastic deformations of concrete
4. to include the effects of night-time and day-time curling and warping of slabs
5. to be able to analyze full and partial depth patched slab sections, and to study the effect of patching on the response, deflections, and stress levels in pavements
6. to include the strains due to shrinkage in the analyses
7. In this investigation, examples of full three-dimensional analyses of pavements and repair sections under combinations of self weight, wheel loads, and temperature are presented and discussed. The study is only of an exploratory nature. It does not include parametric studies on the various pavement configurations and different loading conditions. It also does not cover the distresses due to blow-up which may need a geometric nonlinearity modeling capability.

To be of real value to practicing engineers, the program will have to be used to analyze different pavement configurations on a case by case study, and the results of such an analysis could be employed fruitfully in arriving at alternative rehabilitation procedures.

In this study, a complete distress simulation capability has been built into a three-dimensional analysis program for the first time; and it is expected that analyses using this program will enable better understanding of pavement behavior, which can lead to proper guidelines for evaluation of different materials and repair procedures in rehabilitating rigid-jointed pavements.

ELEMENTS OF CONCRETE PAVEMENT

The main features of a jointed concrete pavement are:

1. A slab cast in portland cement concrete
2. A subgrade, cemented, bonded, or unbonded
3. Joints - Doweled or undoweled
4. Shoulders - concrete or asphalt
5. Reinforcement

A typical section of a concrete pavement is shown in Figure 3.1

1. To develop a specialized finite element computer program for analyzing jointed concrete pavements
2. to be capable of simulating jointed rigid pavement distresses due to loss of support, concrete deterioration due to fatigue, looseness of dowels, etc.
3. to be able to consider the development and propagation of cracks in pavements and inelastic deformations of concrete
4. to include the effects of night-time and day-time curling and warping of slabs
5. to be able to analyze full and partial depth patched slab sections, and to study the effect of patching on the response, deflections, and stress levels in pavements
6. to include the strains due to shrinkage in the analyses
7. In this investigation, examples of full three-dimensional analyses of pavements and repair sections under combinations of self weight, wheel loads, and temperature are presented and discussed. The study is only of an exploratory nature. It does not include parametric studies on the various pavement configurations and different loading conditions. It also does not cover the distresses due to blow-up which may need a geometric nonlinearity modeling capability.

To be of real value to practicing engineers, the program will have to be used to analyze different pavement configurations on a case by case study, and the results of such an analysis could be employed fruitfully in arriving at alternative rehabilitation procedures.

In this study, a complete distress simulation capability has been built into a three-dimensional analysis program for the first time; and it is expected that analyses using this program will enable better understanding of pavement behavior, which can lead to proper guidelines for evaluation of different materials and repair procedures in rehabilitating rigid-jointed pavements.

3.3 ELEMENTS OF CONCRETE PAVEMENT

The main features of a jointed concrete pavement are:

1. A slab cast in portland cement concrete
2. A subgrade, cemented, bonded, or unbonded
3. Joints - Doweled or undoweled
4. Shoulders - concrete or asphalt
5. Reinforcement

A typical section of a concrete pavement is shown in Figure 3.1

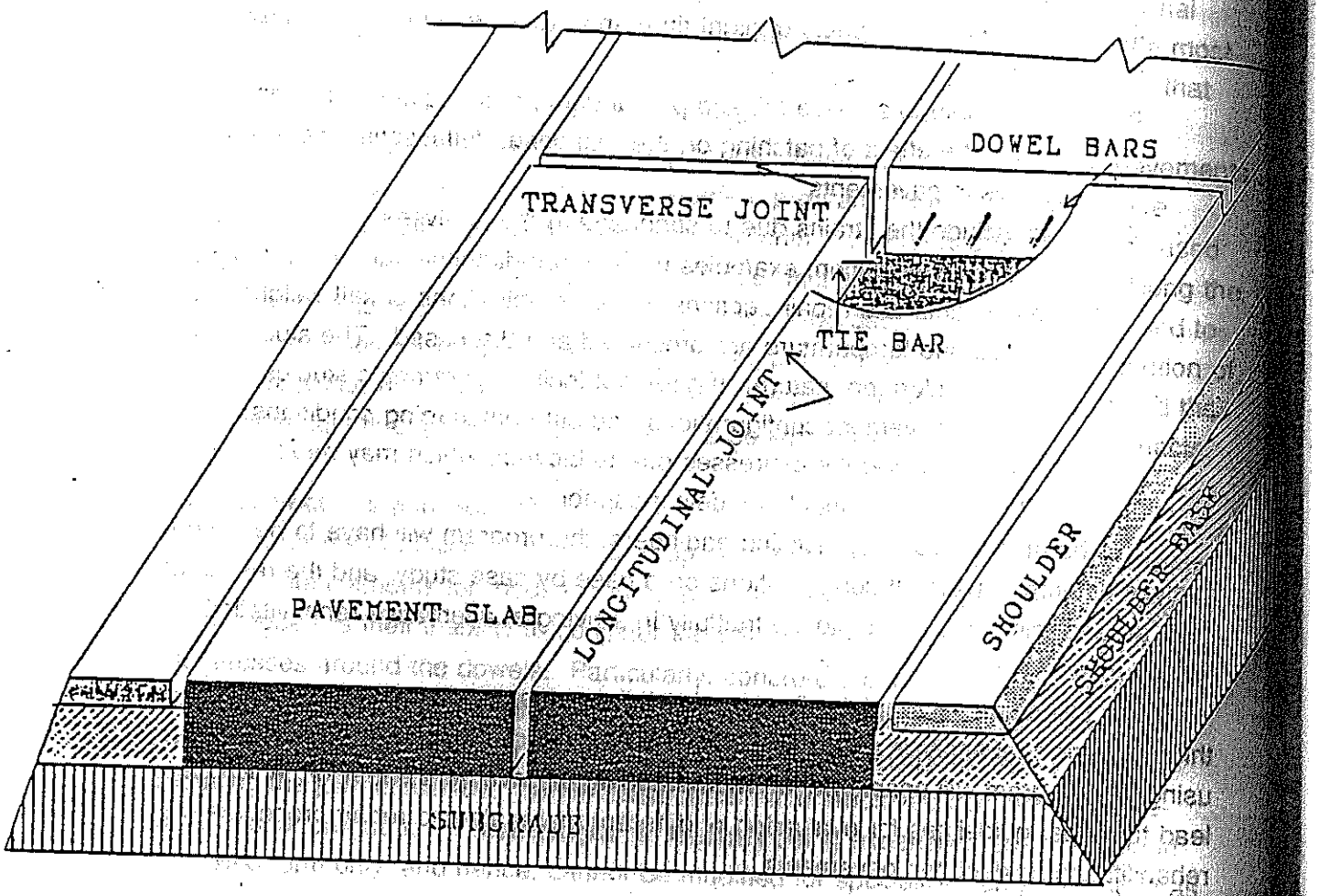

Figure 3.1
Typical section of concrete pavement

3.3.1 Concrete Slab

The pavement slab is usually made up of a concrete slab at least 10 inches thick, cast and cured in place. The minimum strength specifications vary from state to state and is usually specified as a minimum modulus of rupture. A design value of 550 psi (3.875 Mpa) is suggested for pavements in Louisiana *[76]*. The suggested value of Elastic modulus is 4,200,000 psi (29020 MPa.)

3.3.2 Subgrade

The subgrade for concrete pavements may consist of natural soil or stabilized soil. In some places, special concrete bases are used. The purpose of the base courses is to provided a uniform surface for casting the slab. Base courses are sometimes used under rigid pavement for the following purposes:

1. Control pumping damage
2. Control frost action
3. Provide drainage
4. Control shrinkage and swelling of subgrade
5. Expedite construction

The AASHTO design guide *[4]* provides for a reduction in slab thickness for properly drained subgrades.

3.3.3 Joints

Joints in concrete pavements are provided for two purposes:

1. To provide for the release of stresses due to shrinkage of concrete during curing
2. To facilitate expansion and contraction of the slab under temperature variations

There are four types of joints:

Expansion Joints: These are provided to permit free expansion and contraction of pavement slab. They are about .75 to one inch wide and are spaced more than 60 ft. apart. Expansion joints are expensive to construct and maintain. Dowel bars are required to transfer load across these joints. Many times these are sources of pumping distresses. Many states have discontinued the use of expansion joints.

Contraction Joints: These are provided to control cracking due to shrinkage of concrete. These are usually about 0.25 inch wide and are spaced at 15 to 20 ft. apart. They may or may not have dowels to transfer the load across. Recent investigations *[77]* have demonstrated the superiority of doweled joints. Dowels are plain steel rods usually one inch in diameter and 1.5 to two ft. long. They are greased to permit free expansion and contraction of slabs. In some states, the practice is to cut a groove to about half the depth of slab and introduce the dowels at one ft. c/c. The rest of the joint forms during shrinkage.

Construction joints: These are employed to transfer load across old and new castings. Sometimes dowel bars are used. Use of keys is also prevalent.

Longitudinal joints: These are used between two lanes of a multi-lane highway and between the roadway and the shoulder. The two lanes or the shoulder and lane are sometimes tied with tie bars, which are usually deformed steel bars two ft. long and 0.5 to 0.75 inch in diameter placed at two to three ft. intervals. The tie bars are firmly anchored into the concrete at both ends.

3.3.4 Reinforcement

Reinforcement is provided in concrete pavements to control cracks. This consists of a small diameter wire mesh or a bar mat. However, in case of continuously reinforced pavements, the reinforcements take up the stresses due to temperature and shrinkage, and are designed accordingly.

3.3.5 Shoulders

Shoulders protect the highways from drainage related distresses. They also serve as service lanes. They may be paved or unpaved. Usually paved shoulders are made of asphaltic concrete. Cement concrete shoulders are sometimes tied to the lanes through tie bars. The AASHTO Guide *[4]* permits a reduction in the thickness of pavements if they are tied to paved shoulders recognizing the structural participation of the shoulders.

3.3.6 Distresses and Causes of Failure of Concrete Pavements

A concrete pavement is subjected to stress from traffic, change in temperature, change in moisture conditions, change in support conditions, and boundary conditions. Further, a large repetition of wheel loads causes fatigue. Occasionally, when poor quality materials are used, concrete pavements deteriorate with time, and this leads to failure. Insufficient maintenance, particularly with respect to the joints, leads to failure at the joints. The main types of failure/distress encountered in jointed plain concrete pavements are: raveling, spalling, faulting, pumping, blow-up, failure of keyways, corner cracks, and compression cracks. Figure 3.2 shows typical failure modes and Table 3.1 describes each of them briefly. Among these different modes, some lead to functional failures, and others lead to structural failures.

Faulting is mainly a functional failure, though with time, it leads to other structural failures. This is due to an insufficient transfer of loads across the joint. The difference in deflection of loaded and unloaded slab is high enough to cause a rough riding surface. Water may seep into the subgrade through such a joint and repeated pumping of water at high pressure during the passage of vehicles leads to pumping failure. In this mode, subgrade material is removed through the joint and sides along with water under pressure. This gradually leads to loss of support and a resulting

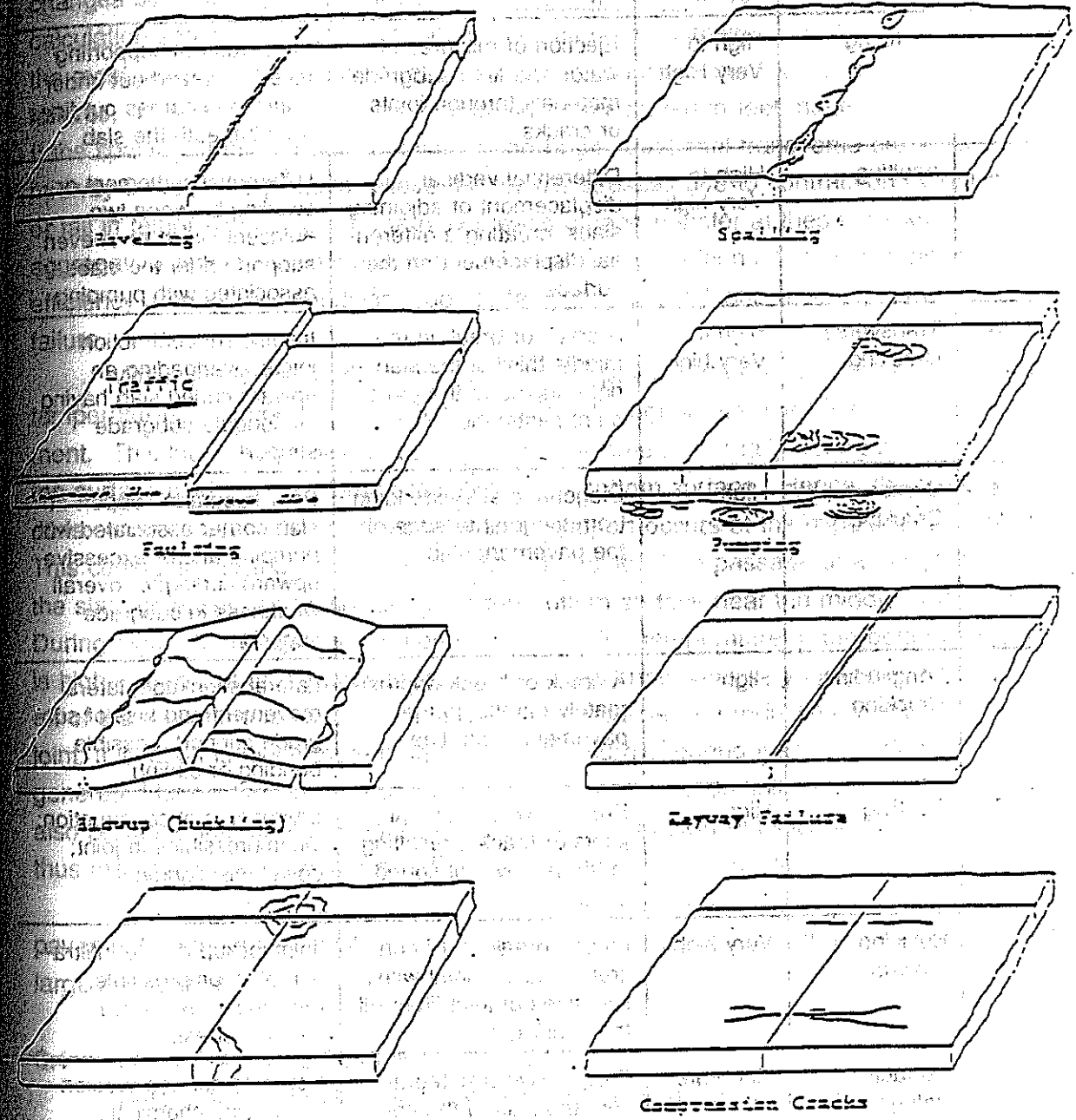

Figure 3.2
Typical failure modes *[66]*

Table 3.1

Distresses in pavements

Sl. No.	Type of Distress	Severity	Description	Mechanism
1	Pumping	High to Very High	Ejection of mixtures of water and finte subgrade materials through joints or cracks	Free water in supporting layer squeezed out und traffic load carries out from beneath the slab
2	Faulting	High to Very high	Differential vertical displacement of adjoining slabs, creating a differential displacement on the surface	Differential settlement or swelling between two adjacent slabs, or uneven support under the slabs associated with pumping
3	Transverse Cracking	High to Very high	A crack or break in the middle third of the slab at right angles to the pavement centerline	Insufficient contraction joints; overloading an upward curled slab having inadequate subgrade support
4	Corner Cracking	High	Diagonal crack extending from the joint to edge of the pavement slab	Poor subgrade support at slab corner associated with pumping and/or excessive upward curling; or overall weakness in subgrade support
5	Longitudinal Cracking	High	A crack or break approximately parallel to the pavement centerline	Lateral shrinkage, lateral movement and loss of subgrade support; possible bending or curling
6	Spalling	High	Breakdown of slabs at joints or cracks, resulting in the removal of sound concrete	Improper joint construction; incompressibles in joint; dowel misalignment
7	Buckling - Blowup	Very high	Lateral break up of concrete near the joint with two sides of joint lifted off the subgrade	Joint lockup due to infiltration of incompressible, resulting in excessive bending stresses
8	Surface deterioration (Scaling, Raveling)	Moderate	Progressive disintegration and loss of the concrete wearing surface	Concrete surface erosion by de-icing chemicals; improper construction techniques; repetitive freeze-thaw cycles

crease in stresses in the pavement. Even with a smaller number of load applications, and the pavement cracks, higher stress levels lead to a faster fatigue deterioration. Thus, pumping by itself does not cause structural failure, but accelerates the failure through side effects and is considered to be a severe distress condition.

When sufficient provision for expansion and contraction under temperature changes does not exist, high stresses are developed in the pavement. Simple calculation shows that these stresses even exceed the stresses due to loads. One of the most severe distress conditions, the blow-up failure, is because of this. Blow-up failures, wherein the lift-off at the joint could be measured in feet, have been observed. If the spacing of the contraction joints is too large, additional transverse cracks develop midway through the joints to relieve the tensile stresses due to contraction (shrinkage or fall in temperature). Since the only means of load transfer at these cracks is by aggregate interlock, with time and a number of load repetitions, the load transfer efficiency is lost. This condition leads to faulting, pumping, and resulting structural failure.

When the top and bottom surfaces of the pavement are subjected to different temperatures, a temperature gradient develops throughout the thickness of the pavement. This leads to warping or curling of the pavement. Usually during the day, the top surface is at a higher temperature than the bottom surface. Hence, the pavement curls convexly upwards and a partial loss of support occurs at the middle of the slab. This curling is resisted by the self weight of the slab. The passage of a vehicle over the slab increases the tensile stress at the bottom surface near the middle of the slab. During night, the reverse phenomenon occurs. The temperature of the bottom surface is higher than that at the top surface and the slab curls concavely upwards, and a lift-off of the pavement is observed at the joints. Because of a reduction in stiffness at the joint, this lift-off is much more than the lift-off occurring during the day. The void generated below the slab leads to collection of water and pumping distress. It should also be noted that on the majority of highways, most heavy vehicles travel at night and thus the upward concave curling of the slab is the more critical mode *[66]*.

When the traffic travels along the edge of a pavement, particularly in case of pavements without tied concrete shoulders, the stresses developed at the corner are large and lead to corner cracks.

3.4 MATERIAL MODEL FOR CONCRETE

Before describing the implemented material model for concrete, it is necessary to highlight the response of concrete to loads.

3.4.1 Behavior of Concrete Under Load

3.4.1.1 Uniaxial Behavior

Compression

A typical stress-strain curve of concrete under uniaxial compression is shown in Figure 3.3. The following observations can be made:

(1) Compressive stress-compressive strain diagram is linear up to about 30 percent of the ultimate compressive strength.

(2) If a displacement controlled test is performed in a rigid testing machine, the strain softening portion of the stress-strain curve beyond the ultimate strength stage can be observed. The final failure of concrete under compression occurs at a limiting compressive strain.

(3) The lateral strain-longitudinal stress plot is linear up to about 80 percent of the ultimate compressive strength.

(4) A plot of volumetric strain vs. longitudinal compressive stress indicates in Figure 3.4 a decrease in volume up to about 80 percent of compressive strength. Beyond this, the volume increases rapidly resulting in an effective increase of the Poisson's ratio even beyond 0.5. This increase in volume can be attributed to the formation of voids and is reflected by a rapid increase in Poisson's ratio.

Behavior Under Cyclic Compressive Loads

Under cyclic loading, the following observations can be made as shown in Figure 3.5:

(1) On unloading and reloading beyond 30 percent of ultimate strength, the unloading and reloading curves show marked nonlinearity. An inelastic deformation can also be observed.

(2) Up to about 85 percent of the ultimate strength the response follows approximately the initial modulus.

(3) Beyond this, a modulus degradation can be observed with an increase in the nonlinearity.

Tension

The following observations can be made if a uniaxial displacement-controlled tensile test is conducted in a stiff testing machine as shown in Figure 3.6.

(1) The uniaxial tensile stress-strain behavior is linear up to about 60 percent of tensile strength.

(2) The initial modulus is nearly equal to that of the compressive stress-strain plot.

(3) Beyond the ultimate stress, a region of strain softening can be observed along with the appearance of microcracks. The final failure is by the coalescence of microcracks and the formation of a macrocrack.

3.4.1 Behavior of Concrete Under Load

3.4.1.1 Uniaxial Behavior

Compression

A typical stress-strain curve of concrete under uniaxial compression is shown in Figure 3.3. The following observations can be made:

(1) Compressive stress-compressive strain diagram is linear up to about 30 percent of the ultimate compressive strength.

(2) If a displacement controlled test is performed in a rigid testing machine, the strain softening portion of the stress-strain curve beyond the ultimate strength stage can be observed. The final failure of concrete under compression occurs at a limiting compressive strain.

(3) The lateral strain-longitudinal stress plot is linear up to about 80 percent of the ultimate compressive strength.

(4) A plot of volumetric strain vs. longitudinal compressive stress indicates, in Figure 3.4 a decrease in volume up to about 80 percent of compressive strength. Beyond this, the volume increases rapidly resulting in an effective increase of the Poisson's ratio even beyond 0.5. This increase in volume can be attributed to the formation of voids and is reflected in a rapid increase in Poisson's ratio.

Behavior Under Cyclic Compressive Loads

Under cyclic loading, the following observations can be made as shown in Figure 3.5:

(1) On unloading and reloading beyond 30 percent of ultimate strength, the unloading and reloading curves show marked nonlinearity. An inelastic deformation can also be observed.

(2) Up to about 85 percent of the ultimate strength the response follows approximately the initial modulus.

(3) Beyond this, a modulus degradation can be observed with an increase in the nonlinearity.

Tension

The following observations can be made if a uniaxial displacement-controlled tensile test is conducted in a stiff testing machine as shown in Figure 3.6.

(1) The uniaxial tensile stress-strain behavior is linear up to about 60 percent of tensile strength.

(2) The initial modulus is nearly equal to that of the compressive stress-strain plot.

(3) Beyond the ultimate stress, a region of strain softening can be observed along with the appearance of microcracks. The final failure is by the coalescence of microcracks and the formation of a macrocrack.

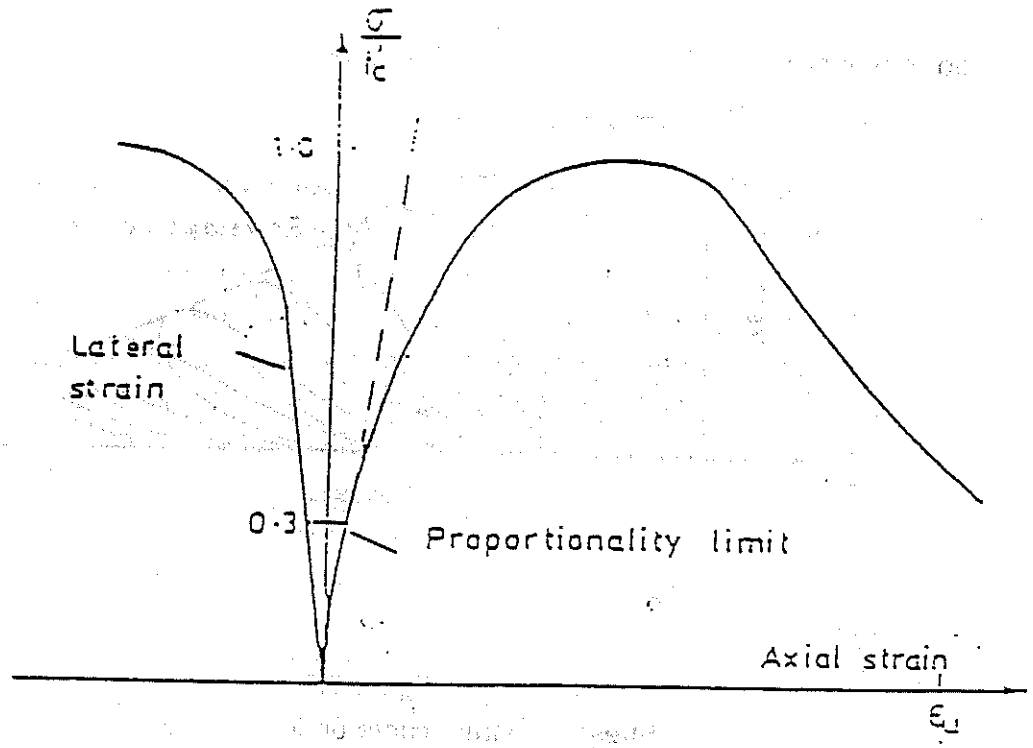

Figure 3.3
Compressive stress vs. axial lateral strain curves

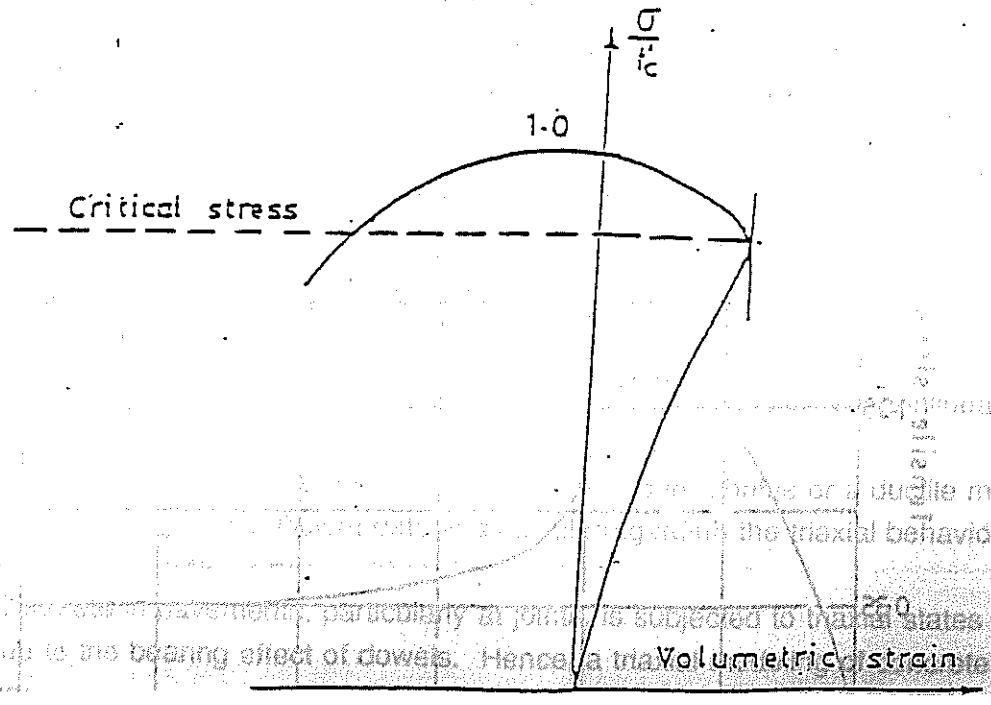

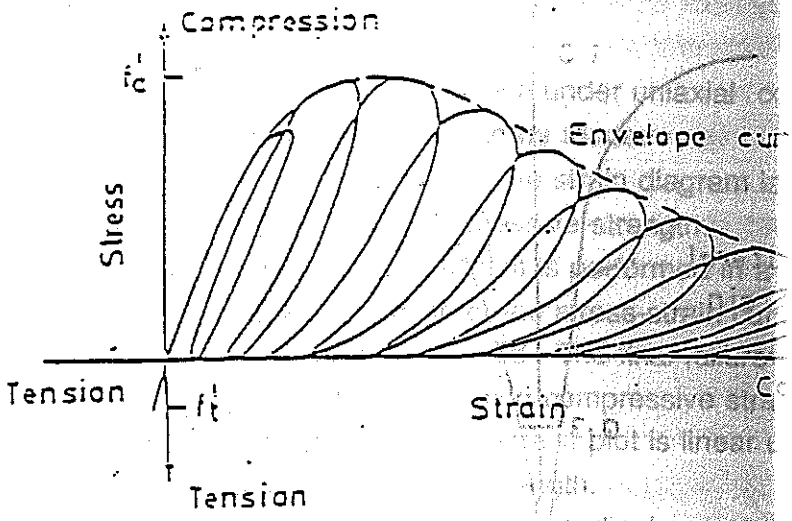

Figure 3.5
Stress vs. strain curve under cyclic loadin

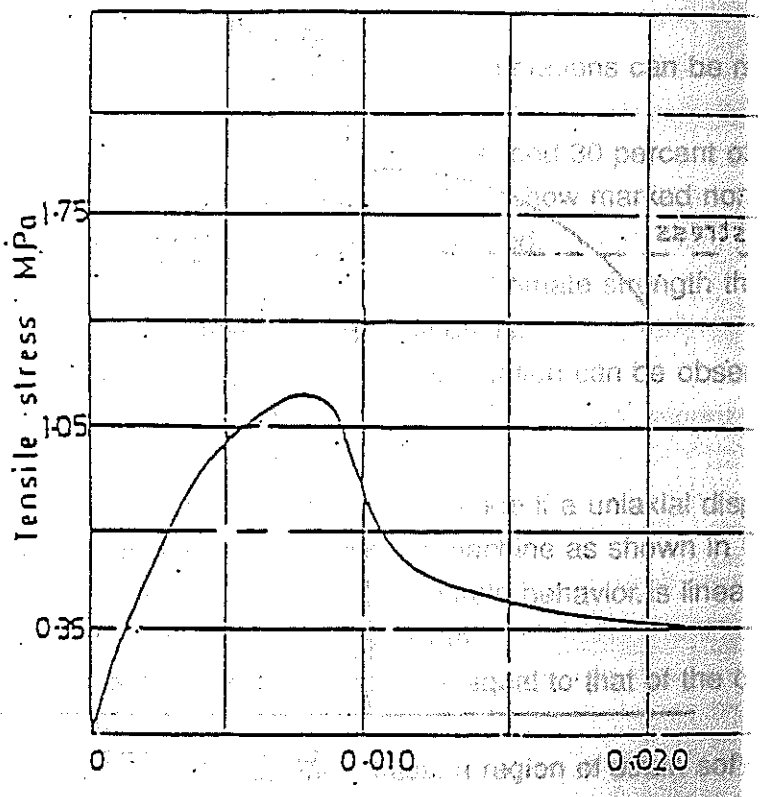

Figure 3.6
Tensile stress vs. strain curve

Biaxial Behavior

An extensive series of tests conducted by Kupfer et al. *[10]* is considered to be standard for comparison of results of most numerical models and other tests. Figures 3.7 - 3.10 indicate some of their observations.

(1) The maximum compressive strength increases for biaxial compression. At a principal stress ratio of 0.5 it is about 27 percent more than the uniaxial compressive strength and at a principal stress ratio of 1.0, it is about 16 percent in excess, as shown in Figures 3.7 and 3.8. The biaxial tensile strength remains almost constant and is equal to the uniaxial tensile strength, as shown in Figure 3.9. In compression-tension, the compressive strength decreases almost linearly with the increase in the tensile stress.

(2) Concrete ductility under biaxial stress fields depends upon the state of stresses. Under uniaxial and biaxial compression, the average maximum compressive strain is about 0.003 and the average maximum tensile strain is about 0.002-0.004. Under uniaxial and biaxial tension, the maximum tensile strain is about 0.00008.

(3) Near the failure stress, the total volume increases under compression. This is due to crack formation and is termed dilatancy.

(4) Failure occurs due to tensile splitting in the direction perpendicular to the maximum principal tensile strain.

(5) The maximum strength envelope shown in Figure 3.10 seems to be largely independent of the load path.

3.4.1.3 Triaxial Behavior

Experiments indicate that concrete does not fail in hydrostatic compression. Chinn and Zimmermann *[78]* reached triaxial stresses of the order of 79 times the uniaxial compressive strength without observing failure. Under lateral compressive stresses, the axial compressive strength and ductility increase as indicated in Figure 3.11. The stress-strain curves under hydrostatic compression are nonlinear and the unloading curve follows the initial modulus.

Depending on the stress level, concrete behaves in a brittle or a ductile manner under triaxial loadings. Insufficient data is available regarding the triaxial behavior of concrete.

Concrete in pavements, particularly at joints, is subjected to triaxial states of stress due to the bearing effect of dowels. Hence, a triaxial modeling of concrete is necessary.

3.6.4 Analysis Procedure

The following are the steps in the analysis:

(1) The pavement slab, subgrade, and joints are discretized as three dimensional finite elements. As many slabs as needed for the problem are considered. The mesh is refined near the regions of interest, such as around dowels, at regions of expected cracking/plasticity, etc. The boundary conditions, applied loads, and their locations are chosen consistent with the field conditions.

(2) An elastic analysis is carried out with the temperature strains and a small proportion of the total wheel load. The strains and stresses at various integration points are computed. These strains and stresses are then checked for cracking and/or yielding.

(3) If cracking and/or yielding is encountered in the 'i'th increment then the following steps are taken:

(a) The fraction of load increment required to reach the critical condition (either cracking or yielding) is computed as a ratio of the current strain increment.

(b) This portion of the strain increment and the corresponding stress increment are added to the current strains and stresses. The state indicator for the stress point under consideration is changed.

(c) The remaining portion of the current strain increment is divided into a prescribed number of sub-increments.

(d) Each sub-increment is added and the current material matrix is computed based on the current state of stress. The increment in stress corresponding to the sub-increment of strain considered is computed. The strains, stresses, and other state variables are updated.

(e) After considering all the sub-increments of strain the results are stored, and the final stresses are integrated to obtain the equivalent nodal forces. The next stress point is then examined.

(4) After completing the above calculations for all the stress point in the structure, equilibrium of the external loads with the equivalent nodal forces is checked for testing convergence. If convergence is not found, the following steps are taken:

(a) If necessary, a new global stiffness matrix is computed based on the current state of stress. This step may be done for every iteration as in the Newton-Raphson method or at a certain prescribed interval of iterations as in the modified Newton-

$$\{\sigma\}^e = [D]\,[\{\varepsilon\}^e - \{\varepsilon_0\}^e] + \{\sigma_0\}^e$$

where $\{\sigma\}^e$ is the element stress vector, [D] is the constitutive
$\{\varepsilon_0\}^e$ is the initial strain vector, and $\{\sigma_0\}^e$ is the initial stress ve

(5) The equilibrium equation at the global level can now be obtai
principle of virtual work and represented as,

$$\{F\} + \{Fb\} + \{Fs\} + \{F(\varepsilon_0)\} + \{F(\sigma_0)\} = [K]\{d\}$$

where {F} is the applied nodal force vector, and {Fb} is the eq
nodal force vector due to body forces b, given by,

$$\{Fb\} = \Sigma^e \int_V [N]^T \{b\}\, dV$$

{Fs} is the equivalent nodal force vector due to surface forces
by,

$$\{Fs\} = \Sigma^e \int_S [N]^T \{s\}\, dV$$

$\{F(\varepsilon_0)\}$ is the equivalent nodal force vector due to initial strains

$$\{F(\varepsilon_0)\} = \Sigma^e \int_V [B]^T [D]\, \{\varepsilon_0\}\, dV$$

$\{F(\sigma_0)\}$ is the equivalent nodal force vector due to initial stress
by,

$$\{F(\sigma_0)\} = \Sigma^e \int_V [B]^T \{\sigma_0\}\, dV$$

[K] is the structure stiffness matrix represented as,

$$[K] = \Sigma^e \int_V [B]^T [D]\, [B]\, dV$$

where {d} is the nodal displacements, and V being the volume
element and S the surface area of the element.

In a structure with material nonlinearity, the structure stiffness matrix [
depends on the stresses/strains. Thus equation 3.6.5 will have to be solved
at each load increment level. For this purpose, several solution techniques a
available. Of those, the Newton-Raphson and the modified Newton-Raphson
most popular. In this technique, the structure stiffness matrix is reformulated
solved at every iteration or after a prescribed number of iterations is complet
present study, this technique of solution is employed.

elements. Three different concrete strengths are considered for the anal material properties are given in Table 3.2. The steel dowel bar was emb distance of 12 inches from the face of the joint. Spring dowel supports o concrete and dowel nodes. A shear load was applied at the tip of the do load is increased gradually and the analyses performed. The reaction of support springs and the displacement of the corresponding nodes are co Figure 3.28 showed the distribution of stresses around the dowel. A larg tion of tensile stresses in the elements above the dowel and large compr stresses in the elements below the dowel can be observed. Figure 3.29 shear load vs vertical displacement of the node at which the dowel enters concrete joint. The curves are nonlinear and a gradual loss of stiffness w in load can be observed.

In the analyses of pavements during this study, a stiff dowel-conc spring representing no local effects and a soft dowel-concrete interface sp representing local yielding and cracking have been employed and compar analyses also indicated that most of the shear is transferred through the c spring while the interior springs remained essentially linear in response. the interface spring at the joint is given 'soft' stiffness during analysis with stiffness.

3.7.5 Selection of Finite Element Mesh

In any finite element analysis, proper choice of finite element mesh necessary to get reasonably accurate results. Particularly, in a pavement thickness dimension is very small when compared to the plan dimensions reliable overall response, the maximum aspect ratio (defined as the ratio dimension to minimum dimension of the element) of the finite element sho than five for linear elements and 10 for quadratic elements. Further, to o accurate stresses and strains for the nonlinear analysis, particularly near regions, a relatively small element size should be selected. The placemen also restricts the choice of finite element mesh.

To select a reasonable reliable and computationally economical me refinement study was conducted. Three meshes, shown in Figures 3.30 to 3.32, with different refinement levels were chosen. The support condition meshes were chosen to be identical. Symmetric loads 6 ft. apart and 0.5 joint were applied. Elastic analyses were performed and deflections were and compared. Table 3.3 shows the comparison of the deflections obtain selected points, shown in Figure 3.33, using these meshes. Based on the

Chapter 4

CONCLUSIONS AND RECOMMENDATIONS

4.1 CONCLUSIONS

In this study the behavior of brittle repair materials in rigid jointed concrete pavements has been examined experimentally and analytically. The following are the main conclusions of the study.

4.1.1 Experimental Study

1. An experimental procedure and corresponding testing set-up is introduced for biaxial testing of the repair material. Accurate measurements and a minimum number of boundary conditions have been shown to provide better understanding by which the strength and behavior of brittle repair material can be fully investigated. The test results show the capabilities of the biaxial tensile-compressive experimental technique.
2. The biaxial tension-compression test program presented herein is simple. The results are in agreement with previous investigations.
3. The bond strength tests used in this study include the slant shear, direct tension, and dire shear tests. These tests are required to determine directly the bond strength and quality of the bonding system.
4. The influence of patch shape and depth were studied by testing concrete specimens of two different patch shapes, namely, rectangular and transition shapes. Each shape includes three different depths. Specimens with transition shape patch were stronger than specimens with rectangular patch. Within each patch, strength decreases as depth increases.
5. Adding steel fibers to concrete increases flexural strength, toughness, and tensile peak stress and the corresponding strain.
6. Duracal cement material has higher flexural strength and ductility than plain concrete but less than fiber concrete. Duracal cement has the highest compressive strength in comparison with plain and fiber concrete. However, it behaves similarly as concrete at high stress ratios of biaxial tension-compression.

4.1.2 Analytical Study

1. Local deformation of concrete around the dowels at the joints due to high stress

premature local failures. These failures, though highly localized, reduce the shear transfer efficiency of the joint.

2. The dowel-concrete interface stiffness has been found to significantly affect the deflection profiles under normal support conditions. This in turn affects the joint shear transfer efficiency, which decreases with an increase in load.
3. With the loss of support under both slabs due to pumping damage, the shear transfer efficiency seems to increase even though the ultimate load decreases.
4. The corner load position due to edge wheel path leads to structural corner cracks. These cracks may appear even at service loads under severe loss of support conditions.
5. Nighttime curling of slabs leads to a loss of support at the joints. It also widens the joint, allowing entry of water at the joint. Most of the heavy traffic on highways travel at night, and hence, the nighttime curling condition of the slab is more critical from a structural point of view.
6. The nighttime curling of slabs, because of the loss of support under the joint, leads to a lift-off of the far end of the slab during the passage of heavy wheel loads. This effect is also present due to loss of support conditions from pumping. Thus, faulting of slabs at a joint may also indicate a loss of support at the far joint of that pavement slab.
7. The daytime curling condition is not critical to the joint. Further, the lift-off for this condition occurs at the center, which is less frequently loaded. Another feature of this mode is that such a lift-off does not encourage entry of water into the base of the slab. The behavior of pavements with daytime temperature gradients and wheel loads is similar to that caused by no temperature gradients.
8. Shrinkage of repair materials is an important characteristic which affects the stresses in both repair and existing materials.
9. Due to shrinkage, corner cracks in the existing material at the junction with repair materials can be expected.
10. The increase in stresses grows with the difference in the Young's modulus of the existing and repair materials and with the maximum differential shrinkage for the two materials.
11. Shrinkage effects are significant only for low traffic loads. At higher traffic loads, the difference in maximum stresses for pavements with and without shrinkage stresses decreases.
12. Because of the increase in stress ratios at lower load levels, the fatigue life of the repaired section decreases.
13. Since the existing material is also affected by shrinkage, the selection of a very high quality repair material will not increase the life of the repaired section

14. Partial patching procedures are more critical for material selection than full depth patching because of the additional interface between existing and repair materials. In these procedures, subgrade damage, if any, cannot be repaired. This also increases the stresses.

4.2 RECOMMENDATIONS

The conclusions given above lead to the following recommendations:

1. Strength under biaxial tension-compression stress states should be investigated before selecting a repair material.
2. It is important to determine the elastic properties of the repair material in order to check for compatibility with the existing material.
3. Fiber concrete, with its higher post-failure energy dissipation capacity, is likely to maintain serviceability even after cracking.
4. Selection of pavement sections for rehabilitation should be done considering the damaged or faulted slab and the conditions at the far end of the adjoining slabs.
5. When measuring shear transfer efficiency to determine the extent of pumping damage, the actual deflections of the slab should also be considered. This is because loss of support under both slabs leads to an increase in shear transfer efficiency.
6. The shrinkage difference between the existing and patch material should be minor for a satisfactory performance of the repair section. Failure of these sections can occur even in the existing material due to shrinkage.
7. The elastic properties of the repair material should be as close as possible to those of the existing material to reduce the shrinkage stresses.
8. Fatigue of existing and repair materials at low traffic loads should be investigated in the selection of a rehabilitation procedure by estimating and including the shrinkage stresses.
9. In some cases, strengthening of the existing materials near the damaged region may be necessary for a satisfactory performance of the repair procedure.
10. The computer program developed in this study can be used as an effective tool in assessing the causes of distress of a concrete pavement and in selecting the optimal repair procedure and material.
11. The procedure described in the analytical part of this study may be employed during the selection of a repair material by considering both fatigue and shrinkage. However, the fatigue characteristics need to be investigated and appropriately combined in the program.
12. If a proper choice of repair materials cannot be made based on the procedure described earlier for economical reasons, reinforcement provisions in the form of a mesh at the top and bottom surfaces of repair material can be made. The

existing material, particularly at the corners, can be improved though epoxy grouting or by suitable modifications in patch geometry. Such modifications, however, should again be checked through analyses before implementation.

4.3 SUGGESTIONS FOR FUTURE RESEARCH

Based on the observations and conclusions of this study, the following suggestions can be made for future research:

1. The simple test setup developed in this study needs to be augmented by a further study on fatigue characteristics of materials under biaxial fields due to cyclic loading. This is important because most of the structural failures of concrete pavement can be linked to fatigue.
2. Shrinkage measurements, particularly the effective shrinkage of repair materials should be made. The total shrinkage of these materials can be split into two parts. The first part takes place before the material has hardened. This part is not likely to lead to additional stresses. The second part of shrinkage leads to stresses in both repair and existing materials. This part is likely to be more for rapid hardening materials. Methods of shrinkage measurements which consider this aspect need to be developed.
3. Testing should be done to consider durability aspects of the repair material particularly under freeze-thaw conditions and surface moisture conditions.
4. Testing of fiber concrete patches with various percentage of steel fibers should be made to decide on an optimum level of fibers.
5. Analytical methods of considering the cyclical damage of concrete in concrete pavements need to be developed. These can be incorporated into the computer program developed in this study for a more realistic assessment of distresses and the effect of rehabilitation procedures on the performance of pavements.
6. The program developed in this study can be improved into a user-friendly software to enable its use by engineers in transportation departments.
7. An investigative study of actual highway patches done under supervision and monitored continuously for one to two years by a research team is needed to fully describe and evaluate the behavior of repair materials under field conditions. Data from such a study would be very useful for development of behavior predictive models. Particular attention with respect to shrinkage and fatigue aspects can be given in such a study.

REFERENCES

1. Hanaor, A., Balaguru, P. N., Kudlapur, S., and Nawy, E. G. (1985) "Repair of Bridge Deck Structures in Cold Weather," Interim Report No. 1, Department of Civil Engineering, College of Engineering, Rutgers University, Piscataway/New Jersey, Department of Transportation, Trenton, 65 pp.

2. Kudlapur, S., Hanaor, A., Balaguru, P. N., and Nawy, E. G. (1987) "Repair of Bridge Deck Structures in Cold Weather," Interim Report No. 1, Department of Civil Engineering, College of Engineering, Rutgers University, Piscataway/New Jersey, Department of Transportation, Trenton, 218 pp.

3. Kudlapur, S., Hanaor, A., Balaguru, P. N., and Nawy, E. G. (1989) "Evaluation of Cold-Weather Concrete Patching Material," ACI Material Journal, Vol. 86, No. M5, pp. 36-44.

4. AASHTO Guide for Design of Pavement Structures (1986) Publ. by the American Association of State Highway and Transportation Officials.

5. Slate, F. O., and Olsefski, 1963. "X-rays for Study of Internal Structure and Microcracking of Concrete," ACI Journal, Proceedings, 60 (5), 575-588.

6. Hsu, T. T., F. O. Slate, G. M. Sturman, and G. Winter, 1963. "Microcracking of Plain Concrete and the Shape of the Stress-Strain Curve," ACI Journal, Proceedings, 60 (2), 209-224.

7. Kotsovos, M. D., 1979. "A Mathematical Description of the Strength Properties of Concrete Under Generalized Stress," Magazine of Concrete Research, 31 (108), 151-158.

8. Kotsovos, M. D., and J. B. Newman, 1977. "Behavior of Concrete Under Multiaxial Stress," ACI, 74 (9), 443-448.

9. Liu, T. C. Y., A. H. Nilson, and F. O. Slate, 1972. "Stress-Strain Response and Fracture of Concrete in Uniaxial and Biaxial Compression," ACI Journal, May, 291-295.

10. Kupfer, H, Hilsdorf, H.K. and Rusch, H. (1969) "Behavior of Concrete under Biaxial Stresses," ACI Journal, Vol, 66, No. 8, August, pp. 656-666.

11. Tasuji, M. E., F. O. Slate, and A. H. Nilson, 1978. "Stress-Strain Response and Fracture of Concrete in Biaxial Loading," ACI Journal, Proceedings, 75 (7), July, 306-312.

12. Mills, L. L., and R. M. Zimmerman, 1970. "Compressive Strength of Plain Concrete Under Multiaxial Loading Conditions," ACI Journal, 57 (10), 802-807.

13. Launay, P., and H. Gachon, 1972. "Strain and Ultimate Strength of Concrete Under Triaxial Stresses," Special Publication, SP-34, ACI, 269-282.